NUCLEAR INSTRUMENTS & METHODS

A JOURNAL ON ACCELERATORS, INSTRUMENTATION
AND TECHNIQUES IN NUCLEAR PHYSICS

EDITOR: K. SIEGBAHN - UPPSALA

VOLUME 4

JANUARY 1959 — JUNE 1959

NORTH-HOLLAND PUBLISHING COMPANY — AMSTERDAM

PRINTED IN THE NETHERLANDS
DRUKKERIJ MEIJER N.V. — WORMERVEER AND AMSTERDAM

64-06907

NUCLEAR INSTRUMENTS AND METHODS

Per.
QC
786
N883
v. 4-5

EDITORIAL BOARD:

J. B. ADAMS (CERN)
F. A. ALSINA (Buenos Aires)
E. AMALDI (Rome)
H. L. ANDERSON (Chicago)
K. T. BAINBRIDGE (Cambridge, Mass.)
C. J. BAKKER (CERN)
P. R. BELL (Oak Ridge)
R. E. BELL (Montreal)
A. BERTHELOT (Saclay)
H. BRINKMAN (Groningen)
E. H. COOKE–YARBOROUGH (Harwell)
S. DE BENEDETTI (Pittsburgh)
M. DE HEMPTINNE (Louvain)
A. DE-SHALIT (Rehovoth)
M. DEUTSCH (Cambridge, Mass.)
S. DU TOIT (Pretoria)
B. S. DŽELEPOV (Leningrad)
W. GENTNER (CERN)
P. C. GUGELOT (Amsterdam)
H. HALBAN (Paris)
O. HAXEL (Heidelberg)
P. HUBER (Basel)
D. J. HUGHES (Brookhaven)
S. KIKUCHI (Tokyo)
J. KOCH (Copenhagen)
M. S. KOZODAEV (Moscow)
S. LIVINGSTON (Cambridge, Mass.)
E. M. MCMILLAN (Berkeley)
M. G. MEŠČERJAKOV (Moscow)
P. B. MOON (Birmingham)
M. L. OLIPHANT (Canberra)
W. PAUL (Bonn)
A. S. RAO (Bombay)
G. SALVINI (Rome)
P. SAVIĆ (Belgrade)
P. SCHERRER (Zürich)
CH. SCHMELZER (CERN)
H. W. B. SKINNER (Liverpool)
R. TANGEN (Oslo)
D. TAYLOR (Northampton)
V. I. VEKSLER (Moscow)
O. WERNHOLM (Stockholm)
G. VON DARDEL (CERN)
R. R. WILSON (Cornell)
S. D. WINTER (Saclay)

JANUARY 1959 VOLUME 4 (1959) No. 1

GREGG M. SINCLAIR LIBRARY
UNIVERSITY OF HAWAII
8-7-63

NUCLEAR INSTRUMENTS & METHODS

A JOURNAL ON ACCELERATORS, INSTRUMENTATION AND TECHNIQUES IN NUCLEAR PHYSICS

EDITOR: K. SIEGBAHN - UPPSALA

CONTENTS

A. W. PRYOR and A. G. KLEIN, Statistical design basis for fast scaling systems 1
SURVEY ARTICLE: GUNNAR BÄCKSTRÖM, Experimental methods for the study of neutron capture gamma rays 5
D. C. COLLEY, J. B. KINSON and L. RIDDIFORD, 9-inch liquid hydrogen bubble chamber in a pulsed magnetic field 26
M. HUQ and G. W. HUTCHINSON, An energy sensitive Čerenkov detector with improved optical focussing 30
A. H. MORTON and W. I. B. SMITH, Improved cyclotron performance from control of initial ion motion 36
HANS M. NYSÄTER, Accurate magnetic field and field gradient measuring instrument for dynamic low fields in a synchrotron magnet 44
W. J. O'NEILL, E. SUNDAHL and H. OSTRANDER, An absorber system for scattering experiments 50
Conferences 51
Book Review 52

NORTH-HOLLAND PUBLISHING COMPANY - AMSTERDAM

NUCLEAR INSTRUMENTS AND METHODS

A journal on accelerators, instrumentation and techniques in nuclear physics

EDITOR: K. SIEGBAHN, UPPSALA

EDITORIAL BOARD:

J. B. ADAMS (CERN)
E. AMALDI (Rome)
H. L. ANDERSON (Chicago)
K. T. BAINBRIDGE (Cambridge, Mass.)
C. J. BAKKER (CERN)
P. R. BELL (Oak Ridge)
R. E. BELL (Montreal)
A. BERTHELOT (Saclay)
H. BRINKMAN (Groningen)
S. DE BENEDETTI (Pittsburgh)
M. DE HEMPTINNE (Louvain)
A. DE-SHALIT (Rehovoth)
M. DEUTSCH (Cambridge, Mass.)
S. DU TOIT (Pretoria)
B. S. DŽELEPOV (Leningrad)
W. GENTNER (CERN)
P. C. GUGELOT (Amsterdam)
H. HALBAN (Paris)
O. HAXEL (Heidelberg)
P. HUBER (Basel)
D. J. HUGHES (Brookhaven)
S. KIKUCHI (Tokyo)
J. KOCH (Copenhagen)
M. S. KOZODAEV (Moscow)
S. LIVINGSTON (Cambridge, Mass.)
E. M. MCMILLAN (Berkeley)
M. G. MEŠČERJAKOV (Moscow)
P. B. MOON (Birmingham)
M. L. OLIPHANT (Canberra)
W. PAUL (Bonn)
A. S. RAO (Bombay)
G. SALVINI (Rome)
P. SAVIĆ (Belgrade)
P. SCHERRER (Zürich)
CH. SCHMELZER (CERN)
H. W. B. SKINNER (Liverpool)
R. TANGEN (Blindern)
D. TAYLOR (Harwell)
V. I. VEKSLER (Moscow)
O. WERNHOLM (Stockholm)
G. VON DARDEL (CERN)
R. R. WILSON (Cornell)
S. D. WINTER (Saclay)

INSTRUCTIONS FOR CONTRIBUTORS

Contributions may be sent to the Editor, Professor K. Siegbahn, Institute of Physics, University of Uppsala, Sweden, either directly or through the intermediation of one of the members of the Editorial Board. Contributions may be written in English, French or German but should always, except for very short papers, be supplied with a brief abstract in English. Figures should be in inked original drawings or glossy prints and they should be sufficiently large. Contributors should make sure that important details in drawings and photographs will show up clearly in the diminished copy used by the publisher.

Books for review should be sent to Professor Siegbahn.

Objective and descriptive material on endeavors and product developments from the industry for the section "Spotlight on Industry" should be sent directly to the publishers, North-Holland Publishing Company, P.O. Box 103, Amsterdam.

Nuclear Instruments and Methods is published monthly. The subscription price of a volume of 360 pages is $ 17.00 (130 s), postage free.

Subscriptions should be sent to the publishers, North-Holland Publishing Company, P.O.Box 103, Amsterdam or to any subscription-agent.

No part of this issue may be reproduced in any form, by print, photoprint, microfilm or any other means without written permission from the publisher. Reprints, photoprints or microfilms are obtainable at cost from the publisher.

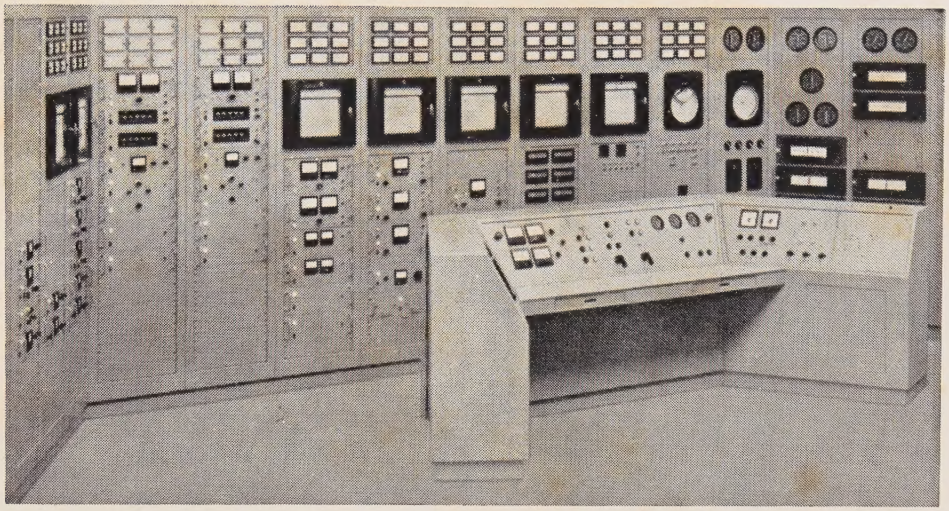

PHILIPS

equipment for Nuclear Physics and Atomic Energy

Instrument console and operators' desk for a 30 MW High-Flux tank-type reactor completed for testing in our Eindhoven works. Visible from left to right in panel are: water monitoring equipment, channels for neutron flux measurement, safety amplifiers and process instrumentation.

Desk contains operational controls as well as remote indication of the most important data.
Equipment was supplied on order from ACF Industries, Incorporated, for installation at AB Atom Energi's new facilities at Studsvik, Sweden.

- Synchro-cyclotrons for various final energies.
- Cockcroft-Walton accelerators.
- Generators for very high d.c. voltages.
- Linear electron accelerators.
- Reactor control instrumentation.
- Radiation measuring and detection equipment.
- Civil defence instruments.
- Area monitoring instrumentation.
- Geiger counter tubes.
- Photomultipliers.
- Radio-active isotopes.
- Air & gas liquefiers.
- Vacuum measuring equipment.

PHILIPS

PHILIPS
Nuclear Equipment

For further information please apply to one of the following addresses:

N.V. PHILIPS' GLOEILAMPENFABRIEKEN, Scientific Equipment Department, Eindhoven-Holland
RESEARCH & CONTROL INSTRUMENTS LTD., Instrument House, 207/215, King's Cross Road, London WC1
PHILIPS ELECTRONICS INC., Instruments Division, 750, South Fulton Avenue, Mount Vernon N.Y. U.S.A.

These names make NUCLEAR POWER

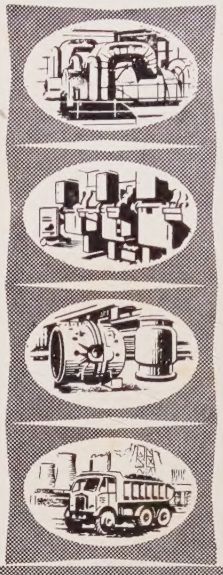

C. A. PARSONS & COMPANY LTD.

A. REYROLLE & COMPANY LTD.

HEAD, WRIGHTSON & COMPANY LTD.

SIR ROBERT McALPINE & SONS LTD.

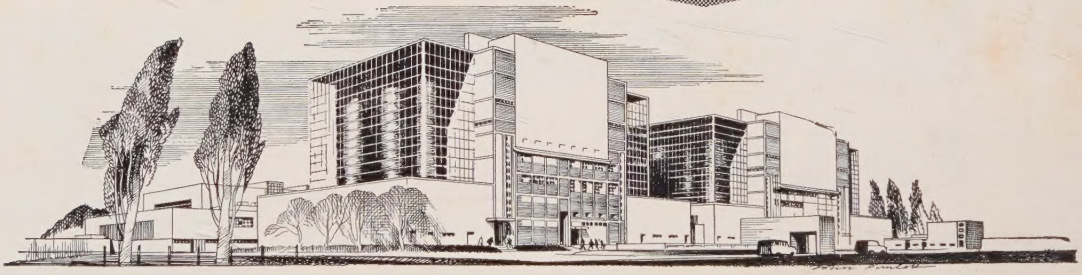

Bradwell, Essex, has leapt into fame as the site of the first commercial nuclear power station in the world to be built by N.P.P.C. Eight names make The Nuclear Power Plant Company Limited. N.P.P.C. thus combines the resources of eight specialist companies whose individual skills are co-ordinated to form a unified team capable of undertaking the construction of complete nuclear power stations throughout the world.

Bradwell nuclear power station will have a guaranteed output of 300 Megawatts. It is being built by The Nuclear Power Plant Co. Ltd. for the Central Electricity Generating Board.

WHESSOE LTD.

STRACHAN & HENSHAW LTD.

ALEX. FINDLAY & COMPANY LTD.

CLARKE, CHAPMAN & COMPANY LTD.

A Greater Britain through Nuclear Power

NPPC

THE NUCLEAR POWER PLANT COMPANY LIMITED · BOOTHS HALL · KNUTSFORD · CHESHIRE · ENGLAND

TGA NPJA4

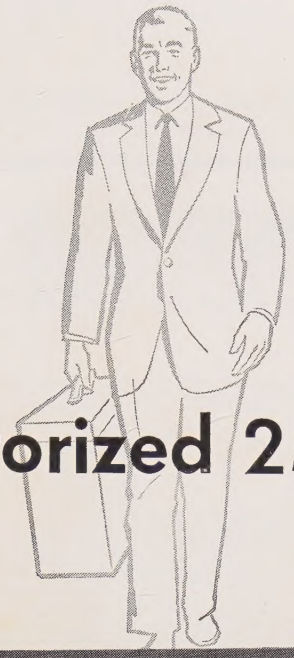

- *only 8¾" high*
- *uses interchangeable plug-in logic units*
- *provides complete versatility and portability*

. . . A Transistorized 256-Channel Pulse Analyzer

MODEL CN-110
256-CHANNEL ANALYZER
WITH PLUG-IN MODEL 210
PULSE HEIGHT ANALYZER UNIT

THE BASIC CN-110 IS THE MEMORY containing all the elements for complete magnetic core data storage — memory current drive, cycle control binaries, address and arithmetic binaries, power supplies, etc.

PLUG-IN LOGIC UNITS make several different analyzers available in the time it takes to interchange units. Standard plug-in units are available for Pulse Height Analysis, Time of Flight Measurements, Count as a Function of Time; units for special programs can be built to order.

CARRY THE SYSTEM TO THE OPERATION — the completely transistorized Model CN-110 weighs only *40* lbs. (including logic unit), and is only *8¾"* high. It is easily carried by one person to any location. With auxiliary readout system, total weight is approximately 100 lbs. — over 1500 lbs. less than equivalent systems using vacuum tubes.

NO COOLING PROBLEMS — the complete use of transistors in the Model CN-110 reduces heat dissipation — air conditioning or bulky blowers are not required; total power less than 10 watts.

MANY TYPES OF READOUT may be used — analog . . . binary . . . octal and decimal. Data can be recorded on strip chart or X-Y recorders . . . printed paper tape . . . magnetic computer tape . . . punched paper tape . . . punched cards. The Model 220 *Decimal Converter,* available as an accessory, is designed specifically for use with the CN-110. It includes a paper tape printer which prints channel number and count number on the same line (with 3-space separation). During the counting period, the Model 220 also functions as a live time indicator and automatic dead time corrector.

Write for complete data on the Model CN-110 and standard plug-in logic units. For details on custom logic units and data readout programmers, outline your specific requirements.

TMC **TECHNICAL MEASUREMENT CORPORATION**

441 WASHINGTON AVE., NORTH HAVEN, CONN.

INTERNATIONAL

advertise

YOUR NUCLEAR PRODUCTS IN

sell

YOUR NUCLEAR PRODUCTS

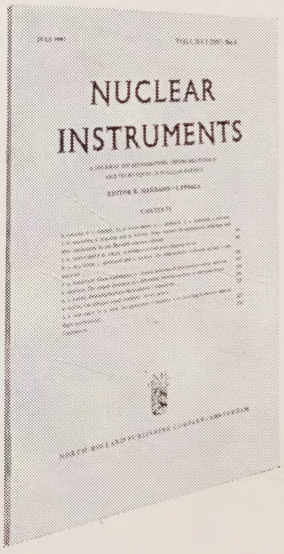

reap

YOUR NUCLEAR SALES
REWARDS

world wide

KEY NUCLEAR MANAGEMENT
NUCLEAR SCIENTISTS
NUCLEAR ENGINEERS
NUCLEAR PRODUCTION
PERSONNEL

SUBSCRIBE TO

you reach

THE WHOLE
NUCLEAR SALES WORLD IN

Entirely international in scope Nuclear Instruments is the one nuclear scientific journal that has an established subscription clientele through-out the whole world-where-ever nuclear men are at work—they want your nuclear products—they need your nuclear products—advertise in Nuclear Instruments and tell them WHAT – HOW – WHERE they can get your nuclear products

GO INTERNATIONAL WITH YOUR SALES PROGRAM TODAY WRITE

WILLIAM F. BAARS - ADVERTISING MANAGER NORTH-HOLLAND PUBLISHING COMPANY

P.O. BOX 103 – AMSTERDAM, HOLLAND

INTERNATIONAL

Elcor inc.
1225 W. BROAD ST.
FALLS CHURCH, VA.

FEATURES

- Wide current range: 1 x 10^{-3} to 3 x 10^{-9} amp. in 12 switch settings.
- High accuracy: 1% of full scale.
- Internal calibrating current source to check proper operation.
- Front panel switch allows instrument to be used with current of either polarity.
- Pre-setting feature provides means of safeguarding against over-exposure.
- Developed especially for use with Van de Graaff and other high-voltage accelerators.
- Permits many experiments with particle accelerators that would otherwise be difficult or impossible.
- Register readout gives digital accuracy on charge measurement.

MODEL A 309
CURRENT INDICATOR AND INTEGRATOR

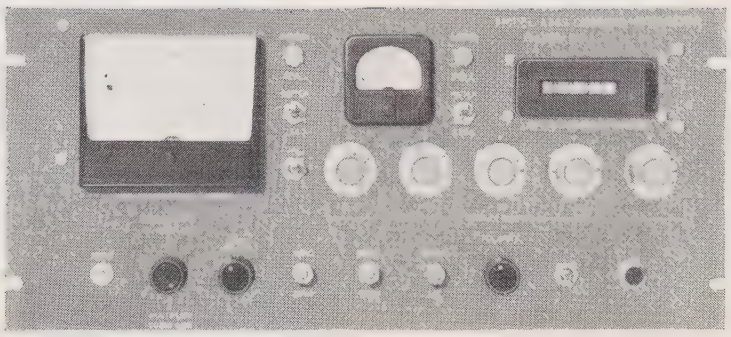

MODEL A 309 A

The versatility and accuracy of two instruments in one!

1. Measures currents from 1 milliampere to 3 milli-microamperes.
2. Integrates input current and registers accumulated charge.

GENERAL DESCRIPTION The Model A309 Current Indicator and Integrator is a sensitive current indicator that also measures the total charge collected in a given length of time. Developed especially for use with high-voltage particle accelerators such as the Van de Graaff generator, the instrument is also ideally suited for other applications requiring the measurement of accumulated charge or the integration of a variable current.

The full-scale sensitivity of the instrument can be varied from 1 milliampere to 3 milli-microamperes in twelve ranges. For convenience in checking the performance and accuracy of the instrument, an internal calibrating current source is provided for each range. The accumulated charge is indicated on a 5-decimal digit register. Any number up to 99,999 can be preset into the instrument, and upon reaching the corresponding charge a relay closes to actuate a warning device or control auxiliary equipment. In applications where X-rays are being generated, this feature affords protection against accidental over-exposure.

Input current of either polarity can be measured and integrated, and a front panel switch enables the instrument to be immediately changed from one polarity to the other. Advanced circuit techniques have been employed to achieve low input impedance, negligible drift, and a high overall accuracy and reliability.

Two models are available with the same specifications except for the method of presetting. In the Model A309A the presetting means consists of five front-panel switches. Presetting in the Model A309B is accomplished by manual adjustment of five presetting wheels that are accessible through the hinged cover of the register used in this model.

SPECIFICATIONS

1. Input current for full-scale meter deflection: 1 x 10^{-3} to 3 x 10^{-9} ampere in twelve switch settings.
2. Polarity of input current: positive or negative, controlled by front-panel switch.
3. Current indicating means: 4½" meter.
4. Charge indicating means: 5-decimal-digit register and 2½" meter
5. Maximum charge indicating capacity: 99,999 units.
   Note: Each unit is equal to one coulomb multiplied by the numerical value of the full-scale current.
6. Maximum integrating time: 28 hours.
7. Integrating rate for full-scale current: 1 unit per second.
8. Method of presetting:
   Model A309A: five front-panel switches.
   Model A309B: five presetting wheels in register.
9. Accuracy (Indicating and integrating accuracy, based on full-scale current): 1%.
10. Maximum drift: .01% per hour.
11. Maximum input voltage for full-scale current: 2 millivolts.
12. Minimum signal-source impedance for 1% accuracy: 1 ohm divided by numerical value of full-scale current.
13. Calibration: Internal reference current provided for each current range.
14. Power Input: 110–125 volts, 50-60 cps.
15. Dimensions: 19" wide x 8¾" high x 13¼" deep.
16. Mounting: standard 19" relay rack.
17. Weight: approximately 25 lbs.
18. Price: Model A309A: $1674.00.
    Model A309B: $1524.00.

ELCOR, — INC. • 1225 W. BROAD STREET • FALLS CHURCH, VA.
Telephone JEfferson 2-7718
A subsidiary of Fairfax Manufacturing Co., Inc.
Bulletin No. 24-1258

A Beta-Ray Spectrometer in commercial production, engineered to highest standards of performance

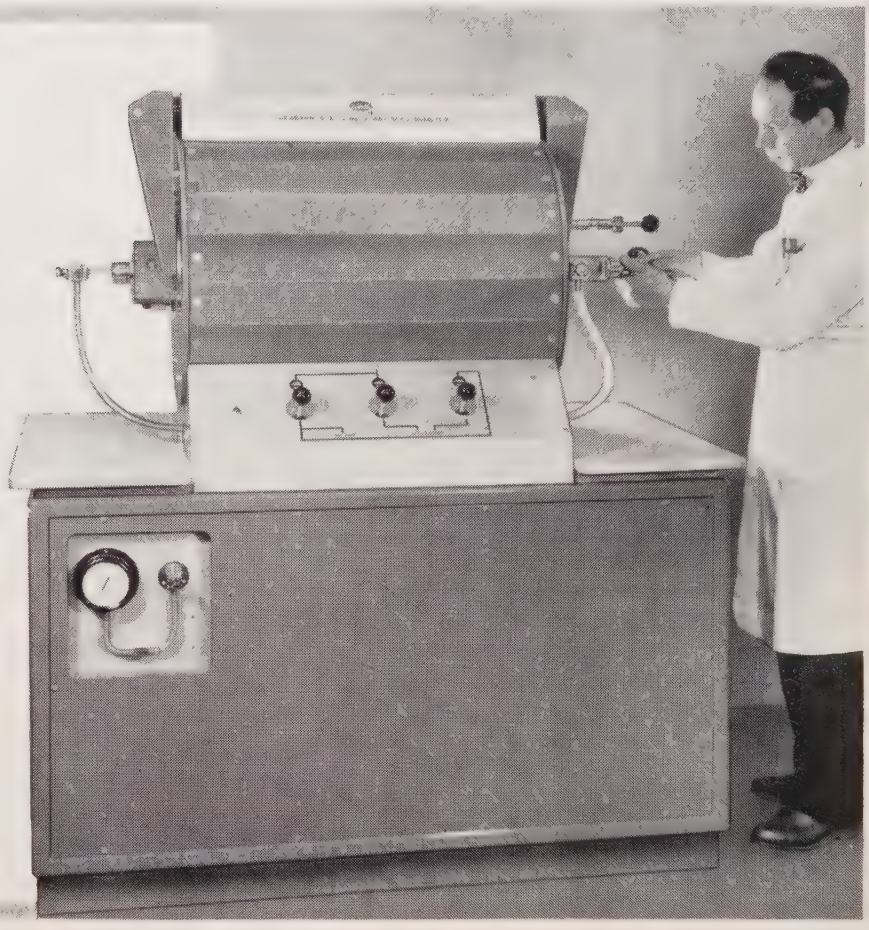

▲ Operator inserting source holder into spectrometer chamber through lock valve. Control console and 50 kW motor-generator set not shown.

The LKB 3024 B Siegbahn-Slätis Intermediate Image Beta-Ray Spectrometer

Features distinguishing the LKB Beta-Ray Spectrometer include:

Energy Range: 1 keV to 8.3 MeV electrons, or, when used as pair spectrometer, up to 17.6 MeV gammas.

Transmission: up to 8% of 4π.

Resolution: 0.7% at 1% transmission or 1.2% at 6% transmission.

Linearity: $B\rho$ proportional to magnet current within ±0.11% between 36 keV and 8.3 MeV.

Shielding: Spectrometer is iron-jacketed, insuring extremely low stray-field level.

Operation: Safe and fast. There are protective devices against all possible kinds of failure. Precision electronic regulator with follow-up servo facilitates current setting.

To be shown at the Geneva "Atoms for Peace" Exhibition, Sept. 1–14, 1958

Other LKB Products for the Nuclear Physicist:
Custom-built Precision-Stabilized and Transient-Free High Current D. C. Power Supplies.
Autovac Vacuum Gauge.

LKB

Write for details and references to:

LKB-PRODUKTER

Fabriksaktiebolag

P.O. Box 12220, Stockholm 12, Sweden

Distributors throughout the world

IF YOU ARE INTERESTED IN

NUCLEONIC COUNTING

Nucleonic Counting Equipment Type 127A.
Designed specifically for use in the nucleonic field where accurate, high speed counting is essential. This range of equipment comprises Scaling Unit, Amplifier-Discriminator, E.H.T. Unit, Head Amplifier, Quench Unit, Ratemeters and Timing Unit.

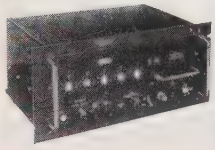

Scaling Unit Type 1221C.
A reliable general purpose Scaling Unit with a resolving time of 500μ secs. and a maximum count of 10^5.

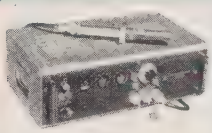

G.M. Counter Type 121A.
An inexpensive and reliable low-speed counting equipment for use in schools and technical colleges.

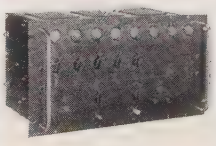

Timing Unit Type 146A.
An advanced design in Timing Units, this instrument employs high speed relay start/stop control.

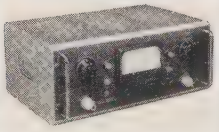

E.H.T. Power Unit Type 105A
Designed for nucleonic work—this gives continuously variable stabilized voltages from 300 - 3,300 volts d.c.

YOU NEED THIS NEW CATALOGUE!

If your interest lies in fact, in any aspect of Nuclear Physics, Radiation Monitoring, Radio-active Ore Surveying and Industrial Control and Measurement, then this new comprehensive catalogue should have a place in your library.

Here at Etelco, research and development are proceeding continuously to widen the range of counting, measuring and control instruments, and we invite you to examine our progress.

See us on Stand No. 97 at the Physical Society Exhibition, Royal Horticultural Hall, Westminster—19-22 January 1959

Cut out and mail today

ETELCO
INSTRUMENT DIVISION
HIGH CHURCH STREET, NEW BASFORD, NOTTINGHAM.
Please send copy of your catalogue **ELECTRONIC & NUCLEONIC INSTRUMENTS**

NAME _____

ADDRESS _____

POSITION _____

ETELCO
INSTRUMENT DIVISION
HIGH CHURCH STREET, NEW BASFORD, NOTTINGHAM
The Authority on Electronic & Nucleonic Counting

ETELCO LIMITED, HEAD OFFICE: 22 LINCOLN'S INN FIELDS, LONDON, W.C.2 Tel: HOLborn 6936

E106A-84A(R)

LELAB METAL-WALLED G-M TUBES
for anti-coincidence applications
where uniformity counts !

Lelab Counter Tubes are individually constructed, filled, and tested. Each is fabricated almost entirely of metal. All components are confined within the diameter of the tube shell to permit close stacking.

Compare our low prices on these superior tubes!

(Makers of Lelab [Robinson-Selverstone Type] Probe Counters for neurosurgery and where a fine needle-like probe for highly localized measurements is useful.)

Write for complete information

H. W. Leighton Laboratories

York & Sunset Lane-Hatboro, Pa. U.S.A.

1mV	full scale	1V	full scale
3mV	full scale	3V	full scale
10mV	full scale	10V	full scale
30mV	full scale	30V	full scale
100mV	full scale	100V	full scale

These are the Ranges of the BRAND NEW
Mercury Relay **PRECISION SLIDING PULSER,** model 413
for precise calibration and test of pulse-height analyzers and other nuclear instrumentation. Write to us for complete specs.

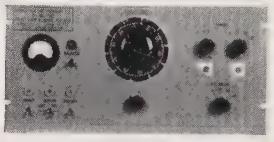

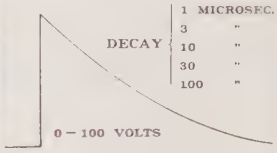

The Model 413 has manual and motor drive. Its fast rise and exponential decay simulate pulses from scintillation, proportional, or Geiger counters.

Window widths are determined AUTOMATICALLY, 10 × MORE ACCURATELY, 40 × FASTER than with conventional pulsers

Power Supply	Highly stable regulated supply with built-in potentiometer circuit.
Calibration	Self-contained standard cell and null indicating circuit for precision adjustment.
Rise Time	Less than .003 microsec.
Decay Time Constant	1, 3, 10, 30, 100 microseconds.
Polarity	Polarity switch for positive or negative pulses.
Ranges	0–100 volts in 10 ranges. All ranges continuously variable from zero.

Price $ 630.00 f.o.b. Silver Spring, Md.

RADIATION INSTRUMENT CO.

P. O. BOX 733, SILVERSPRING, MARYLAND, U.S.A.

NORTH-HOLLAND BOOKS

just out

Internal Conversion Coefficients

by

M. E. ROSE

Chief Physicist, Oak Ridge National Laboratory

9 × 12½″ **XXII + 176 pages** **40 s.**

THE CONTENTS

I INTRODUCTION
1. Definition of the Internal Conversion Process
2. The Selection Rules, Mixtures of Multipoles
3. Theoretical Considerations
4. Method of Calculation and Explanation of the "Tables"

II NUMERICAL RESULTS

K shell Internal Conversion Coefficients; L_I, L_{II}, L_{III}, subshell Internal Conversion Coefficients; Total M shell Internal Conversion Coefficients, $Z \geqslant 65$; M_I, M_{II}, M_{III}, M_{IV}, M_V, subshell Internal Conversion Coefficients, $Z \geqslant 65$; Radial Integrals for K Conversion

Sole Agency for U.S.A.: Interscience Publishers Inc. – New York

NORTH-HOLLAND PUBLISHING COMPANY — AMSTERDAM

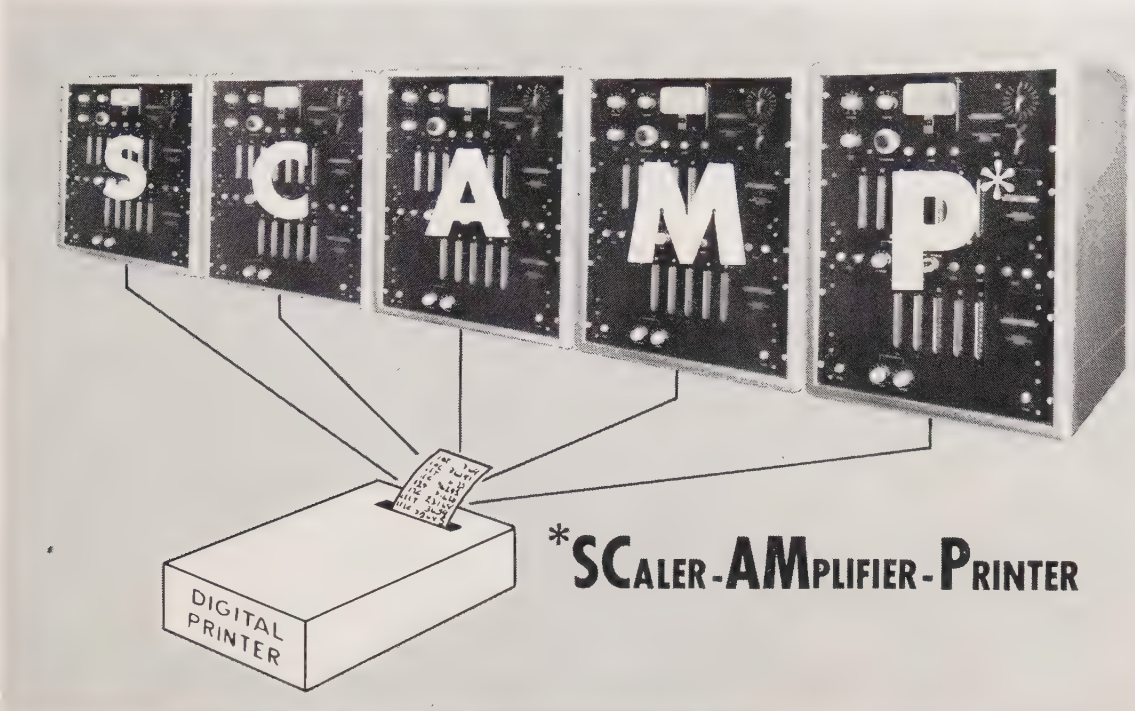

RIDL is proud to announce the Model 49-4 SCAMP System, consisting of a Model 49-4C Printing Count Scaler, a Model 49-4T Printing Time Scaler and a Model 30-1 Amplifier and High Voltage Supply. SCAMP offers *preset count* from 20 to 10^7 counts and *preset time* from 0.02 to 1000 minutes.

When used with an external decimal printer, SCAMP provides a completely *automatic* counting system. In the automatic mode of operation, the scaling operations will stop whenever a preset time or count is reached, whichever occurs first. If the preset time is reached first, the accumulated count data is printed – if the preset count is reached first, the elapsed time is printed. The system will automatically reset at the end of the print-out operation and commence a new count. This automatic operation will continue indefinitely or until stopped by a manual operation.

Any number of these units may be used with a single printer. The data will be read out from the scalers sequentially to the printer. In the event that more than one scaler reaches a print cycle simultaneously, the scalers will hold themselves in abeyance and await their turn at the printer.

SPECIFICATIONS

AMPLIFIER—

Gain: 1600—Coarse and Fine adjustment (Gain of 8000—OPTIONAL).
Input Polarity: Negative.
Input Sensitivity: ½ mv.
Resolving Time: 1 microsecond.
Discriminator: Adjustable from 0 to 80 volts. Linearity of 1%.
Test: Internal precision mercury pulse generator.

HIGH VOLTAGE SUPPLY—

Range: 300 to 1500 volts (400 to 5000 volts—OPTIONAL).
Output Current: 1 ma.
Polarity: Positive.
Line Regulation: A 10% change in line voltage results in less than 0.1% change in output high voltage.
Load Regulation: 0.3%, independent of output voltage.
Long Term Stability: 0.1% per week.
Ripple: 10 mv rms.

SCALER—

Count Capacity: 10^7
Time Capacity: 1000 minutes (10,000 minutes—OPTIONAL).
Resolving Time: One microsecond.
Input Sensitivity: 1/4 volt or 5 volts.
Preset Count: 20 to 10^7 in 24 steps.
Preset Time: 0.02 to 1000 minutes in 20 steps.
Printout Time: Approximately 0.4 seconds.

The Model 49-4 is just one of the many excellent instruments manufactured by RIDL. REMEMBER, whatever your instrumentation problem may be, RIDL has the solution. Our staff is always available to answer your inquiries. Write today for complete information.

RIDL INC.

Radiation Instrument Development Laboratory, Inc.

5737 South Halsted Street, Chicago 21, Illinois • TRiangle 3-2345

Representatives in major cities

MARSHALL

PULSE HEIGHT ANALYSER

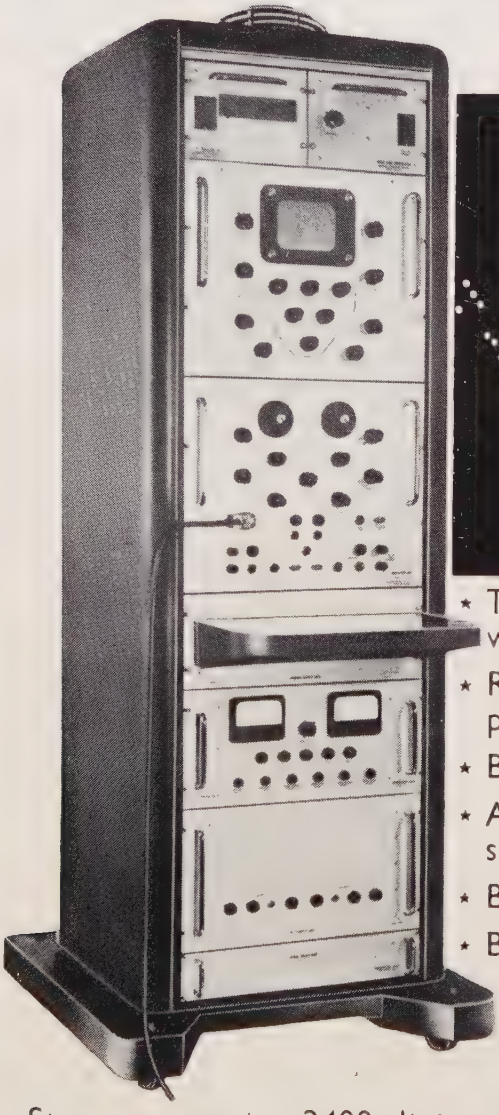

* Torsional delay line data storage with computor reliability.
* Resolution constant or proportional to amplitude.
* Background subtraction.
* Analysis of pulses of either sign from 1 mV to 50 V.
* Binary and decimal storage.
* Both digital and analogue display.

* Storage capacity 2400 digits.
* Analogue readout and automatic printout using either adding machine or electric typewriter.
* High stability and linearity.
* Total count scaler.
* Accurate live time integrator.
* Built-in precision test pulse generator.

M A R S H A L L
THE AIRPORT CAMBRIDGE, ENGLAND
TELEPHONE CAMBRIDGE 56291 TELEGRAMS AND CABLES MARELY CAMBRIDGE

Société d'Applications Industrielles de la Physique
S.A.I.P.
38, rue Gabriel Crié - MALAKOFF (Seine)

NUCLEAR PHYSICS

RECORDING SCINTILLATION SPECTROMETER "SPI 3"

- Resolution 8 to 10% at 0.661 MeV
- Non-saturable amplifier
- Stability: better than 1 Volt per day
- Linearity of the electronic equipment: better than 1%
- Detection starting from 5 KV
- Control oscilloscope
- 3 Scanning speeds
- Meci Speedomax recorder

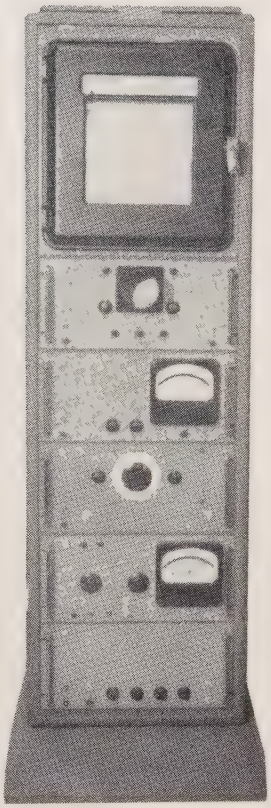

SCINTILLATION SPECTROMETER "SPE 3"

Same performance as "SPI 3"
Threshold variations are controlled by a 10-turn helipot.

OTHER PRODUCTS:

Single-channel kicksorters
Scalers
50-Channel Kicksorter "SA 50"
Proportional counters
Circulation counters
Pressurised ionisation chambers
Linear amplifiers
Vibrating condensator type D.C. amplifiers
Automatic sampling dispensers.

AGENTS:

BELGIUM: DRUA, 205 Avenue Van Volxem, BRUSSELS
DENMARK: LANGEBAEK & SON, Trondhjemsgade 9, COPENHAGEN
NETHERLANDS: ENRAF-EVERSHED, Van Leeuwenhoeksingel 69, DELFT
ITALY: AMPERE, Via Felice Casati 8, MILAN
FINLAND: ISOTEKNO, 13 A Mikontaku, HELSINKI
JAPAN: RIKEI TRADING C°, Kosato Building, 12-4 Chome Shiba Tamura-Cho Minato-Ku, TOKYO
SWITZERLAND: A. MAGAT, 28, rue de Vermont, GENEVA
U.S.A.: LEVIANT, 239 Broadway, N.Y. 7., NEW YORK

The place of the Particle Accelerator in Basic Research...

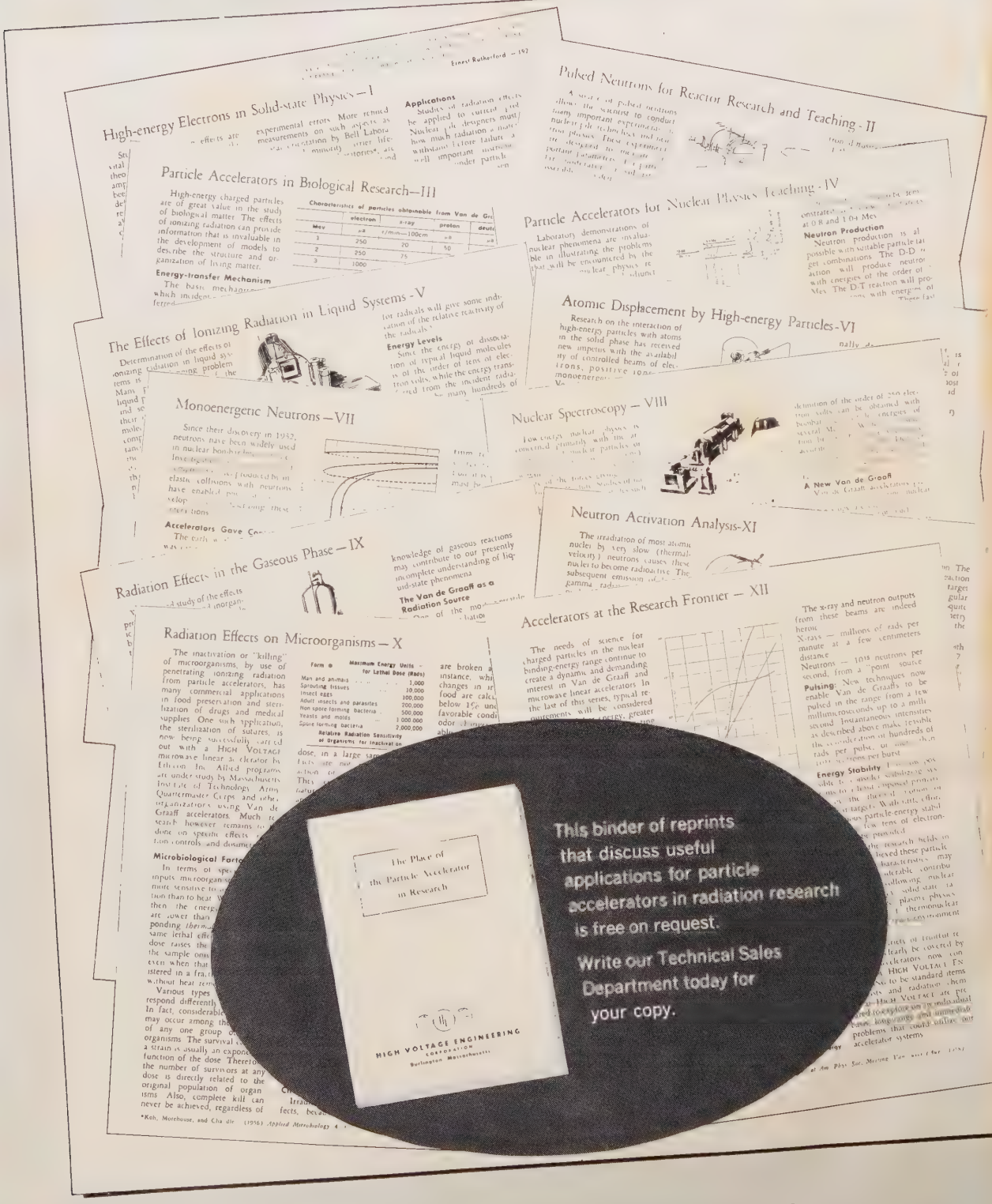
High-energy Electrons in Solid-state Physics—I
Particle Accelerators in Biological Research—III
Pulsed Neutrons for Reactor Research and Teaching - II
Particle Accelerators for Nuclear Physics Teaching - IV
The Effects of Ionizing Radiation in Liquid Systems - V
Atomic Displacement by High-energy Particles-VI
Monoenergetic Neutrons—VII
Nuclear Spectroscopy—VIII
Radiation Effects in the Gaseous Phase—IX
Neutron Activation Analysis-XI
Radiation Effects on Microorganisms—X
Accelerators at the Research Frontier—XII
The Place of the Particle Accelerator in Research
HIGH VOLTAGE ENGINEERING CORPORATION
Burlington Massachusetts
This binder of reprints that discuss useful applications for particle accelerators in radiation research is free on request.
Write our Technical Sales Department today for your copy.

Ionizing Radiations for Mankind. A 17-minute, 16mm, color sound-film on the application and design of particle accelerators. Apply to High Voltage Engineering for booking. Specify narration in English, French, or German.

HIGH VOLTAGE ENGINEERING CORPORATION

BURLINGTON MASSACHUSETTS

NUCLEAR INSTRUMENTS AND METHODS 4 (1959) 1–4; NORTH-HOLLAND PUBLISHING CO.

STATISTICAL DESIGN BASIS FOR FAST SCALING SYSTEMS

A. W. PRYOR and A. G. KLEIN

Australian Atomic Energy Commission, Australia

Received 15 November 1958

Considerations of the statistics of random pulses show that design criteria of fast scalers for nuclear particle detection are essentially different from those of equipment intended for operation with regularly spaced pulses. The regularizing action of scalers on random pulses is discussed and conclusions relating to practical systems are given.

1. Introduction

Radioactive disintegrations occur, for all practical purposes, in an infinitely short time and are completely random in distribution. For any method of detecting them, however, there is a time interval following each event during which no other events can be detected. This time interval is referred to as the *Dead Time* or *Resolving Time*. Both the particle detector ("counter") and the instrument for recording the number of events ("scaler") have resolving times. But the resolving time of the counter is usually a little indefinite and it is normal practice to make the resolving time of the scaler greater than that of the counter. The known resolving time of the scaler may then be used to calculate the counting losses.

If the resolving time is very small compared with the average pulse spacing, these counting losses are negligible. For fast counting rates, however, a correction must usually be applied.

2. Counting Loss Correction

The probability of there being 0, 1, 2... m counts in any given time interval t follows a Poisson distribution

$$P_m(U) = \frac{e^{-U} \cdot U^m}{m!}$$

where U = mean no. of counts expected in time t
$= Nt$ if N is the actual counting rate.

The probability of there being exactly zero counts during the dead time is, therefore

$$P_0 = e^{-Nt}$$

Hence the observed counting rate is given by

$$n = NP_0 = Ne^{-Nt} .$$

This usually approximated by

$$n \approx N(1 - Nt) \approx N(1 - nt) .$$

The true counting rate is therefore obtained in terms of the observed counting rate and the dead time, i.e.

$$N \approx \frac{n}{1 - nt} .$$

The counting loss correction factor is seen to be approximately equal to $1/(1 - nt)$. E.g. if it is required to detect 10^4 counts per second, i.e. pulses with an average spacing of 100 μsec an instrument with 1 μsec dead time will produce 1% counting loss whilst one with 10 μsec dead time will produce roughly 10% (more precisely 9.5%). In practical cases it is desirable to keep the counting loss below about 5%.

3. Regularizing Action of Scalers

If a scaler consisting of a number of decade units is required to operate on regularly spaced pulses, the resolving times of the several decades should be in the ratios of 1:10:100 etc. for a given maximum counting speed. If, however, the scaler is required to work with random pulses, as is the case in particle detection applications, the situation is modified considerably. After passing through the first decade scaler the statistics of the pulse train are modified in such a way that the speed requirements of the subsequent decade can be appreciably relaxed.

In general, scalers have a regularizing effect on initially random pulse trains, the counting losses in subsequent circuits being reduced by factors much greater than the scaling factors involved.

Consider a random train of ideal (i.e. infinitesimally narrow) pulses entering an ideal scale of K (i.e. one with zero dead time) at an average rate of N per second. The probability of exactly m input pulses arriving in the time interval t is given by the corresponding term of the Poisson distribution

$$P_m(Nt) = \frac{e^{-Nt}(Nt)^m}{m!} .$$

If this scaler is followed by a circuit having a dead time t, then an output pulse will be missed if K or more pulses appear at the input of the scaler during the time t.

The probability of this event is

$$Q_K(Nt) = \sum_{m=K}^{\infty} P_m(Nt) = \sum_{m=K}^{\infty} \frac{e^{-Nt}(Nt)^m}{m!}$$

$$\text{i.e.} \quad Q_K(Nt) = 1 - \sum_{m=0}^{K-1} \frac{e^{-Nt}(Nt)^m}{m!} .$$

The assumption is made here that the dead time is extended by t after each pulse arrives.

Since the loss of one output pulse corresponds to the loss of K input pulses, the fraction of input pulses that are not detected will be

$$x = K\,Q_K(Nt)$$

i.e. $NKQ_K(Nt) = Nx$ counts will be lost per second.

Fig. 1 shows graphs of the counting loss x plotted against Nt, the ratio of dead time to the average input pulse spacing for a number of scale factors K. The graph for $K = 1$ corresponds to a "scale of one" i.e. the simple case of circuit dead time discussed in section 2.

The regularizing action is already well apparent in the case of a scale of two. A dead time which would cause a counting loss of 10% with random pulses will cause only about 1% loss if the pulses have passed through an ideal scale of two. Hence by using a fast scale of two in front of a circuit the allowable response time may be increased by a factor of ten in that circuit if a counting loss of 1% is tolerated. This effect is much more pronounced in the case of higher scaling factors, as may be seen from the graphs.

Since in fast counting applications circuit complexity and cost increase considerably with the speed required, the above considerations are important in the design of fast counting systems.

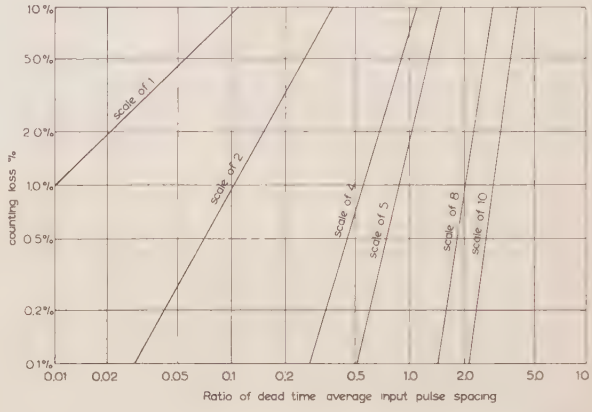

Fig. 1. Regularizing action of scales.

4. Design of Fast Scalers

These principles have been employed in the design of scalers for high counting rates. The general approach adopted is to have a 5-decade indicating scale built from 10-element gas tubes (Ericsson Dekatrons) which have a comparatively long resolving time. This Dekatron scale is preceded by a fast decade stage using transistor fed-back binary circuits. Except for very high speed counting, there will be only one of these fast scales preceding the Dekatron scales and it is quite possible that the maximum input rate will be limited by the onset of counting loss in the Dekatron scale rather than in the input scale as is the usual case.

It is quite impracticable to apply counting loss corrections in the Dekatron scale when the originally random input pulses have been through a scale of ten, so such losses must be kept small. On referring to fig. 1, it is seen that such losses are negligible up to a certain frequency and then begin to increase quite sharply.

For the indicating scale GC10B Dekatrons have been used. The resolution time is 250 μsec.

For the fast transistor stages three possibilities are under consideration:

(a) 0C71 Transistors giving 10 μsec resolution,

(b) 0C44 Transistors giving 1.5 μsec resolution,

(c) SB 102 Transistors giving 0.2 μsec resolution.

These figures have been obtained experimentally using binary circuits similar to those described by Aitchison[1]).

Consider the case of the 0C44 decade. If one of these decades precedes the main indicating scale using the Dekatrons, then the limitation of maximum input rate is set not by the input scale, as is the usual case, but by the main scale. If we take the 0.1% level as the point for negligible loss in the main scale, then we have from fig. 1

$$\frac{\text{Dead Time}}{\text{Av. Input Spacing}} = 2.2.$$

Using 250 μsec as the dead time we would, therefore, have a maximum rate of 8.8 kc/s to the input or 880 counts/sec to the main indicating scale. At this rate the counting loss in the fast decade is only 1.32%.

The problem of feeding a slow scale through one fast decade may be stated in more general terms. Either of two criteria may limit the maximum input rate:

(a) A loss of q% in the input scale (q is usually taken at less than 10%, but, for accurate counting, it may be desirable to have q as low as 1%).

(b) The onset of loss in the main scale, say the 0.1% level.

$$\text{Let} \quad R = \frac{\text{Input Resolution time of Main Scale}}{\text{Input Resolution time of Input Decade}}.$$

Then, using fig. 1 we may deduce that, if R is greater than $220/q$ then criterion (b) limits the input rate and if R is less than $220/q$ criterion (a) limits the input rate.

If q is taken at 5% and the resolution time of the main scale is taken at 250 μsec then, if the resolution time of the input decade is less than 5.7 μsec, the speed of the main scale limits the input rate; if it is greater than 5.7 μsec then the input scale itself limits the input rate.

The treatment may be extended to the case where two pre-scales are used before the main scale. For this case, when the random input pulses have been passed through two scales-of-10, the criteria for the ratios of the three resolving times involved then become:

$$1 : \frac{220}{q} : \frac{7000}{q}$$

where, as before, q% is the allowable loss in the input decade.

(The calculation for the resolution time of a circuit preceded by a scale of 100 is based on the fact that the time intervals between pulses have been regularized very markedly and may be approximated by a Gaussian distribution with a standard deviation of 0.1 average spacings.)

If we have an SB102 decade (0.2 μsec) feeding into an 0C44 decade (1.5 μsec) and then into a GC10B Dekatron main scale (250 μsec); and if we take $q = 5\%$ then the maximum input rate is limited by the SB102 input scale where 5% loss occurs at 250 kc/s. When the input rate exceeds 280 kc/s then losses in the main scale commence, losses in the input scale then being 5.6%. Losses never occur in the 0C44 decade in second place; it could be replaced by an 0C71 scale (10 μsec) but this scale would then be the limiting factor and the input rate would have to be kept below 220 kc/s.

5. Indication

The problem of indication does not arise with the Dekatron scales as they indicate the count by their very nature. In the case of the fast input scales using transistors two methods of indicating the stored count are commonly employed:

(i) *Meter Indication* in which the four binary stages draw currents proportional to their numerical value through a small meter calibrated directly 0 to 9. This system necessitates a fairly careful control over the supply voltage and usually requires "Set Zero" and "Set Nine" controls.

[1]) R. E. Aitchison, Symposium on the Peaceful Uses of Atomic Energy, Sydney (1958).

(ii) *Neon Tube Indication* in which the four collector waveforms are used to switch transistors which control neon tubes to give a binary indication of count. This requires four extra transistors whose collector voltage rating must be at least 30 V. In any case binary indication of a decimal count is not inherently quite satisfactory. The recent Indicating Triode Type DM160 may be used for the same purpose, but extra supplies are required and its reliability is still unknown.

These methods are, to a certain extent, inconvenient. Moreover, on statistical grounds indication of the last digit is not essential. Due to the random nature of the process, the observed counts N_0 will have a Gaussian distribution with standard deviation $\sqrt{N_0}$. Accordingly, if the total observed count exceeds a few hundred the last digit has no significance and its indication is superfluous.

It is possible, therefore, to omit count indication and resetting from the input decades. This necessitates, of course, a high standard of reliability and facilities for testing the operation of the fast scales.

6. Conclusion

Methods of calculating counting losses after the random input pulses have passed through a fast pre-scale have been discussed. The theory has been used in the discussion of possible designs for fast scalers.

NUCLEAR INSTRUMENTS AND METHODS 4 (1959) 5–25; NORTH-HOLLAND PUBLISHING CO.

EXPERIMENTAL METHODS FOR THE STUDY OF NEUTRON CAPTURE GAMMA RAYS

GUNNAR BÄCKSTRÖM

Institute of Physics, Uppsala, Sweden

Received 4 November 1958

The methods for the determination of energies and intensities of neutron capture gamma rays are reviewed. Special attention has been given to the comparison of various types of instruments that have been or may be used in such studies. The problem of establishing decay schemes is discussed, as well as the possibilities of assigning spins and parities to the levels. Methods of determining multipolarities and lifetimes of transitions are also included.

Introduction

Slow neutrons interacting with matter may be elastically scattered or absorbed since the energy is generally too low for the emission of charged particles. After neutron capture, the product nucleus is formed in an excited state with an energy (Q) characteristic of the nucleus. The average Q-value for all nucleids is about 8 MeV, but extreme Q-values of 2 MeV and 11 MeV are encountered. The excitation energy is accurately $Q + T$, where T is the kinetic energy of the neutron, and is of the order of eV. The energy thus imparted to the nucleus may accidentally correspond to an excited state and therefore resonance peaks are usually found superimposed on the well known $1/\sqrt{T}$-dependence of the cross-section. The compound nucleus is formed in one of the existing states with an energy close to the value $Q + T$. With captured slow neutrons, the orbital angular momentum is practically always zero. Thus the spin of the capture state must be $J_1 \pm \frac{1}{2}$, where J_1 is the ground state spin of the initial nucleus. For a similar reason, the parity will be that of the initial nucleus. The compound nucleus releases the energy $Q + T$ by sucessive emission of quanta. The energy factor favours a transition to the lowest states and consequently no transitions between the extremely dense uppermost levels are expected to be observed. On the other hand, the various selection rules may retard the highest energy transitions and lead to population of levels at a few MeV. Such cascade transitions are quite frequent as shown by experiments[1]) which indicate an average number of 3–4 photons per capture. Thus even if only dipole radiation is emitted, the spin of a level so populated may differ by 3–4 units from that of the capturing state.

It is evident that the study of capture gamma rays may yield information on levels which for energy or spin reasons are not populated in radioactive decay. In particular, it should be possible to complete the knowledge of the higher bands predicted by the unified model. The systematics of transition lifetimes may also be extended to higher energies.

Although capture gamma rays were discovered[2]) in 1934, very few data have been published until the last years, when research reactors have become generally available. Few complete decay schemes have been presented because of the complexity of the spectra coupled with present experimental limitations. A review of existing results up till 1955 has been given by Kinsey[2B]).

[1]) C. O. Muehlhause, Phys. Rev. **79** (1950) 277.

[2]) D. E. Lea, Nature **133** (1934) 24.

[2B]) B. B. Kinsey, Beta and Gamma Ray Spectroscopy, K. Siegbahn, ed. (Amsterdam, 1955) 795.

1. Methods of Measuring Gamma Energies and Intensities

1.1. SCINTILLATION METHODS

With many radioactive isotopes, it has been possible to establish unique decay schemes by means of scintillation techniques only. Naturally therefore, there have been attempts to extend the usefulness of this method to the field of capture gamma rays. While in radioactive isotopes the decay energies seldom exceed 3 MeV, capture gamma spectra often extend up to 10 MeV. The resolution of a NaI(Tl) crystal

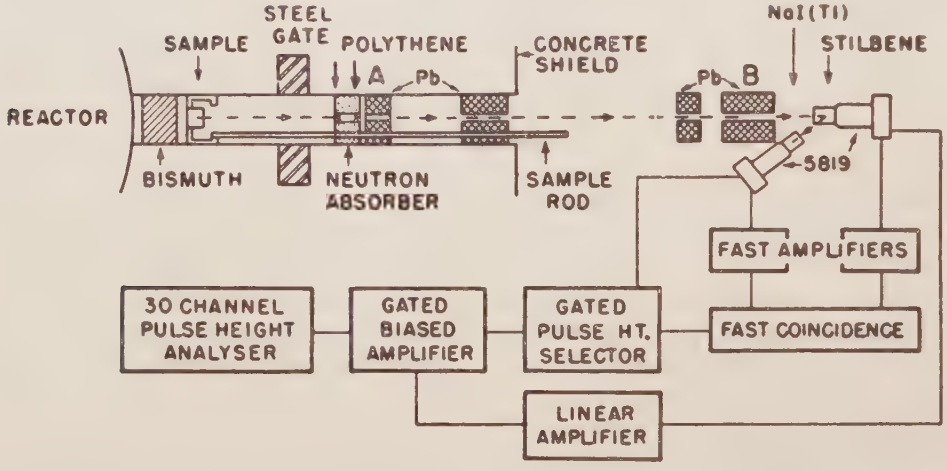

Fig. 1. Compton coincidence apparatus (from T. H. Braid, Phys. Rev. **102** (1956) 1109).

tends to improve with increasing energy, and its efficiency is almost constant from 1 MeV to 10 MeV. On the other hand, certain difficulties arise because the samples have to be examined under continuous neutron irradiation.

Except in the early works with Be(α,n) sources, reactors have been used to provide the neutrons flux. Hammermesh and Hummel[3]) collimated a neutron beam onto a circular target plate of 2 cm diameter, located at some distance from the reactor wall. The gamma radiation from this target was observed perpendicularly to the beam by a 0.8 cm height and 3.4 cm diameter NaI(Tl) crystal shielded with Bi walls from the intense stray gamma flux. A LiF absorber in front of the detector protected it against slow neutrons scattered from the target. The spectrum was recorded with the slow neutron beam hitting the target plate. A background curve was taken while the slow neutron beam was shut off by means of a Cd foil across the collimator. The foil did not appreciably attenuate the flux of fast neutrons and of stray photons. Thus the difference in counting rates could be regarded as arising from slow neutron capture in the source. In the spectra so obtained, the high energy parts were easily interpreted. However, at low energies, the peaks were superimposed on a very strongly sloping Compton background of higher energy gammas and here definite energy assignments were possible only for a few prominent peaks. This investigation covered the region 0.02–10 MeV, and it was possible with most target elements to resolve a few transitions.

Estulin *et al.*[4]) have quite recently applied a similar method, using the same detector techniques but confining the investigation to the region below 1 MeV. In order to reduce the background arising from capture and decay gamma rays from the centre of the reactor, a 12 cm Bi absorber was put in between the neutron collimator and the fuel elements. The direct background was still considerable and it

[3]) B. Hammermesh and V. Hummel, Phys. Rev. **88** (1952) 916.

[4]) I. V. Estulin, L. F. Kalinkin and A. S. Melioransky, Nuclear Physics **4** (1957) 91.

was found necessary to take readings with and without the slow neutron beam. Further, in order to ascertain the origin of peaks superimposed on the high Compton background, pulse height spectra were taken with various thicknesses of Pb in front of the crystal. Lines that were attenuated as expected from absorption data were considered to represent genuine capture gamma transitions. These authors also noticed that the line width increased with target weight, because part of the forward Compton distribution fell under the peak of the original gamma ray. Therefore, intensity generally had to be sacrified for resolution.

The continuous background of scintillation spectra comes mainly from Compton scattering events, where the secondary gamma ray escapes from the detector in an unknown direction. Braid[5]) made an attempt to overcome this difficulty by using a coincidence method which selected those events in which the secondary quantum is scattered into a definite angular interval and taking the spectra of the corresponding electrons. A schematic drawing of the experimental equipment is shown in fig. 1. A Bi block close to the reactor core supresses the gamma radiation from the central parts. Next to this shield is the target, which has here been placed at a point of high neutron flux. The photon beam is extracted to impinge on a stilbene crystal operated in coincidence with a NaI(Tl) crystal which accepts radiation scattered through angles between 130° and 160° and having energy in the range 120–250 keV. Photoelectric and pair creation events are thus excluded and in the coincident pulse spectrum of the stilben scintillator there is a peak corresponding to each gamma ray. Some background was still present, however, because of random coincidences and to stray photons (fig. 2).

A similar experiment was carried out by Reier and Shamos[6]) who used a NaI(Tl) for analyzing the Compton electrons. This type of crystal was preferred because of its higher inherent resolution. The sample was irradiated outside the pile in a collimated neutron beam and the secondary quanta were detected by a system of four counters distributed over a ring. An advantage of this arrangement over the one just described seems to be that the electron detector may be shielded from stray gamma rays. On the other hand, there will be radioactivity near the detectors because of scattered neutrons. Since the detectors subtend a relatively large solid angle as seen from the sample, cascades of prompt gamma rays may produce genuine coincidences, which are misinterpreted as Compton events.

A device which allows excellent suppression

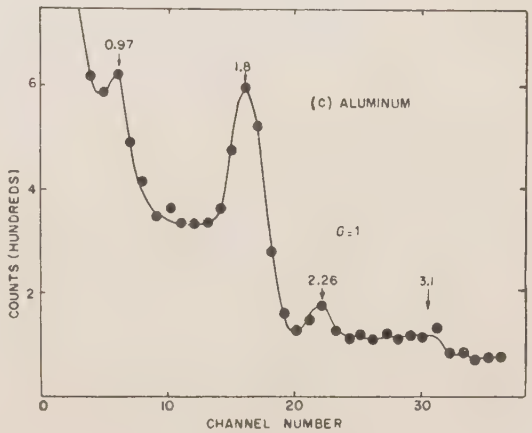

Fig. 2. Two-crystal scintillation spectrum of Al (from T. H. Braid, Phys. Rev. **102** (1056) 1109).

of background is the 3-crystal arrangement suggested by Hofstadter and Mc Intyre[7]). A NaI(Tl) detector receiving a collimated gamma ray is operated in triple coincidence with two similar crystals placed one on each side of and collinear with the first one. Photons of energy higher than $2\,mc^2$ produce electron pairs in the centre crystal, and the occurence of a triple coincidence consequently means that a positron has been stopped and has annihilated. Generally the negatron component of the pair has also been stopped, and the coincident pulse spectrum of the centre crystal consists only of peaks corresponding to energies $E_\gamma - 2\,mc^2$. In the

[5]) T. H. Braid, Phys. Rev. **102** (1956) 1109.
[6]) M. Reier and M. Shamos, Phys. Rev. **100** (1955) 1302.
[7]) R. Hofstadter and J. A. McIntyre, Phys. Rev. **79** (1950) 389.

work by Mann *et al.*[8]), this device was shown to give as good a resolution as 6.5% at 2.8 MeV and 5.1% at 4.8 MeV in response to radioactive gamma rays. In spite of its merits, this method has not yet been applied to capture spectra.

1.2. THE PHOTOPROTON METHOD

The (γ,p) process has been used successfully in attacking special problems of radioactive decay where a weak gamma ray of high energy could be detected in the presence of a strong background of gamma rays with lower energies which fall below the threshold of proton production. In the photodisintegration of deuterium, the energy excess $(E_\gamma - 2.23)$ MeV is roughly equally shared between the proton and the neutron. The partition depends to some extent on the angle of ejection of the particles. In response to a definite photon energy, the protons will therefore show a certain energy spread when detected with an ordinary ionization chamber. The relative width of the proton peak is then about 22%, implying that with $E_\gamma <$ 5 MeV the gamma energy resolution is 12% or better. Thus it seems possible that the method will be found useful in work with (n,γ) reactions, especially if the resolution can be improved by accepting only the protons ejected at a definite angle to the gamma ray. Such a development seems indeed possible, since the electron collection time is sensitive to the angle between the proton track and the collecting electrode. Other types of photonuclear reactions will perhaps also be found suitable for use in this field.

Although the method has frequently been applied to radioactive decay, there has been little attempt yet to record spectra from the decay of compound nuclei. Hammermesh[26]) used photographic emulsions soaked in D_2O and measured the tracks of the photoprotons. He was thus able to obtain a rough view of the gamma spectra from some elements. Better results were obtained by Wilson[27]), who investigated the spectra of Cd, Cl and C in the region 3–9 MeV by means of a deuterium filled ionization chamber.

1.3. THE CRYSTAL DIFFRACTION METHOD

Spectrometers operating on the principle of photon diffraction from crystal lattices were originally used in the X-ray field in the photon energy region below 0.1 MeV. The extension to radioactive gamma rays of the same energies presents only the extra difficulty that the collimation system used to shield the detector from the direct, undiffracted beam must be able

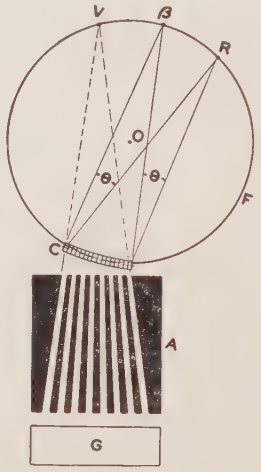

Fig. 3. Principle of the curved crystal diffraction spectrometer (from Muller, Hoyt, Klein and DuMond, Phys. Rev. 88 (1952) 775).

to absorb sufficiently even the higher energies that may be present in the source. The most important attempt to extend the usefulness of this type of instrument to the energies usually encountered in radioactive decay has been made by DuMond[9]) and others, who constructed a transmission type spectrometer (fig. 3) which is capable of measuring photons with energies up to 1 MeV. A quartz lamina (C) was bent along a circle of 2 m radius with its centre at β. A sample R, placed on the focal circle will be reflected according to the Bragg law and transmitted through the crystal as if it came from a virtual image V. Reflection thus takes place at angles determined by the formula $n\lambda = 2\,d \sin\theta$, where n is the order of reflection

[8]) L. G. Mann, W. E. Meyerhof and H. I. West, Jr., Phys. Rev. **92** (1953) 1481.

[26]) B. Hammermesh, Phys. Rev. **80** (1950) 415.

[27]) R. Wilson, Phys. Rev. **80** (1950) 90.

[9]) J. W. M. DuMond, Rev. Sci. Instr. **18** (1947) 626.

and $n = 1$ is most often used. The angle θ at which reflection occurs yields a relative measure of λ, which can be made an absolute one by calibration with X-ray emission lines. In order to find the angles corresponding to the gamma lines present, the intensity of the diffracted beam is measured by a scintillation counter (G) as θ is varied. At high energies, θ has decreased to the point where the diffracted and the factor f, the focal volume and hence the source strength obtainable are proportional to f^3, if self-absorption effects are disregarded. The angles of aperture remain constant while the crystal thickness and hence the reflectivity increase by the factor f. On the other hand, the area of the detector must be increased by f^2. This implies that the fraction of the background counts that is independent of the source strength

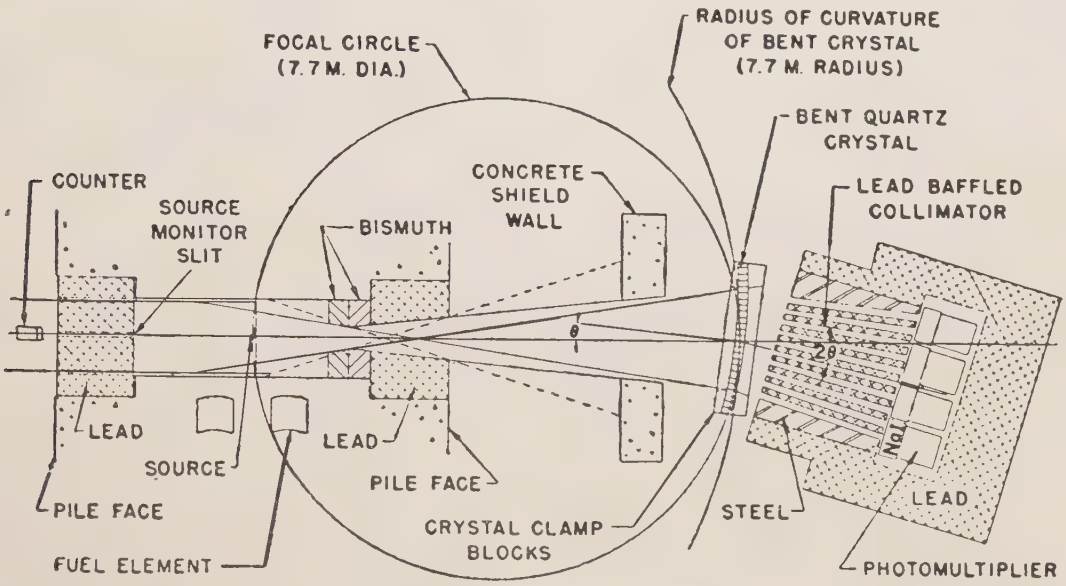

Fig. 4. Schematic drawing of the Argonne curved crystal arrangement (D. Rose, H. Ostrander and B. Hammermesh, Rev. Sci. Instr. 28 (1957) 233).

undiffracted beam partially overlap. In order to discriminate against the much stronger direct radiation, DuMond provided the detector with a collimator which consists of an array of tapered lead foils that point in the direction of the virtual focus.

An instrument for prompt gamma ray work[10]) has recently been built for use in conjunction with the Argonne reactor (fig. 4). Except for the mechanical arrangement necessary for varying θ, this spectrometer is constructed similarly to the one just mentioned but is enlarged to a crystal radius of 7.7 m in order to increase the counting rate and the line-to-background ratio. If the scale is changed by the also increase by f^2. Consequently, there would seem to be an improvement in the peak to background rates by the factor f^2 apart from the gain in absolute counting rate. However, selfabsorption indeed becomes appreciable, and there should be some background which depends on the source strength and arises from Compton scattering from the crystal, its holder, and the collimator plates. The scattering cross section is high in the forward direction, and the energy of the quanta scattered through a few degrees readily fall under the scintillation peak of the diffracted gamma ray.

The crystal of the Argonne instrument has a useful area of 16×16 cm^2 and a thickness of 0.4 cm. The collimator, of 100 cm length, consists of lead plates and yields a transmission

[10]) D. Rose, H. Ostrander and B. Hammermesh, Rev. Sci Instr. 28 (1957) 233.

of 50%. At 0.4 MeV the Bragg angle is 0.7° and the corresponding resolution is 0.5% for a source of zero width. The resolution will accordingly be 5% at 4 MeV on the same assumption. The total efficiency of the spectrometer at 0.4 MeV is 3×10^{-10} and should depend on energy according to εE^{-2}, where ε is the efficiency of the detector system.

As a direct consequence of the Bragg law, the resolution $\Delta E/E$ is about equal to $\Delta\theta/\theta$, the relative angular spread.

$\Delta\theta$ contains contributions from crystal imperfections, aberration, and source width. The first contribution is mainly set by the type of crystal chosen. The possibility of decreasing the source width by increasing R has already been discussed. Improvement may still be had however, by chosing a small lattice constant so as to increase the diffraction angle. This possibility has been considered by Knowles[11]) for Au crystals. It was estimated that reflections up to about the 8th order could be used with good efficiency but that thermal lattice vibrations rapidly impair the reflectivity at higher orders. A considerable practical difficulty would presumably arise in discriminating between spectra of different order. Knowles has also discussed the use of crystals of higher electron density for improving the reflectivity.

When comparing the efficiency of curved crystal spectrometers to that of other types of instruments, it must be born in mind that the source width and thereby the source strength is

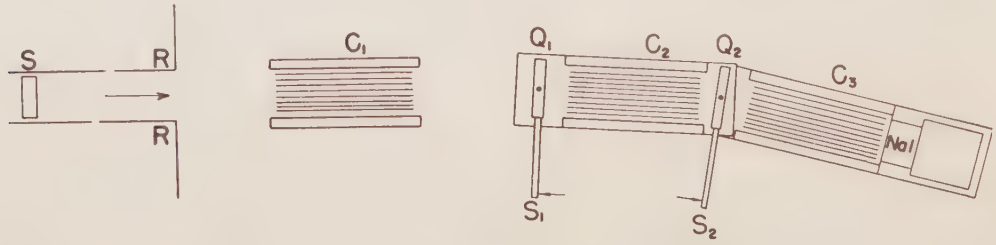

Fig. 5. Principle of the double flat-crystal spectrometer (from J. W. Knowles, Chalk River Report (1957) GPI–42).

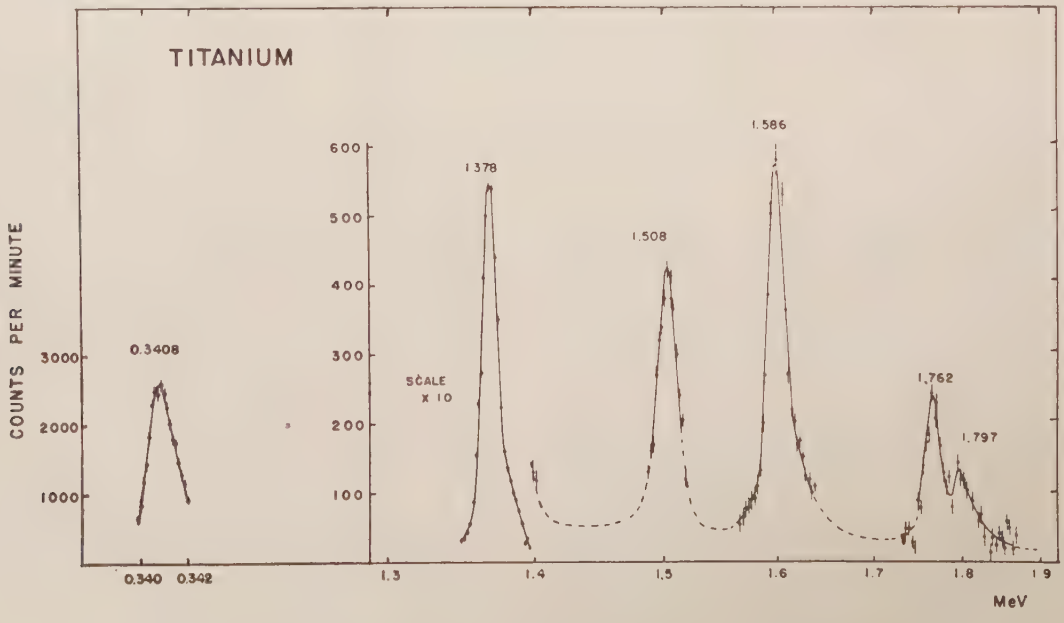

Fig. 6. Diffraction spectrum of Ti (from J. W. Knowles, Chalk Rever Report (1957) GPI–42).

[11]) J. W. Knowles, Chalk River Report (1957) GP I–42.

limited. Knowles[11]) has shown experimentally that the use of a non-focusing diffraction device, allowing larger source volumes, may yield about the same counting rate as the focusing type at still higher resolving power. The instrument (fig. 5) comprises two thick calcite crystals which are cut so that the lattice planes to be used for reflection are perpendicular to the directions S_1–Q_1 and S_2–Q_2. A photon can be successively reflected (1st order) in both crystals only if these make an angle of 2φ, where φ is the Bragg angle. The spectrum is scanned by varying the relative angle 2φ, while maintaining approximately an angle $\frac{1}{2}\pi - \varphi$ between the beam and the first crystal and observing the twice diffracted intensity. The acceptance solid angle, which is determined by the width of the diffraction pattern, is extremely small in this instrument. This enables one to use strict collimation of the gamma rays throughout the apparatus. Knowles used a system of three collimators, (C) which confined the beam to within 45 seconds of arc. An advantage of the double, flat crystal spectrometer over the focusing types is that its mosaic angles and hence the line width is appreciably smaller as a result of not applying stress to the crystals (fig. 6). The background is lower due to the excellent collimation, which becomes especially efficient as the total deviation is twice as large as in the curved crystal instrument. Another background reducing feature is that the detector area need not be much larger than that of the source. The smaller solid angle may generally be compensated by using stronger sources and thicker crystals. The type of crystal may be chosen with regard to diffraction properties only, since the mechanical strength is unimportant. Table 1, due to Knowles, compares the properties of different instruments. Naturally, gamma ray attenuation in the crystals reduces the low energy efficiency for the particular flat crystal arrangements.

TABLE 1

Comparison of diffraction spectrometers

Spectrometer type	Energy MeV	Spectrometer efficiency	Resolution $\Delta E/E$ (%)
Double flat C	0.1	0.5×10^{-10}	0.04
2.3 cm calcite	1.0	3.0×10^{-10}	0.4
mosaics: 3 sec	2.0	1.0×10^{-10}	0.8
Double flat C	0.1	1.0×10^{-10}	0.004
2.3 cm quartz	1.0	0.25×10^{-10}	0.04
mosaics: 1 sec			
200 cm radius curved C	0.1	1.0×10^{-7} †	0.2
1 mm quartz	0.5	4.0×10^{-9}	1.0
mosaics: 2 sec	1.0	1.0×10^{-9}	2.0

† The Argonne group report the efficiency 3×10^{-10} at 0.4 MeV for a similar instrument.

1.4. PAIR PRODUCTION INSTRUMENTS

In interaction with a nucleus, a photon of energy $h\nu$ may produce a positron-negatron pair, sharing the kinetic energy $(h\nu - 2\,mc^2)$. The energy distribution of each component is essentially constant, except at the extreme ends of the spectra. The angles θ that the electrons make with the gamma rays show a wide distribution[12]), gradually accentuated in the forward direction with increasing energy in such a way that the mean angle of ejection is of the order of $mc^2/h\nu$. At $\theta = 0$, however, the differential cross-section possesses a higher order zero. If the interaction with the nucleus is

[12]) W. Heitler, The Quantum Theory of Radiation (Oxford, 1954) p. 256.

neglected, the photon and the electron pair should lie in the same plane. Although the nucleus does not practically receive any energy in the process, its momentum may be high enough to attenuate appreciably this opposite azimutal correlation of the pair.

Kinsey and Bartholomew[13]) made use of a pair spectrometer for the study of capture gamma rays. The instrument is a specially designed semicircular spectrometer and is shown in fig. 7. The collimated gamma beam impinges on a thin pair converter foil of high atomic number. The components of the electron pair are deflected to opposite sides and focussed on two detectors connected in coincidence. Because the total energy of the pair depends to a first approximation only on the sum of the radii, a wide converter may be used. The device thus utilizes a large electron energy interval. The best focusing is had, however, in a cone around $\theta = 0$ where the cross section is low, even though electron scattering in the radiator tends to improve the situation. An important advantage of this intrument is that the detectors are far apart and may be well shielded from each other. Both features reduce the background of false coincidences. The line halfwidth was almost independent of energy and equal to 0.1 MeV. Because of the low cross section and the unfavourable angular distribution near the threshold of pair production, the instrument could be used only occasionally below 3 MeV. In this energy region, the efficiency of the spectrometer rises strongly. At 7 MeV it reaches the value 10^{-7} coincidences per photon incident on the radiator. By means of a special analyzing technique, the energies may be determined to the accuracy of $\pm$ 0.01 MeV. The capture gamma spectra of most elements have been successfully explored with this instrument (fig. 8).

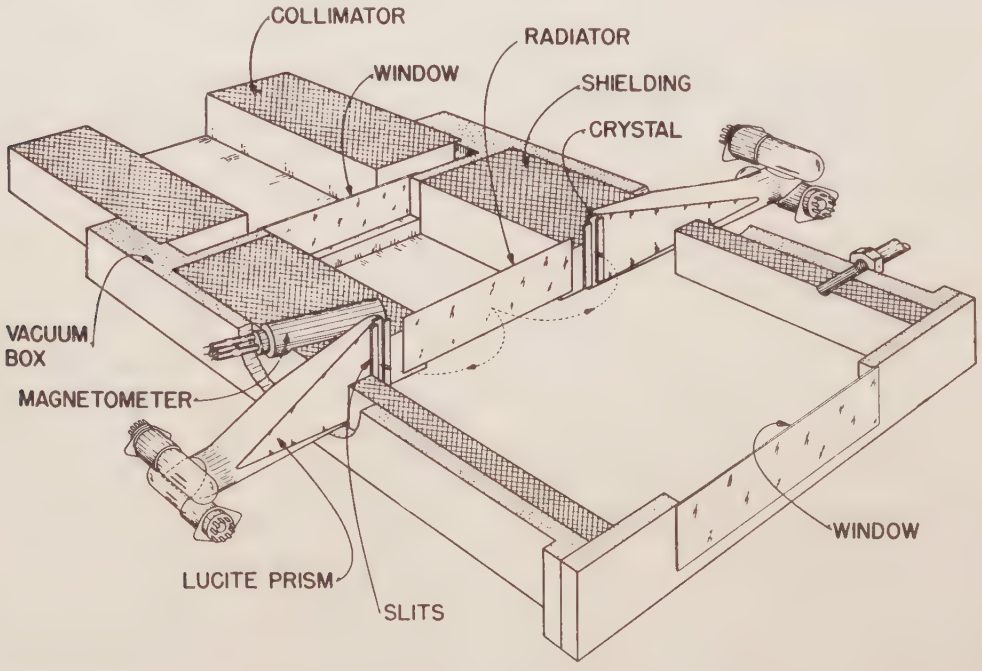

Fig. 7. External pair spectrometer (from B. B. Kinsey and G. A. Bartholomew, Can. J. Phys. **31** (1953) 537).

Several workers have attempted to convert a lens spectrometer into a pair detecting device. Alburger[14]) used an ordinary thin lens producing an annular focus (fig. 9). After passing through the ring-shaped slit, the related electron pairs distribute themselves in a statistical way over the detector area. The detector was split in two

[13]) B. B. Kinsey and G. A. Bartholomew, Can. J. Phys. **31** (1953) 537.

[14]) D. E. Alburger, Rev. Sci. Instr. **23** (1952) 671.

half-circles and each of the two scintillators was coupled via its photomultiplier to a coincidence circuit. When the spectrometer is set to focus use of a high transmission instrument such as the Siegbahn-Slätis type would probably permit a resolution of 3% with a reasonable signal-to-

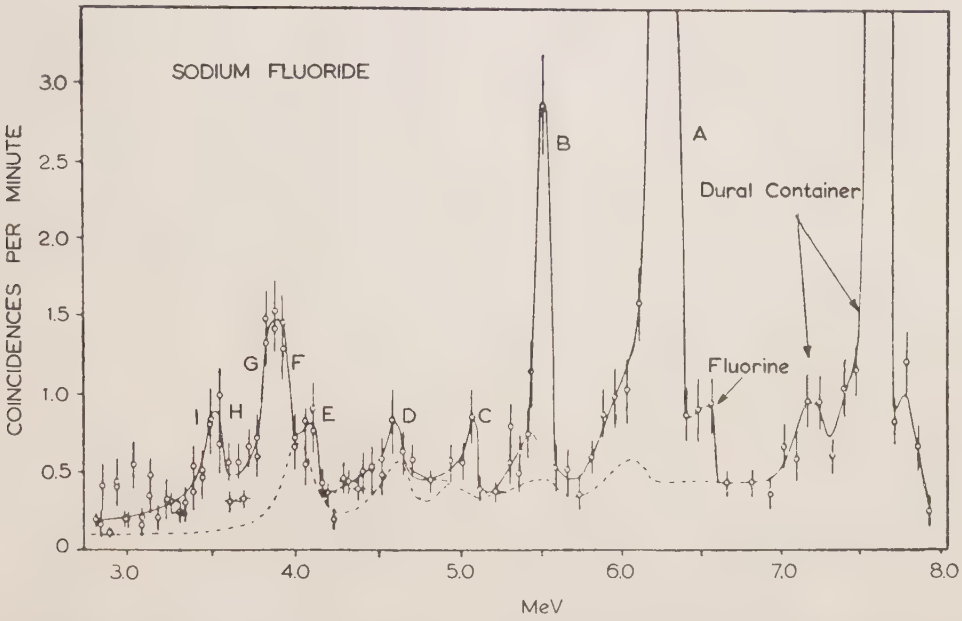

Fig. 8. Pair spectrum of NaF (from B. B. Kinsey, G. A. Bartholomev and Walker, Phys. Rev. 83 (1951) 519).

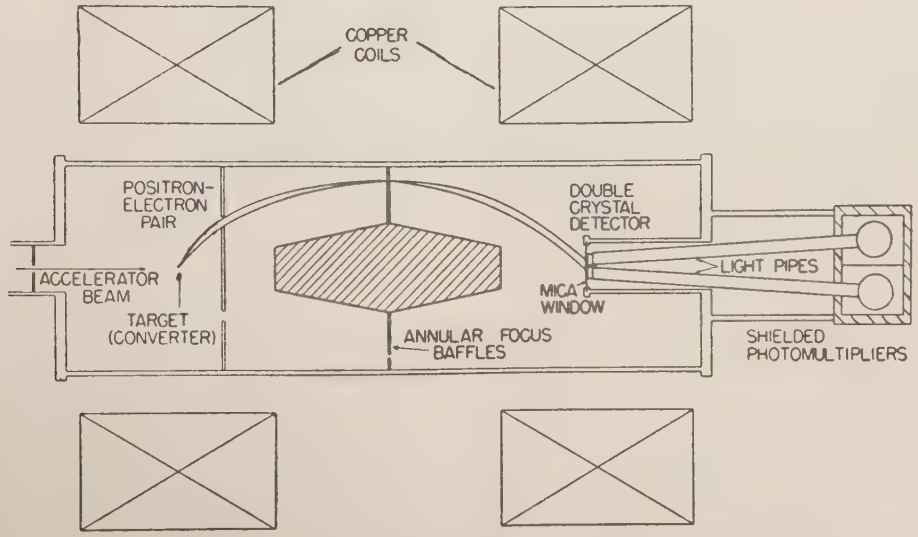

Fig. 9. Lens type pair spectrometer (from D. E. Alburger, Beta and Gamma Ray Spectroscopy, K. Siegbahn, ed. (Amsterdam, 1955) 767).

the energy $\frac{1}{2}(h\nu - 2\,mc^2)$, there is 50% probability that an electron pair which has passed the annular focus will produce a coincidence. The best momentum resolution obtained in this way was 4.5%. It was pointed out[15]) that the noise ratio. The main advantage of a lens spectrometer over the semicircular one for this sort of work is, of course, the higher solid angle and the more efficient utilization of the angular

[15]) D. E. Alburger, Rev. Sci. Instr. 25 (1954) 1025.

distribution. On the other hand, only a few percent of the energy distribution is accepted. Furthermore, the solid angle from one counter to the other is high and there is not much space available for shielding. This causes a comparatively high coincident counting background due to cosmic rays and to annihilation events, where a photon escapes to the other scintillator. Such pulses are, however, greatly rejected by means of energy discrimination.

It seems as if a combination of advantages would be obtained with a flat spectrometer which also has some double focusing properties. Such a solution has been suggested by O. B. Nielsen[16]) on the basis of the "orange" spectrometer.

Malmfors[17]) recently proposed a very promising instrument which uses the principle of time-of-flight measurement. The radiator is placed in a specially shaped inhomogenous magnetic field that makes the emerging pairs drift in different directions while describing trochoidal orbits. By means of a baffle system, it is possible to select, say, positrons of a narrow energy interval. With the momentum and hence the drift velocity of this component thus being known, the time-of-flight difference of the electrons uniquely determines the gamma energy. It seems possible in this way to obtain an energy resolution as high as 1% with an acceptance angle which by far exceeds that of the instruments mentioned above. If the delay times are recorded with a multichannel device, it is possible to measure simultaneously a large part of the gamma spectrum. The signal-to-background ratio is expected to be extremely favourable. Although the instrument has not yet been applied to pair spectrometry, preliminary experiments[18]) with radioactivity seem to bear out the practicability of this scheme.

1.5. THE PHOTOELECTRON METHOD

In the photo-effect, a photon transfers its energy $h\nu$ to a bound atomic electron, which is liberated with the kinetic energy $h\nu - E_1$, where E_1 is the ionization potential of the shell from which it originates. In the larger part of the energy region in concern, the cross section for the photo-effect is lower than that for pair production or Compton scattering. However, the discreteness of the photoelectron energies allows an efficient use of this interaction for the study of γ-spectra. The differential cross-section depends strongly on the angle θ between the photon and the photo-electron. The intensity maximum, which at very low energies occurs at $\theta = 90°$, gradually shifts toward smaller angles as the gamma energy is increased. In the vicinity of $\theta = 0$, the emission probability is very small. With the radiator thicknesses ordinarily used in practice, electron straggling makes this forward minimum unimportant.

Motz[19]) tried an arrangement in which samples were irradiated in an external neutron beam. The sample was located as close as possible to a Pb converter and the photoelectrons were analyzed in a thin lens spectrometer. The results indicated that, although fair intensity could be produced in this way with targets having high capture cross-sections, difficulties arose from the high continuous background of Compton electrons. The spectra were further complicated by the weaker photolines from L and M shells. In most cases, the beta decay of the residual nuclei would produce an additional background which would have to be el minated by some suitable absorber. The neutrons scattered from the target tend to contaminate surrounding metal parts.

In a measurement of the deutron binding energy, Bell and Elliot[20]) used the photo-effect in conjuction with an internal target. A paraffin cylinder was placed in the high neutron flux near the core of the reactor, the γ-beam being extracted through a lead collimator. The electrons were admitted into a thick lens spectrometer with its axis parallel to the beam. The relative halfwidth obtained for the 2.23

[16]) O. B. Nielsen, private comm., quoted by D. E. Alburger, Beta and Gamma Ray Spectroscopy, K. Siegbahn, ed. (Amsterdam, 1955) 767.

[17]) K. G. Malmfors, Nuclear Instruments **1** (1957) 251.

[18]) K. G. Malmfors, Arkiv f. Fysik **13** (1958) 237.

[19]) H. T. Motz, Phys. Rev. **104** (1956) 1353.

[20]) R. E. Bell and L. G. Elliot, Phys. Rev. **79** (1950) 282.

MeV gamma transition was 3%. The lines were superimposed on a high, sloping background.

Motz[19]) has achieved a very important improvement in this arrangement by taking coincidences between the photoelectrons and the X-ray quanta following its emission (fig. 10). With a heavy element converter, the energy of the flourescent radiation is within the range of a NaI(Tl) counter. Also, the K radiation is well

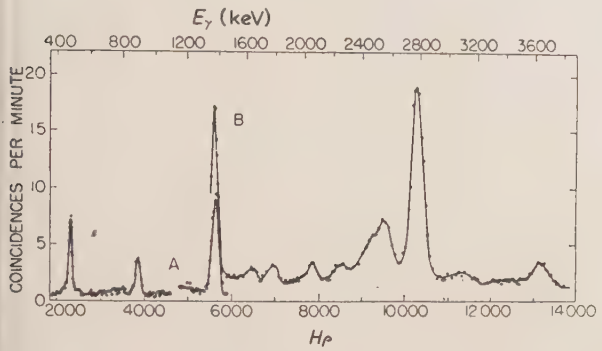

Fig. 10. Photoelectron spectrum of Na (from H. T. Motz, Phys. Rev. **104** (1956) 1353).

distinguished from the radiation caused by holes in higher shells since these energies are a factor of 5 lower. Since the gamma beam is collimated, the crystals can be taken quite close to the converter. This permits the acceptance of a large percentage of the coincident photons. Without serious loss in counting rate, the following desirable features are gained. There is only one photoelectron line corresponding to a given gamma energy. The background due to Compton electrons and pair production is drastically reduced, as well as the contribution from stray radiation reaching the electron detector. The chance coincidence rate appears to have been negligible in Motz' experiment. The sensitivity of this arrangement can be calculated with reasonable accuracy using the theoretical cross-section, modified by straggling in the converter.

1.6. COMPTON ELECTRON METHOD

When a photon $h\nu$ undergoes Compton scattering, its energy and momentum are completely transferred to an electron and a secondary quantum $h\nu'$. Accordingly, the three particles involved are in the same plane and the scattering directions may be described by the angles θ and φ, as shown in fig. 11. The energy distribution[21]) of the electrons is roughly constant, except near the high energy limit where it reaches an intensity 2–5 times the average value. In order to measure $h\nu$, a simultaneous knowledge of two quantities is required, for instance $h\nu'$ and E. For high intensity and resolution, it seems most advantageous to select electrons of maximum energy. $h\nu'$ will then assume its minimum value which can be calculated instead of explicitly measured. The fact that the highest electron energies are found in a small cone around $\varphi = 0$ also favours this choice, since it makes possible an economical

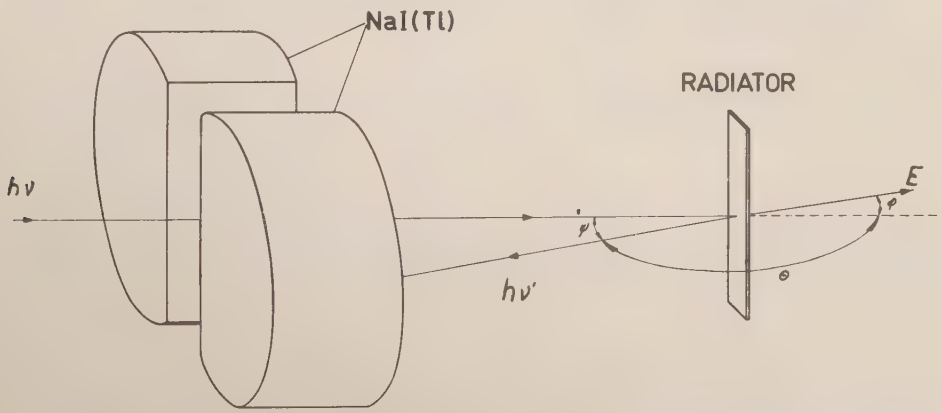

Fig. 11. Compton radiator arrangement for a flat, double focusing spectrometer.

[21]) C. M. Davisson and R. D. Evans, Revs. Mod. Phys. **24** (1952) 79.

measurement with a magnetic spectrometer.

Fig. 12 shows the experimental set-up that Mladjenoviç and Hedgran[22]) used in a study of radioactive decay. The collimated γ-ray hits an Al radiator perpendicular to the radius. A thin bundle of forward electrons is admitted through the first baffle. The resolution obtained using source strengths of a few hundred mC was 2.7% in the energy region 1–3 MeV. A double Geiger

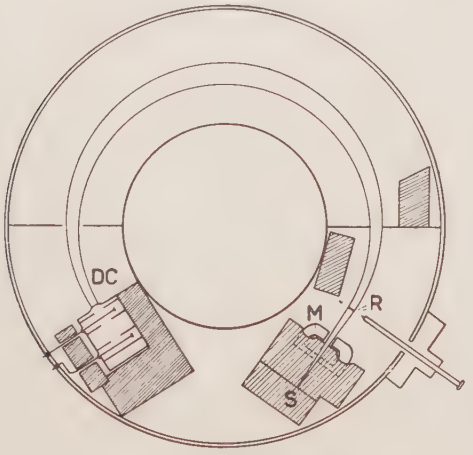

Fig. 12. Simple Compton electron instrument (from A. Hedgran and M. Mladjenovic, Arkiv f. Fysik 8 (1954) 49).

counter was used in order to suppress the direct background of stray gamma radiation.

Apart from the normal line width of the instrument, when used with the same source area, the following factors contribute to the Compton line width in this case. As is seen from the formula for the electron energy,

$$E = \frac{2\alpha\, h\nu}{1 + 2\alpha + (1+\alpha)^2 \tan^2 \varphi},$$

where $\alpha = h\nu/mc^2$, the energy spread is proportional to φ^2 for small angles. The poor collimation of the gamma ray and the finite electron acceptance angle cause a distribution of φ up to a certain maximum value. Multiple scattering further introduces an angular uncertainty such that some electrons having the right energy are scattered out of the aperture angle and vice versa. The application of the same arrangement to a study of capture gamma rays would result in better collimation and hence somewhat higher resolution.

Groshev *et al.*[23]) have constructed and used the instrument in fig. 13. The gamma ray passes into and out of the vacuum tank through thin windows. The secondary electrons leave the converter B in all possible directions. By using a uniform magnetic field and by suitably curving the radiator only electrons corresponding to $\varphi \simeq 0$ were admitted through the entrance slit A of the actual spectrometer, whose pole pieces were shaped in order to improve focusing. The foil could in this way be kept rather large, $4 \times 5\ \mathrm{cm}^2$. In order to obtain a reasonable peak-to-background ratio, it was found necessary to introduce a second Geiger counter behind the slit A and to take coincidences with the counter B. Since a coarse energy selection was made already in the first part of the instrument, the counting rate at A was rather

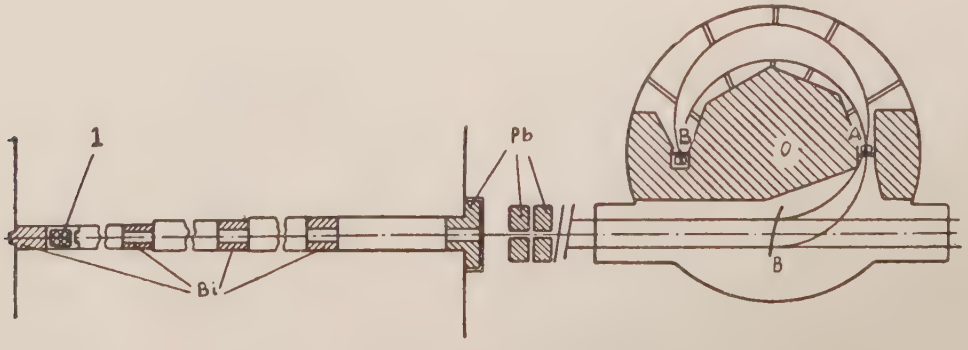

Fig. 13. Compton electron spectrometer (from L. V. Groshev B. P. Adyasevich and A. M. Demidov, Proc. International Conference on the Peaceful Uses of Atomic Energy, Geneva 1955, Vol. 2 (New York, 1956) p. 39).

[22]) M. Mladjenovic and A. Hedgran, Arkiv f. Fysik 8 (1954) 49.

[23]) L. V. Groshev, B. P. Adyasevich, and A. M. Demidov, Proc. International Conference on the Peaceful Uses of Atomic Energy, Geneva 1955, Vol. 2 (New York, 1956) p. 39.

low and random coincidences were negligible. The spectrometer was found useful in the wide energy region 0.3–12 MeV. A resolution of 2.3% was obtained at energies higher than 1.5 MeV†. The efficiency, defined as the number of coincidences per photon incident on the radiator, was 2.5×10^{-7} at 1.3 MeV and increased almost linearly to the figure 10^{-6} at 10 MeV. The capture collected. At 1 MeV, for instance, the associated relative energy spread is only 2×10^{-4} compared to the total line with 2.3×10^{-2}. This large area of the converter also combines with the disadvantage of having to focus a highly divergent ($\simeq 16°$) electron bundle. The coincidence possibility is a definite advantage of this method.

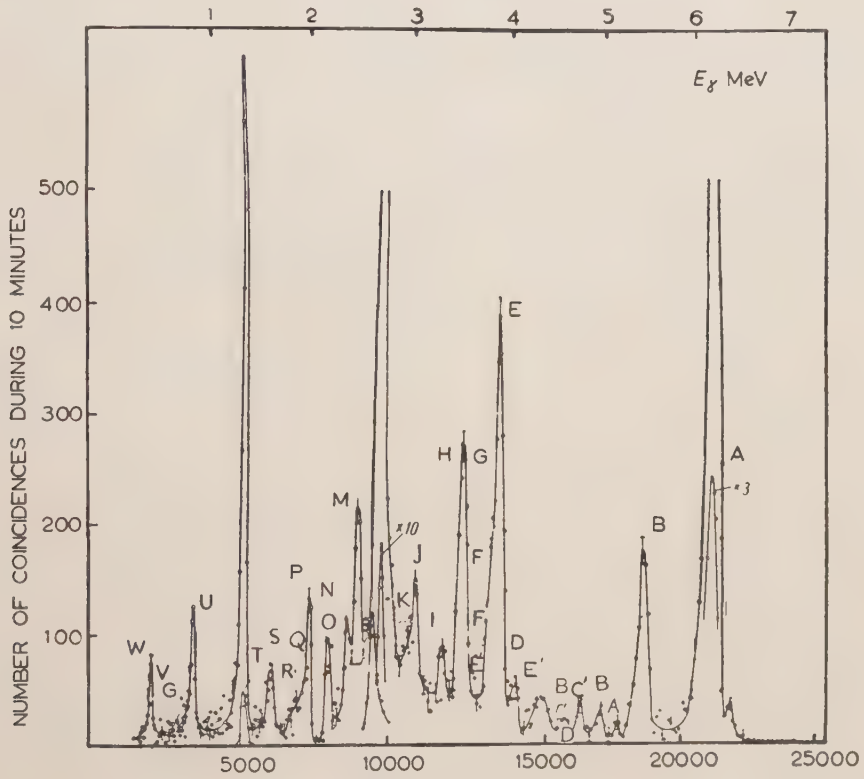

Fig. 14. Compton electron spectrum of Na (from L. V. Groshev, B. P. Adyasevich and A. M. Demidov, Proc. International Conference on the Peaceful Uses of Atomic Energy, Geneva 1955, Vol. 2 (New York, 1956) p. 39).

spectrum of Na^{24} recorded with this device is shown in fig. 14.

The remarkable feature about this instrument is the large radiator area in comparison with the analyzer radius (15 cm). However, considering that the Compton acceptance angle 2φ is only about 1° in the plane of the orbit, one realizes that the Compton electrons are not efficiently

† From a recent publication (Groshev *et al.*, Atlas of Gamma Ray Spectra from Capture of Thermal Neutrons, Moscow, 1958 [in Russian]) it appears that a resolution of 1.3% has occasionally been reached by this instrument.

H. T. Motz[19]) used for the first time a set-up in which the Compton electrons accepted into the annular baffle of a lens spectrometer were counted in coincidence with the backscattered gamma rays in the region $120° < \theta < 160°$. This amounts to a simultaneous measurement of E and θ, whereas the other schemes reviewed here rather involve a measure of E and φ. Apart from the background suppression which is achieved by means of the coincidence arrangement, this principle is definitely superior from the point of view that the gamma scattering

angle is not affected by straggling. In the experiment of Motz, the type of spectrometer was not well suited to the method and the best resolution that could actually be obtained was 5%. The same spectrum was run with singles as well as with coincidences. It was verified that the background could be reduced and that limiting the cone of secondary gamma rays rather than that of the electrons improved resolution as expected.

The author emphasizes that the geometry of the spectrometer used is unfavourable to the method and that with a flat, double-focusing instrument a resolution of 1% or better should be feasible. This would again correspond to the case $\varphi \simeq 0$. The electron energy as a function of the emission angle φ may be written

$$E = h\nu \frac{2\alpha}{1 + 2\alpha}\left[1 - \varphi^2 \frac{(1 + \alpha)^2}{1 + 2\alpha}\right]$$

for small φ. If the electron bundle used is limited to the solid cone $\varphi < \varphi_0$, the electron energy distribution will be approximately rectangular with a relative width

$$\frac{\Delta E}{E} = \frac{(1 + \alpha)^2}{1 + 2\alpha}\varphi_0^2 .$$

The height of the distribution obviously is independent of φ_0 and the peak counting rate cannot be raised much by increasing the solid angle, if the energy spread is larger than the width of the window curve of the analyzer. The acceptance solid angle necessary to make economic use of secondary electrons with an energy spread $\Delta E/E$ is thus

$$\frac{\pi \Delta E}{E} \frac{1 + 2\alpha}{(1 + \alpha)^2} \text{ steradians} .$$

The highest solid angle is encountered at low energies and is less than 0.25% of the sphere for an energy spread of 1%. From this point of view, the flat, double-focusing instrument may conveniently be used even at the lowest energies. The spectrometer should in practice be worked at a higher solid angle than that defined by the initial directions of the electrons in order to allow for multiple scattering. The maximum backward angle ψ_0 of the secondary photons is approximately given by

$$\tfrac{1}{2}\psi_0 \simeq \tan(\tfrac{1}{2}\psi_0) = (1 + \alpha)\varphi_0 = \sqrt{(\Delta E/E)(1 + 2\alpha)} .$$

Still taking $\Delta E/E = 10^{-2}$, we obtain $\psi_0 = 0.2$ at low energies, $\psi_0 = 0.45$ at 1 MeV, and $\psi_0 = 1.3$ at 10 MeV. The detector for the gamma rays cannot, of course, utilize the whole region $0 < \psi < \psi_0$, since the direct beam has to be avoided. The area of this crystal should accordingly be large compared to the unused area of the beam itself. It is very fortunate therefore that the angles ψ_0 required are rather large, so the gamma detector may be located at a reasonable distance from the foil. As the flat spectrometer allows the use of an extended source, it is advantageous to arrange the detector system in a way shown in fig. 11. The actual line shape of the set-up is obtained by mathematical folding of the instrument window curve with the rectangular Compton electron distribution and the energy loss distribution. These operations tend to shift the centroid of the line towards lower energies and it will be necessary to make a detailed analysis of these factors in order to obtain the best determination of energies.

The energy of the back-scattered gamma ray is $\frac{1}{3}mc^2$ at $\alpha = 1$ and approaches $\frac{1}{2}mc^2$ at higher quantum energies. This is a fortunate situation since it allows a high and constant detector efficiency. Apart from a possible small variation of this efficiency, the sensitivity of the instrument would be computable from the Klein-Nishina formula which must be considered a very dependable basis for intensity measurements.

1.7. TARGET CONSIDERATION

For various reasons, the flux of a reactor is not constant in time. Thus it is necessary to monitor continuously the strength of the target. This is not satisfactorily done by measuring the flux of the gamma beam, since this would yield a contribution from the induced radioactivity which does not follow strictly the variations of the neutron flux. Probably the best solution of this problem has been realized by Rose *et al.*[10])

TABLE 2

Comparison of the properties of gamma-ray spectrometers working with an extended source. The efficiencies are the number of counts at line maximum per photon emitted from the source inside the reactor

Spectrometer type	Energy MeV	Total efficiency	Resolution $\Delta E/E$ (%)
Double flat crystal, 2.5 cm calcite (Knowles)	0.1	0.5×10^{-10}	0.04
	1.0	3.0×10^{-10}	0.4
	2.0	1.0×10^{-10}	0.8
Semicircular pair spectrometer (Kinsey and Bartholomew)	2.0	$< 2 \times 10^{-14}$ †	5.0
	4.0	1×10^{-13}	2.5
	10	2×10^{-12}	1.0
Compton spectrometer (Groshev *et al.*)	1.0	1.0×10^{-12} †	3.0
	2.0	1.3×10^{-12}	2.4
	10	4.0×10^{-12}	2.3
Double focusing spectrometer ($\varrho = 50$ cm)†† with the Compton coincidence arrangement due to Motz	1.0	1.0×10^{-12}	1.0
	4.0	2.7×10^{-12}	1.0
	10	5.0×10^{-12}	1.0
Double focusing spectrometer ($\varrho = 50$ cm)†† with photoelectric radiator	1.0	2×10^{-12}	0.5
	2.0	2×10^{-12}	0.5
	10	$\simeq 3 \times 10^{-12}$	0.5

† These efficiencies refer to a source-to-radiator distance of 6 m.

†† Since these two experimental arrangements have not yet been put to a practical test, the efficiencies had to be estimated. The Compton yield was computed for a foil of area 0.4×3 cm² and a thickness of 10 mg/cm² per MeV. The source-to-foil distance was 6 m. The back-scattering detector was assumed to be 50% efficient. The resulting line width was inferred from experience with a general purpose instrument in use at this institute.

In the photo-electric case the uranium foil has the area 0.4×3 cm² and a thickness of 5 mg/cm² per MeV. At 1–2 MeV it was assumed, on the basis of the results of Hultberg[42]), that the resultant angular distribution is constant within the bipartition cone[21]). At 10 MeV the actual photo-electron distribution is concentrated to such small angles that the electron scattering should dominate its width. An effective bipartition angle of 10° was assumed for this energy. The efficiencies refer to a singles experiment. If the X-ray coincidence method of Motz is introduced, these figures are reduced by a factor of 2 or more.

for use with the Argonne diffraction spectrometer. The target is placed in a through channel passing close to the reactor core. In this way the drawback of the spectrometer "seeing" the fuel elements is avoided. Through a collimator at the opposite end of the channel, a BF_3 counter monitors the flux of neutrons scattered from the target.

Especially with the even Z elements, several isotopes contribute to the prompt gamma spectrum if the natural element is used. It is essential to have some method of assigning each transition to the decay of a definite isotope. Since the isotopes may have very different cross-sections and Q-values, an identification will frequently be possible on energy or intensity arguments, but separated isotopes will probably have to be used in many cases.

In the construction of an efficient internal target, the following factors have to be taken into account. High specific activity is desirable because of the attenuation of the gamma beam in the target itself and the production of degenerated quanta, which cause a continuous background. In order to achieve a high specific activity everywhere in the source, it should preferably consist of an array of plates

[42]) S. Hultberg Arkiv, Fysik **9** (1955) 245.

perpendicular to the channel direction. The plate thickness should be of the order of the mean neutron range and the distance between the units should be chosen large in order to reduce "shadowing" effects. Such an arrangement was used by Motz[19]) in an investigation of Cd.

nucleus is radioactive, some daughter gamma ray with known intensity may be present in the capture spectrum and provide normalization. Finally, the source under investigation may be mixed in known proportions with an isotope of simple capture decay, for instance H^1 which

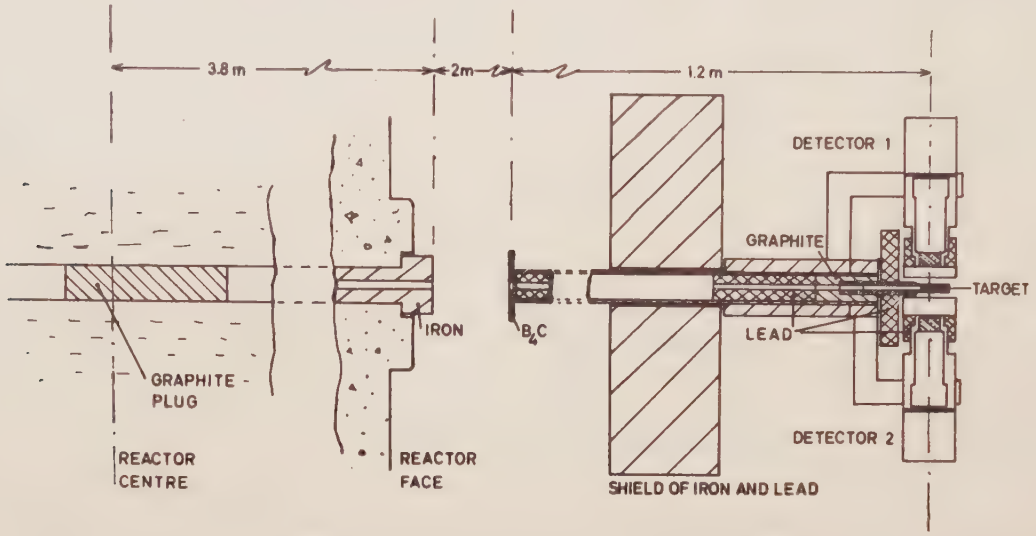

Fig. 15. Set-up for (γ, γ) angular correlation from G. Trumpy, Jener Publications **13** (Oslo, 1957)).

2. Construction of Level Schemes

2.1. GENERAL CONSIDERATIONS

Unlike radioactive decay where part of the disintegration energy escapes unobservably, the transition between the capturing level and the ground state proceeds mainly by gamma radiation. The relation $\Sigma E_\nu = Q$ is therefore valid for each cascade of gamma rays E_ν following the capture and Q is generally known. The intensities, I_ν, expressed as the number of quanta per capture, should yield $\Sigma I_\nu = 0$ for the intermediary states and $\Sigma I_\nu = 1$ for the ground state. Isomeric states which decay partly by β-emission are of course exceptions. Given a capture spectrum with its relative intensities, I'_ν, there are three methods of normalizing these to obtain I_ν. The normalization constant C may be taken from $\Sigma E_\nu C I'_\nu = Q$. This equation expresses the fact that the probable energy released in a decay must equal the energy actually available. This method is applicable to an unresolved spectrum if the sum is substituted by an integral. If the product emits only one gamma ray. A knowledge of the relative cross-sections is then sufficient for conversion to absolute intensities.

Whether the above energy and intensity considerations leads to a unique decay scheme depends on the accuracy of the measurements. In any case, however, the pattern of transitions may always be reversed. It is therefore necessary to make use of additional level data. Such information may often be had from other fields. For instance, one or more levels may be known from radioactive decay, inelastic neutron scattering, or from charged particle reactions. The position of isomeric states might also be known, although no systematic investigation of the isomers excited by (n,γ) reaction seems to be available at present.

2.2. COINCIDENCES

If the target is located in an external beam, counters may be placed sufficiently close to the target to make possible coincidence measurements. Fig. 15 shows the set-up of the (γ,γ)

experiments of Trumphy[24]). It appears from this investigation that difficulties arise which are not usually met with in radioactive work. Scattered neutrons which are captured in one of the phosphors yield coincident quanta which may be registered by the detectors. Pair

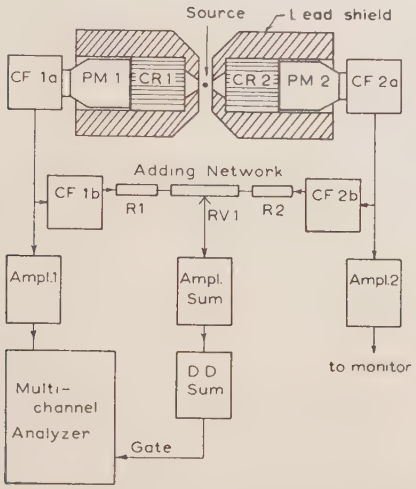

Fig. 16. Sum coincidence circuits (from A. M. Hoogenboom, Nuclear Instruments 3 (1958) 57).

created positrons annihilate producing coincident radiation. The crystals may not be taken as close to the source as in radioactive work because of the space taken up by the beam and the neutron shields. However, coincidences between the highest energy transition and the strong low energy lines were easily carried out.

Hoogenboom[25]) has recently described a new method for (γ,γ) coincidences which effectively improves the resolution of the NaI scintillator and removes the Compton distribution. The technique is especially useful in cases of transitions between a definite capturing state and the ground state. The principle of the arrangement is shown in fig. 16. The pulses from the two channels are added and fed into a differential discriminator, which selects pulses corresponding to a direct transition between the extreme levels. These pulses are used to gate the multichannel analyzer. As a result, one obtains the spectrum only of those cascade gamma rays which have spent all their energy in the detectors. If one component of the cascade has lost appreciable energy in scattering within the source or has not been fully absorbed in the crystal, the event does not contribute to the spectrum. The coincidence resolution of this set-up is rather poor ($\approx 3\ \mu$ sec) but may be improved by including a fast coincidence cirquit between CF 1 a and CF 2 a. This also leads to the exclusion of events in which the total decay energy Q has been absorbed in one detector only, i.e. the sum peak is eliminated. The spectrum registered by the kicksorter does not reflect the true gamma intensities. Apart from the normal variation of the photo-peak efficiency ε with energy, the detection of cascades of two gamma rays is favoured over that of cascades of higher multiplicity by a factor of $\simeq 1/\Omega\varepsilon$ or more. Comparison of the sum-coincidence spectrum with a singles spectrum will therefore disclose which pairs of gamma rays form a cascade, although the order in which they are emitted will be unknown.

The above scheme may be extended by adding a third counter in a similar way, in which case no single or two-stage decay are observed, but only cascades of higher multiplicity.

The method is readily adapted for angular correlation work. On the whole, it seems to be a powerful tool which no doubt will find use in investigations of (n,γ) reactions.

In complicated spectra, conversion electron coincidences may be required to establish relations between low energy lines. Especially since there is no coincident beta background, the use of this method is conceivable at least with the isotopes of high cross-sections.

2.3. SPINS AND MULTIPOLARITIES

The spin of the target nucleus is usually well known. This generally leaves two possibilities for the spin of the capture state. Usually both spins will be present in an unknown mixture. The ground state spin of the compound nucleus, usually radioactive, may be known from atomic beam resonance methods, from its radioactive decay, or from nuclear reactions. Experiments to determine the spin of intermediate states may

[24]) G. Trumpy, Jener Publications **13** (Oslo, 1957).
[25]) A. M. Hoogenboom, Nuclear Instruments **3** (1958) 57.

be carried out by the indirect method involving multipolarities or more directly by means of (γ,γ) angular correlation.

Some difficulties with (γ,γ)-coincidences have been mentioned in the preceeding section. With the thick targets sometimes necessary for intensity reasons, corrections have to be applied for the dependence of gamma ray attenuation on the correlation angle. Trumpy[24]) has discussed the sources of error in detail and has obtained definite spin sequences for several cascades.

After neutron capture, the compound system is to some extent aligned with the spin of the neutron. One might expect that some azimuthal unsymmetry would be observed in the emission of capture gamma rays from nuclei exposed to polarized neutrons. As has been shown by Wolfenstein[30]), the vanishing orbital angular momentum of the neutron implies an isotropic distribution of capture gamma rays. On the other hand, the radiation is circularly polarized[32]) to a degree depending on the spin of the target nucleus, the spin of the capture state, and the multipole order of the gamma ray. Using a neutron beam, polarized by attenuation in magnetic iron, Trumpy[24,31]) has confirmed this fact experimentally by observing the capture gamma rays through magnetic absorbers which could determine the sense and percentage of circular polarization. Although the observed transmission asymmetry was very small ($\simeq 1:10^4$), conclusions could be drawn about spins in a few cases. In view of the large experimental difficulties, the use of this method is restricted to levels fed by prominent transitions.

In cases of high cross-section, it is possible to produce, in an external neutron beam, sufficient specific activity for studying internal conversion of capture gamma rays. Since this method requires very small quantities of target material, separated isotopes can always be used. Gamma ray and conversion line intensities together yield relative conversion coefficients which carry much multipolarity information, especially at low energies. Low energy lines from a few elements have been measured by Hibdon and Muehlhause[28]) by means of a semicircular spectrograph. Fig. 17 shows a conversion spectrum of Cd, recorded by Motz[19]) with his lens spectrometer. The conversion spectra of many isotopes have the desirable feature of being free of continuous beta rays. The background level is then mainly set by the possibilities of shielding against scattered radiation.

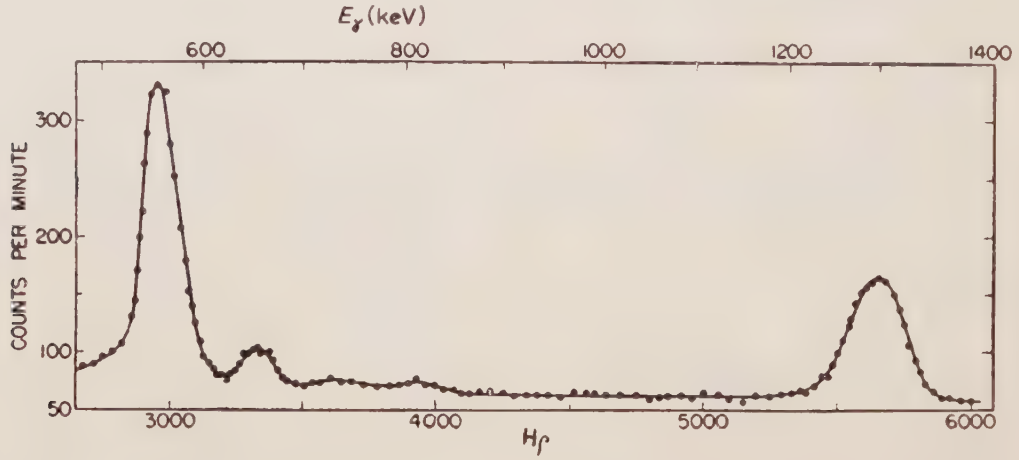

Fig. 17. Internal conversion spectrum of Cd (from H. T. Motz, Phys. Rev. **104** (1956) 1353).

The coefficient of internal pair production increases with energy, contrary to the internal conversion coefficient, and does not depend

[28]) C. T. Hibdon and C. O. Muehlhause, Phys. Rev. **83** (1951) 235; **87** (1952) 222.

[30]) L. Wolfenstein, Phys. Rev. **75** (1949) 1664.

[31]) G. Trumpy, Nuclear Physics **2** (1957) 664.

[32]) L. C. Biederharn, M. E. Rose and G. B. Arfken, Phys. Rev. **83** (1951) 683.

strongly on Z. It may be experimentally obtained by comparing the area of the positron distribution to that of some known conversion line or beta continuum. According to the calculations of Rose[29]), the E1 coefficient, which is the highest one, rises from 10^{-3} at 2.5 MeV to 3×10^{-3} at 10 MeV. It is of some interest to compare the counting rate of a pair production spectrum with that of the corresponding conversion line that is recorded in a typical magnetic spectrometer ($\Delta B\varrho/B\varrho \simeq 10^{-2}$). The pair production coefficients have only to be reduced by a factor $\simeq 10^{-2}$ in order to be directly comparable to the internal conversion coefficients. At 2.5 MeV, $Z = 33$, and E1 multipolarity the counting rate of the conversion line is thus estimated to be higher by a factor of 3 and at 4 MeV the heights should be about equal. For higher Z or higher multipole order, internal conversion is more favourable at these energies, whereas for $h\nu > 4$ MeV and E1 multipolarity pair production dominates. With either of these internal effects, the dependence of angular momentum gradually vanishes at high energies. The ratio of internal pairs E1/E2, for instance, becomes 1.7 at 2.5 MeV and 1.23 at 10 MeV. A corresponding figure for internal conversion is 1.45 at 2.5 MeV and $Z = 33$. A disadvantage with the pair production method is, of course, that the effect of stray background and the contribution from other transitions are not as easily taken into account as with internal conversion. The angular correlation of pairs depends more strongly on multipolarity, but the experimental difficulties involved seem correspondingly larger. On the whole, the problem of multipolarity assignment for high energy capture gamma rays seems a most difficult one.

3. Transition Lifetimes

When the intensities of the various transitions depopulating a definite level have been measured, it is sufficient to know the radiative lifetime ($\tau = \hbar/\Gamma_\gamma$) of the level in order to compute the partial lifetimes of the transitions. Neutron spectroscopy[33]) provides values for the radiation widths (Γ_γ) of the various resonances and occasionally their spins. With nuclei exposed to the mainly thermal neutrons of a reactor, absorption will take place mostly in the $1/v$ region, where several resonances may contribute to the cross section. It is thus not possible to assign unique properties to the capture level, although the lowest resonance (of positive or negative energy) usually gives the strongest contribution. Even if the exact population of the capture states is not known, a reasonably good value of Γ_γ may still be obtained, since this quantity does not differ much between resonances of the same isotope. A more serious obstacle to the interpretation of transition lifetimes is the uncomplete knowledge of spin, which may take either of the values $I_1 \pm \frac{1}{2}$. This generally leads to multipole mixing of the transitions depopulating the capture levels.

The contribution from a positive energy resonance may possibly be distinguished from that of a negative energy resonance by enclosing the target in a capsule which strongly absorbs thermal neutrons. The observed capture gamma spectrum would then contain a larger contribution from the positive energy state, because of the enrichment in neutrons falling under the resonance peak.

Investigation of the gross features of the decay of a definite resonant state may be carried out by the use of a neutron monochromator. Because of the resulting low intensity the high efficiency of scintillation techniques is essential.

Wood[34]) studied the production rate of isomers resulting from the decay of a particular capture state. This method should be very sensitive to the spin of the resonance but can only give a partial picture of the relative population of lower states.

Scintillation spectra from neutron capture in various resonances have been taken by Landon and Rae[35]) and by Fenstermacher *et al.*[36]). In

[29]) M. E. Rose, Phys. Rev. **76** (1949) 678.

[33]) J. Rainwater, Encyclopedia of Physics, S. Flügge, ed. **40** (1957) 373.

[34]) R. E. Wood, Phys. Rev. **95** (1954) 453.

[35]) H. H. Landon and E. R. Rae, Phys. Rev. **107** (1957) 1333.

[36]) Fenstermacher, Bennett, Walters, Bockelman and Schultz, Phys. Rev. **107** (1957) 1650.

order to make possible a more detailed investigation of the gamma ray branching from the capture states, Kennett *et al.*[37]) recently used a scheme in which low energy transitions were detected in coincidence with the group of direct gamma transitions to the low lying states. In this way, the coincidence counting rates of the various low energy gamma rays could be taken as measures of the intensities of the direct capture transitions, which could not be resolved in a singles spectrum. Comparison with the corresponding branching ratios for thermal neutrons disclosed the contribution of a negative energy resonance.

Lifetime measurements of bound states present greater difficulties. Current methods of delayed coincidences should, of course, be applicable in their usual lifetime range. However, some of the levels excited will be at several MeV and consequently possess very short lifetimes. In fact, near the binding energy their widths should approach the value found for capture resonances. These widths centre around 0.1 eV[33]) and thus correspond to lifetimes in the region of 10^{-14} sec, i.e. the region in which the resonant scattering method[38,39]) is most easily applied.

The cross-section for resonant absorption of gamma radiation is

$$\sigma(E) = \frac{2J+1}{2I+1} \cdot \frac{2\pi\,\lambda^2}{1 + \left(\frac{E - E_r}{\frac{1}{2}\Gamma}\right)^2}$$

where E and λ are the energy and wave-length of the incident radiation. E_r is the energy of the level and Γ its total width. J and I are the spins of the level E_r and of the ground state respectively. Γ may obviously be determined by means of some measure of the area of the resonance curve. The re-emitted photons may easily be distinguished from Compton scattered photons on the basis of energy discrimination, if the observation is made at large angles ($> 90°$). Fortunately the cross-sections of competing elastic scattering processes assume their lowest values at these angles. Thus, for $E = E_r$ the cross-section for resonant scattering exceeds that of ordinary elastic scattering by several orders of magnitude. However, the thermal motion of the target nuclei introduces a random Doppler shift which has the effect of increasing the width of the macroscopical resonance curve and reducing its peak value correspondingly.

The main difficulty with this method, however, is to provide a gamma ray of the right energy for exciting the level. In the rather small number of cases where a resonant scattering effect has actually been observed[39]), the gamma ray emitted in the decay of the same level is used for the excitation. The energy available for the excitation is, however, then only $E_r - E_r^2/Mc^2$, where M is the mass of the nucleus, since part of the level energy is imparted to the nucleus as recoil energy. Several workers have therefore attempted to restore the resonance condition by opposing the recoil motion to some extent. This has been achieved by giving the source a high velocity by means of a rotor or by the use of thermal agitation. In an external neutron beam the latter method could be used but would yield inconveniently weak sources. With gamma rays following a nuclear reaction, the momentum of the incoming particle is often sufficient to restore the recoil energy loss. The momentum carried by neutrons in the eV range is however inadequite. Another possibility is to have a preceeding photon imparting the necessary recoil velocity to the nucleus. Since the decay of a bound level, excited in an (n,γ) reaction has a high probability of being preceeded by the emission of a gamma ray of higher energy, it seems possible to extend this method to this field. The limitation of all these techniques is that the product isotope has to be stable and available as a scatterer in at least gram quantities.

In a scheme first proposed by Cormack[40]), the quanta from a suitable transition are degraded by Compton scattering through a definite angle

[37]) T. J. Kennett, L. M. Bollinger and R. T. Carpenter, Phys. Rev. Letters **1** (1958) 76.

[38]) K. G. Malmfors, Beta and Gamma Ray Spectroscopy, K. Siegbahn, ed. (Amsterdam, 1955) 521.

[39]) F. R. Metzger, Proc. Rehovoth Conf. Nucl. Structure, H. J. Lipkin, ed. (Amsterdam, 1958) 560.

[40]) A. M. Cormack, Phys. Rev. **96** (1954) 716.

to fit the energy of the level to be excited. In principle any level decaying to the ground state of a stable nucleus may be excited in this way. With the source strengths obtainable in a pile, this method should be practicable in many cases. The counting rates will be very low, however, if reasonably narrow lines are to be obtained. The success of the experiment is thus determined by the suppression of general background that can be achieved.

With all methods of resonant scattering, a knowledge of the spectral shape of the exciting line is necessary for the calculation of Γ. In an alternative method due to Metzger[41]) the attenuation in an absorber is measured and the resonant scattering process serves as a detector.

The author wishes to thank Professor K. Siegbahn for following the progress of this work with such encouraging interest. My thanks are further expressed to Dr. O. Beckman for illuminating discussion on the crystal diffraction methods and to Dr. J. Hamilton for correcting the English of the manuscript.

[41]) F. R. Metzger, Phys. Rev. **103** (1956) 983.

NUCLEAR INSTRUMENTS AND METHODS 4 (1959) 26–29; NORTH-HOLLAND PUBLISHING CO.

9-INCH LIQUID HYDROGEN BUBBLE CHAMBER IN A PULSED MAGNETIC FIELD

D. C. COLLEY, J. B. KINSON and L. RIDDIFORD

Department of Physics, University of Birmingham

Received 1 November 1958

The construction and operation of a liquid hydrogen bubble chamber nine inches in diameter is described. It is expanded in the liquid phase by a stainless steel bellows and the construction is such that it may be used in an intense pulsed magnetic field. The latter is provided by an air-cored solenoid.

1. Introduction

The liquid hydrogen bubble chamber[1]) is now well established as a research tool in high energy physics[2,3]). The density of the liquid is about 30 times that of the gas usually employed in diffusion cloud chambers[4]). Further, there is no limit to the sensitive depth as with diffusion chambers. Multiple scattering is still small except for particles of very low energy. We have constructed a chamber 9 inches in diameter and 4 inches deep which uses a liquid expansion system. It operates in an intense pulsed magnetic field produced by an air-cored solenoid. The assembly is light and compact.

2. The Chamber

Fig. 1 is a line drawing and fig. 2 a photograph of the apparatus. The chamber is a composite structure. The pressure is maintained within a 0.1 inch thick stainless steel cyclinder (1) lightly flanged at the ends. Small V-grooves machined two in each end locate 1 mm diameter lead gaskets which seal the cylinder to $\frac{7}{8}$ inch thick end windows of toughened glass (2). The gaskets are compressed by 36 0.25-inch diameter stainless steel bolts passing through clamping rings on the glass. The space between each pair is usually evacuated. Within the cylinder is another of 0.125 inch thick oxygen-free copper (3), to minimize temperature gradients in the chamber. This is split in the vertical direction to prevent the substantial loss of liquid hydrogen which would otherwise occur as a result of eddy current losses due to the pulsed magnetic field. The clamping rings are also split. The cylinders are separated one from the other by a thin sheet of the plastic Mylar.

Expansion is achieved by means of a three-ply stainless steel bellows of mean diameter 4 inches and 5 inches long (4). This is immersed in a cylinder of freely boiling liquid hydrogen (5) supported from the top of the vacuum tank (6) and fed from the main liquid hydrogen container (7). It is driven by a control rod operated by an external air-cylinder (8). The large bellows is connected to the chamber by a tellurium-copper tube of $\frac{7}{8}$ inch inside diameter silver-soldered to both the chamber and its copper liner. The small bellows (9) is inserted for assembly purposes. Two 25-watt heaters embedded in a copper-block (10) attached to the expansion pipe are used to increase the chamber temperature appropriately.

The bubble chamber is supported by three 0.25 inch diameter stainless steel rods from a liquid hydrogen container of capacity about 20 litres (7). The hydrogen level in the container is monitored by a capacitor level indicator[5]). The

[1]) D. Parmentier and A. J. Schwemim, Rev. Sci. Instr. **26** (1955) 954.

[2]) L. Baggett, University of California, Radiation Laboratory Report UCRL 8302.

[3]) F. Eisler *et al.*, Columbia University Report Nevis-70, R-210.

[4]) A. P. Batson, P. N. Cooper and L. Riddiford, J. Sci. Instr. **33** (1956) 302.

[5]) W. E. Williams and E. Maxwell, Rev. Sci. Instr. **25** (1954) 111.

liquid nitrogen container (11), to which is attached the radiation shield (12), is of similar capacity. Both containers are suspended from the top plate of the vacuum chamber (6) by thin-walled tubes. The chamber is evacuated by

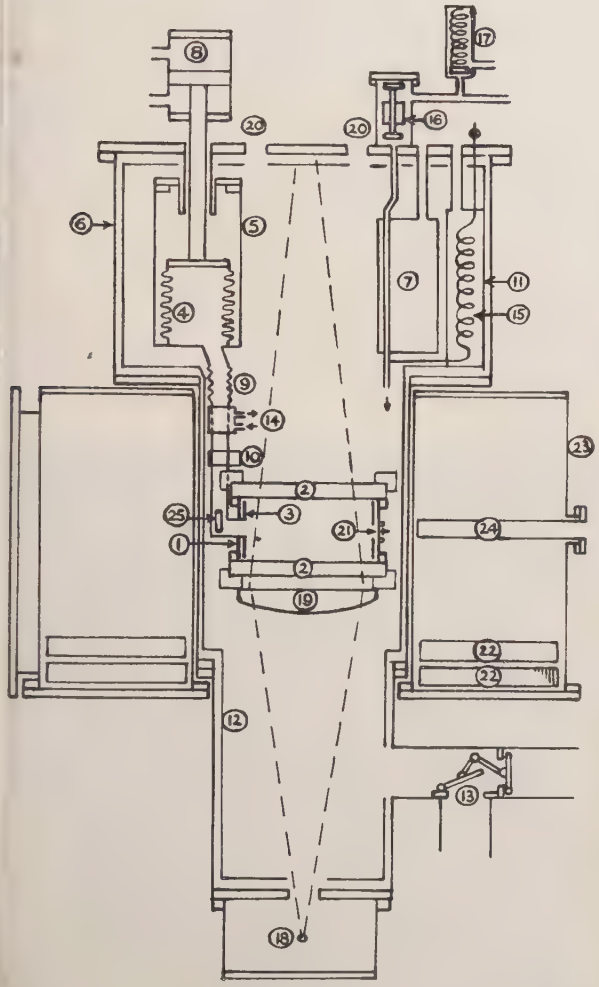

Fig. 1. Line drawing of chamber and magnet assembly.

pressure gas in either the bellows case (5) or the condenser (14) which is also fed from the hydrogen container (7). The gas is pre-cooled by a heat exchanger (15) in the nitrogen container. Just prior to an expansion the filling line is sealed off from the gas supply by the electromagnetic valve (16). The chamber is protected against pressure surges by the spring-loaded valve (17).

Illumination is by a xenon-filled flash tube (18) (spark 0.5 cm long) located in a box bolted

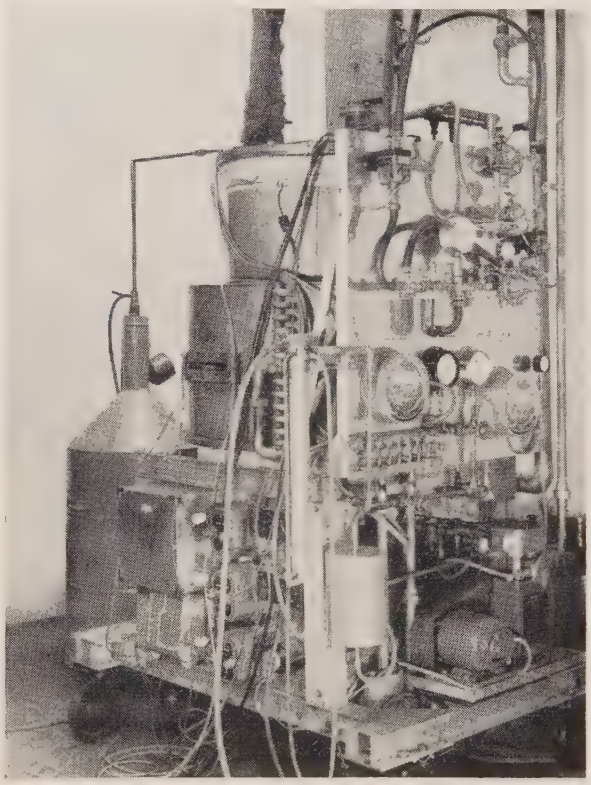

Fig. 2. General view of the apparatus.

a 2-inch diffusion pump at the top of which is a safety valve (13). This is normally sealed by atmospheric pressure, but in the event of window failure a hydrogen pressure in excess of one atmosphere would isolate the pump and connect the chamber to a 2-inch pipe (14) passing through the roof of the building. Hydrogen evaporating from the storage reservoir is normally conducted through the roof. The bubble chamber is filled by condensing high

to the bottom of the vacuum chamber. A plano-convex lens (19) 9.5 inches in diameter and of 16-inch focal length, attached to the bottom clamping ring of the bubble chamber, images this source between the viewing windows (20). The cameras thus see mainly the light scattered from bubbles. The transducer for observing the pressure pulse in the chamber is a capacitor[6])

[6]) W. I. Linlor, Q. A. Kerns and J. W. Mark, Rev. Sci. Instr. 28 (1957) 535.

connected in a radio-frequency bridge circuit. The elastic diaphragm (21) is a 0.025 inch thick stainless steel disc silver-soldered to the chamber wall. It is insulated from the rigid element by an annulus of 0.003 inch Mylar.

3. Magnet and Hydrogen Supply

A 500 V, 1000 A generator was available to excite the magnet. On pulsed operation it would deliver about 1000 kVA. The air-cored solenoid consists of 860 turns of 1.25 × 0.10 inch copper strip disposed in 12 layers (22) in a sealed vessel (23) to permit cooling. The re-entrant cavity (24) in the vessel is a beam entry port. Cooling is by transformer oil circulated by a centrifugal pump of nominal capacity about 1800 GPH through an external water-cooled heat exchanger. Insulation between turns is by 0.010 inch Presspahn tape and between layers by bakelite webs shaped to permit the oil flow. Strips of an oil-resistant plastic sponge confine the flow to the appropriate channels.

The magnet is excited in the same way as was that of the diffusion cloud chamber[4]), and the field is monitored by the same electronic integrator[4]). A current of 900 A provides an intensity of 15 kilogauss. The pulse length is about two seconds. For a pulse repetition rate of 8 per minute and this field the mean power dissipation is about 50 kilowatt and the operating temperature about 70° C†. The entire assembly weights about two tons and is mounted on the trolley evident in fig. 2.

Liquid hydrogen is supplied by a liquefier manufactured by S.E.C.M.E.R. (Grenoble). The daily output is 70–100 litres. It is stored and transferred to the bubble chamber in 50-litre dewars. The static heat input to the chamber assembly is about 20 watts, mainly down the expansion control rod, the corresponding hydrogen loss being 2 litres per hour. The dynamic loss under normal conditions (§4) is also about 2 litres per hour, and in addition the heater power is about 10 watts. About 50 litres of liquid hydrogen are required to cool and fill the chamber.

† Operation at higher power would require a lower repetition rate.

4. Operation

Fig. 3 is a block diagram of the control system. The sequence timer provides the coarse controls necessary for magnet switching and a signal to initiate the expansion at the top of the

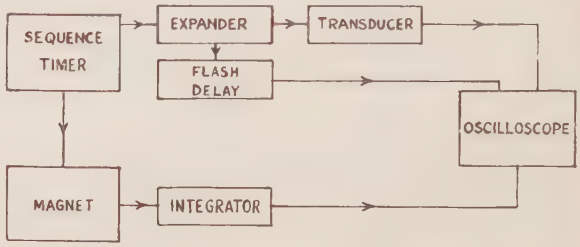

Fig. 3. Block diagram of control system.

magnet pulse. The cylinder for the control rod uses compressed air at 150 PSIG. The pressure is removed and re-applied at the appropriate

Fig. 4. Typical photograph of electron tracks from a ^{60}Co source.

instants by a $\frac{3}{4}$ inch Barksdale valve. Expansion takes place in about 10 milliseconds, the bubble growth time is about 10 milliseconds, and recompression is achieved in a further 10 milliseconds. A volume change of 1.5% is sufficient. The system behaves as if pressure

defined for there appears to be no self-pressurization after 0.25 seconds, the longest interval used.

Chamber temperature is recorded by a vapour pressure thermometer (25) attached to the base of the expansion line. Tracks are obtained at temperatures corresponding to the pressure range 55–80 PSIG, the bubble density increasing with temperature. The chamber starting pressure is maintained a little above the vapour pressure. Fig. 4 is a photograph of typical electron tracks produced by a 5 millicurie ^{60}Co source and curled up in the 15 kilogauss field. The pulse repetition rate during the run was 8 per minute. At the higher temperatures or for extended expansions this would need to be lowered to prevent the formation of a bubble in the chamber. The vapour pressure thermometer reads about 5 PSI lower when the chamber is expanding. The heat input from the magnet is about 10 watts.

Acknowledgments

We are grateful to Professor P. B. Moon for his encouragement in the work. It would not have been possible without the excellent technical assistance of Mr. C. Barrow and the steady supply of liquid hydrogen by Mr. G. Guest. Mr. A. W. Williams and Mr. J. G. Hill have helped with the apparatus. The Cryogenic Data Book of the University of California, Radiation Laboratory Report UCRL 3421, has proved invaluable.

NUCLEAR INSTRUMENTS AND METHODS 4 (1959) 30–35; NORTH-HOLLAND PUBLISHING CO.

AN ENERGY SENSITIVE ČERENKOV DETECTOR WITH IMPROVED OPTICAL FOCUSSING

M. HUQ† and G. W. HUTCHINSON

Physics Department, University of Birmingham

Received 15 November 1958

A Čerenkov detector is described having improved energy selecting properties for protons of energy about 900 MeV. Good focussing from an extended area of a spherical reflecting surface has been realised by minimising astigmatism in the optical system. The light is produced in a liquid radiator and detected by photomultipliers used in coincidence. The energy resolution is largely determined by the dimensions of the optical stop used. It is about ± 4% in the instrument constructed.

Several authors have described Čerenkov detectors in which the light from individual incident particles was focussed by an optical system so that the position of the image could be used to define their velocity. The resolving power of these detectors is limited partly by the slowing down and scattering of the particles in the radiator, partly by optical dispersion and partly by imperfections of their geometrical focussing properties. It is with an improvement in the latter that we are here concerned.

A system using a cone shaped radiator was proposed by Getting (1947)[1]) and used by Dicke (1947)[2]) in an unsuccessful attempt to detect cosmic ray particles. This system can be made to give a point focus for the light produced by particles of a particular velocity travelling along the axis of the cone. It does not, however, give a sharp focus for particles travelling along paths either at an angle to the axis or displaced from it (Huq, 1958)[3]) and cannot therefore be used to detect particles in a beam of finite width comparable with the dimensions of the apparatus. This difficulty is general to all systems using an optical system with only cylindrical symmetry about the beam axis.

Detectors in which the optical elements have spherical symmetry can give first order focussing for light produced over a finite area perpendicular to the axis. Marshall (1951)[4]) and Mather and Martinelli (1953)[5]) have used detectors of this type in which the Čerenkov light was produced in a solid cylinder ending in a spherical surface.

The optical behaviour of these detectors may be most easily visualised by considering the light produced by particles of a monoenergetic parallel beam to strike the refracting surface as if coming from an annular source at infinity. A real annular image of this source is produced, but it is astigmatic because of the finite angle at which the light strikes the focussing surface. If the particles are all near the axis of the system, a sharp ring focus is obtained in the plane in which the astigmatism is circumferential, but when the beam of particles has finite width most of the light rays are skew to the axis and the focus obtainable becomes progressively worse as the beam diameter becomes significant in comparison to the focal length of the optical system. Precise velocity selection therefore requires a rather large optical system whose size increases in proportion to the acceptable beam diameter.

† Now at the Physics Department, University of Malaya, Singapore.

[1]) I. A. Getting, Phys. Rev. **71** (1947) 123.
[2]) R. H. Dicke, Phys. Rev. **71** (1947) 737.
[3]) M. Huq, Nuclear Instruments **2** (1958) 342.
[4]) J. Marshall, Phys. Rev. **81** (1951) 275; **86** (1952) 685.
[5]) J. W. Mather and E. A. Martinelli, Phys. Rev. **92** (1953) 780.

Baldwin, Caldwell, Hamilton, Osborne and Ritson (1957)[6]) have further improved the focussing in gas-filled detectors by applying the techniques developed for large angle astronomical telescopes. Gas detectors can be used conveniently when the velocity of the particles is very close to that of light and sufficiently high refractive indices can be obtained in gasses at reasonable pressures.

The detector described in this paper was designed to detect particles with a good degree of velocity selection, when their velocity is too low for the convenient use of gas radiators. The width of the beam accepted was a large fraction of the width of the detector. Good focussing conditions with such a beam width was achieved by producing a non-astigmatic image by reflection at a spherical concave surface so placed that all the light is incident on it nearly normally.

1. Description

1.1 THE OPTICAL SYSTEM

An axial section of the detector is shown in fig. 1. The radiator is a liquid filling the space between the front silvered mirrors C and M. C is spherical and concave and M is plane. Each mirror is 6 inches in diameter. They are held in rubber O-ring seals in a brass tube. Their distance apart is adjustable by means of a screw thread cut on part of the length of the inside of the tube. Suitable filling holes with light-tight stoppers are provided in the sides.

Particles to be detected travel from the left. The Čerenkov light that they produce in the liquid is, first reflected from M. It is then incident on C in directions such that it appears to have come from a region to the right of M, defined by the image in M of the radiating portion of the liquid. The radius of curvature of C is so arranged that this region is as close as possible to its centre of curvature. The effect is then as though the light rays came from an annular source at infinity seen through a stop placed near the plane of the centre of curvature of C. Under these conditions they come to a fairly sharp annular focus in a plane nearly coincident with that of M.

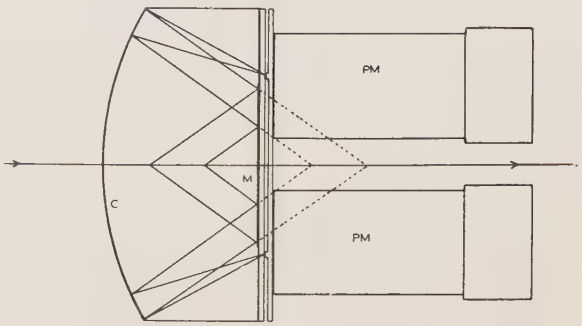

Fig. 1. Schematic Diagram: C and M = Curved and flat mirrors, PM = Photomultipliers.

An annular stop is placed in this focal plane and defines the limits of acceptance for the conical angle of the Čerenkov light relative to the axis of symmetry of the system. Photomultipliers are placed to the right of the stop so that each receives light passing through a segment of the annulus. A particle which produces Čerenkov light within the accepted cone is detected by coincident pulses from the multipliers.

The stop used consisted of a $\frac{1}{8}$ inch thick perspex disc, turned down to $\frac{1}{16}$ inch and blackened on one side except in the area of a ring of internal radius 4.25 cm and external radius 4.50 cm. This ring made optical contact with the back surface of mirror M. It defined an accepted Čerenkov angle, $\theta = 35° \pm \frac{1}{2}°$. The silvering on the front surface of M covered only the central portion to a radius of 4.0 cm.

1.2. THE RADIATING LIQUID

The desirable properties of the liquid radiator are:

(a) adjustable refractive index so as to produce Čerenkov light at 35° for any particle velocity selected within a reasonable range

(b) good optical transmission

(c) low optical dispersion

[6]) D. E. Baldwin, D. O. Caldwell, S. G. Hamilton, L. S. Osborne and D. M. Ritson, Proceedings of the Conference on Mesons and Recently Discovered Particles, Padova (September, 1957).

(d) low mean atomic number so as to minimise multiple Coulomb scattering

(e) low density to minimise the change of velocity of the particle in traversing the radiator.

Mixtures of water and glycerine were used. This gives a range of refractive indices of 1.33 to 1.47, and corresponds to a range of velocities $\beta = 0.918$ to $\beta = 0.825$; or for protons, to a range of kinetic energies $E = 1400$ MeV to $E = 730$ MeV.

Light from particles of "correct" velocity along the axis of the apparatus is accepted from a path length of about 4 cm. The number of Čerenkov photons emitted within the range of the spectral response of the photomultipliers is about 800. Therefore if the mean photo-electric efficiency is taken as 15%, the mean number of photo-electrons produced if all this light were collected would be about 130. For particles whose paths are parallel to the axis, but displaced from it the path length from which light is collected is progressively reduced as the displacement increases. There will be some loss of light because of imperfect optical transmission and reflection.

The path length, and thus the number of photo-electrons, would change in proportion to the linear dimensions of the whole apparatus. However in a larger apparatus, the increase in light collection would be offset by a reduction in energy resolution because of increased energy loss and multiple scattering. The dimensions chosen were a convenient compromise.

1.3. THE LIGHT COLLECTING SYSTEM

It is very desirable to use more than one photomultiplier in coincidence. This practically eliminates background counts due to photomultiplier noise and avoids counting particles of the wrong velocity which produce Čerenkov light in other parts of the apparatus than that intended as the radiator. The optimum number and disposition of the multipliers round the axis of the apparatus depends to some extent on the type of experiment for which the detector is to be used.

Fig. 2 shows the relative positions of the focal annulus and the stop for particles (a) travelling parallel to the axis with the accepted velocity, V_0, and - for particles whose velocities are different either in (b) direction or (c and d) in magnitude. If the annular stop is divided into three or more equal azimuthal sections and light is required to fall on all of them for a particle to be detected, then, the system will discriminate against variation either of the direction or magnitude of particle velocity. Provision is made for using the apparatus in this way with three 2″ diameter photomultipliers evenly spaced round the annulus.

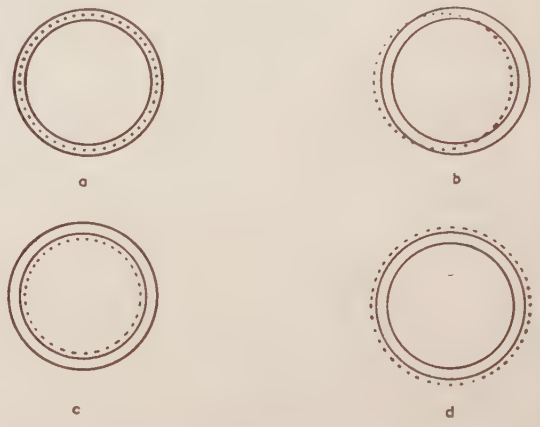

Fig. 2. Relative positions of annular stop (solid lines) and image of Čerenkov cone for: a. particles of correct velocity; b. particles whose velocity is wrong in direction; c. particles whose velocity is too small; d. particles whose velocity is too large.

If, however, light is only collected from two segments of the annulus, at opposite ends of a horizontal diameter, the apparatus will be sensitive to variation in the magnitude of the particle velocity and to variation of direction in the horizontal plane, but not very sensitive to variation fo direction in the vertical plane. This is desirable when the detector is used in scattering experiments carried out in the horizontal plane. Since it was intended for such experiments, the apparatus has been tested with two photomultipliers arranged in this way.

Light may be collected from the whole annulus by using suitably shaped perspex light guides, but sufficient light is collected by making

optical seals directly from the back of the perspex annulus to the ends of the photomultipliers. The photocathodes of two Dumont 6292 multipliers covered about 35% of the area of the annular stop. This method avoids the background of large, non-coincident pulses which may be produced by Čerenkov light from light guides. It also restricts the light collection to those parts of the annulus within about $\pm 30°$ of the horizontal azimuth, and this is a suitable limit for the type of velocity and direction discrimination desired.

The detector was normally used in coincidence with scintillation counters placed on its axis both in front of and behind it, so as to define the width of the accepted beam to a region of the counter in which the response was independent of the lateral position of the particle tracks.

2. Energy Resolution

The different factors affecting the resolution of the detector are shown in table 1, for the case of mono-energetic proton beams (900 MeV) with angular spread of $\pm \frac{1}{2}°$. The over-all resolution, obtained by taking arbitrarily a square root of the sum of squares of the individual contributions, is $\pm 3.6\%$. The resolution is mostly determined by the width of the annulus. This also largely determines the angular acceptance and thus the counting rate in a scattering experiment. The choice in the present case was made with this in mind.

TABLE 1

Origin of Contribution to total resolution	du/u
1. Basic Contribution due to width of the annulus (2.5 mm)	$\pm$ 2.42%
2. Angular spread among the protons in the beam ($\pm \frac{1}{2}°$)	$\pm$ 1.73%
3. Slowing down of the protons in the radiator	$\pm$ 0.60%
4. Multiple Coulomb Scattering	$\pm$ 0.93%
5. Optical dispersion	$\pm$ 1.76%
Estimated Overall Resolution	$\pm$ 3.6 %

3. Experimental Performance

The apparatus has been tested in the external proton beam produced from the Birmingham proton synchrotron by scattering out and subsequently focussing and collimating. The direction and position of the beam were defined by scintillation counters in front of and behind the detector. These remained fixed while the detector could be moved horizontally across the beam or rotated about vertical and horizontal axes passing through the radiating liquid. Double coincidences were formed between the two photomultipliers of the detector and also between the two scintillation counters, using conventional circuits of resolving time 10 mμsec. Four-fold coincidences were then formed by combining these outputs in a further coincidence.

The angular homogeneity of most of the proton trajectories in the beam as measured from the proton tracks in an emulsion plate exposed in the beam, was better than $\pm \frac{1}{2}°$, but there was a significant tail to the angular distribution through multiple scattering in the

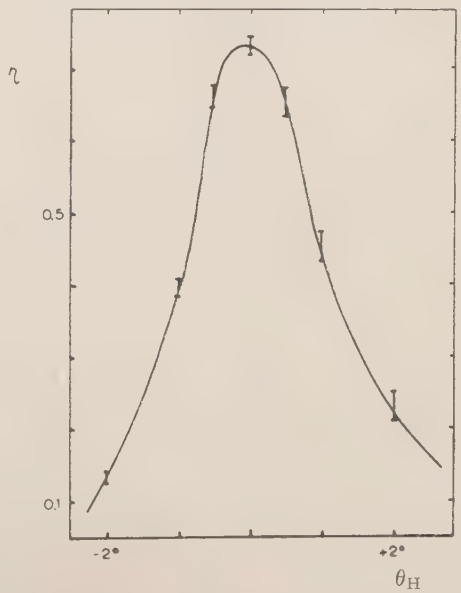

Fig. 3. Variation of efficiency η with horizontal direction θ_H of axis.

front scintillator and the walls of the collimators.

The efficiency, η, of the detector under these

conditions is defined as the ratio of the four-fold coincidence counting rate to the double-coincidence counting rate of the scintillation counters.

Fig. 3 shows the variation of η with the angle between the axis of the detector and the axis defined by the two scintillators, when the detector is rotated around a vertical axis

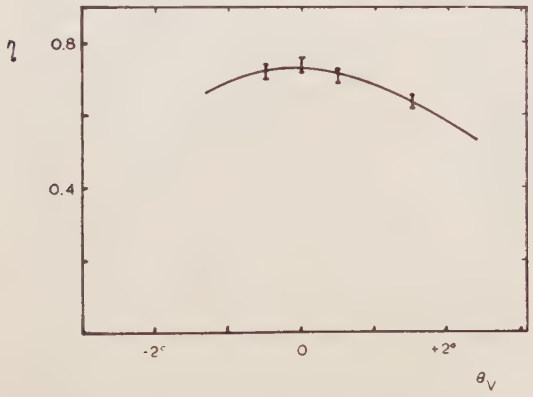

Fig. 4. Variation of efficiency η with vertical direction θ_V of axis.

passing through the centre of the effective volume of the radiator liquid. Fig. 4 shows the variation of η, due to a similar rotation of the detector around a horizontal axis. Fig. 5 shows the variation of η with the transverse displacement of the detector. Fig. 6 shows the variation of η with the mean energy of the beam. In this case the energy was varied by placing slabs of Cu in the beam at a large distance in front of the detector. It is to be expected that this will increase the spread of proton energies in the beam.

Figs. 3, 4 and 5 were obtained with beams of energy corresponding to the maximum of the curve of fig. 6, i.e. at 900 MeV, and fig. 6 was obtained with the position and orientation of the detector corresponding to peak efficiency as given by figs. 3, 4 and 5. The diameter of the scintillators was 1″.

The efficiency is not expected to reach 100% partly because of the Poisson distribution in the number of photoelectrons produced by any one proton, and partly because of the inhomogeneity of the proton beam both in energy and direction.

The angular acceptance shown in fig. 4 is, as expected, much larger than that of fig. 3. The flat response for $\pm$ 2 cm in the horizontal traverse of the detector (fig. 5), and the displacement between the points at which η is reduced to half its central value indicates the useful acceptance area of the detector. Taking into consideration the width of the scintillators,

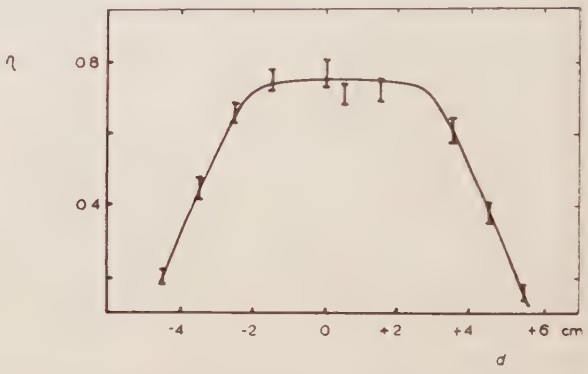

Fig. 5. Variation of efficiency η with horizontal transverse displacement d.

it appears that the response of the detector is nearly constant over most of the silvered area of the flat mirror.

The energy resolution experimentally obtained

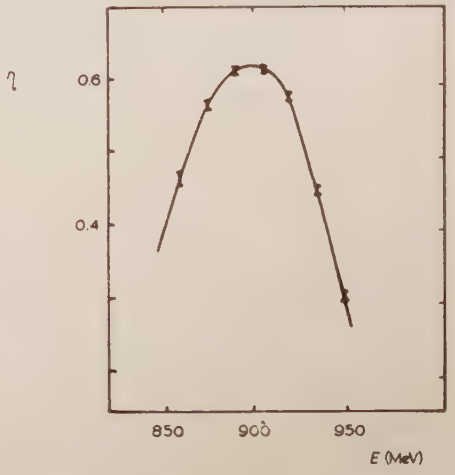

Fig. 6. Variation of efficiency η with proton energy E.

is $\pm$ 45 MeV (fig. 6), whereas the theoretical resolution is only $\pm$ 33 MeV. This discrepancy should be almost wholly accounted for by the energy spread in the beam, both inherent and

introduced by the considerable thickness of the absorbers. This statement is justified by the fact that the angular acceptance of the detector agrees very closely with the calculated value. The energy resolution corresponding to the observed horizontal angular acceptance (1.1°) is $\pm$ 34 MeV. An energy spread of $\pm$ 30 MeV in the beam would account for the discrepancy of the observed and calculated resolutions. According to Van der Raay (1957)[7]) a spread of $\pm$ 20 MeV is expected in the external synchrotron beam. A further spread is certainly introduced by the copper absorbers.

The apparatus has been used in experiments on the polarisation and angular distribution of protons scattered from carbon. Accounts of these are in course of publication.

Acknowledgments

We are grateful to Professor P. B. Moon and Professor O. R. Frisch for stimulating discussions during the design of the apparatus. One of us (M. Huq) wishes to thank the Government of East Pakistan and the University of Birmingham for Research Grants.

[7]) H. B. Van der Raay, Nuclear Instruments **1** (1957) 351.

NUCLEAR INSTRUMENTS AND METHODS 4 (1959) 36–43; NORTH-HOLLAND PUBLISHING CO.

IMPROVED CYCLOTRON PERFORMANCE FROM CONTROL OF INITIAL ION MOTION

A. H. MORTON and W. I. B. SMITH

Research School of Physical Sciences, The Australian National University, Canberra

Received 3 November 1958

Techniques have been developed to improve cyclotron beam characteristics by the use of slits near the ion source to obtain defined internal beams concentric with the cyclotron centre resulting in high extraction efficiencies, and monoenergetic external beams of small angular spread. The optics of the ion source and the use of focussing grids on early revolutions of the ions are discussed.

1. Introduction

The beam from a fixed frequency cyclotron usually has a wide spread in energy and a large angular divergence. These characteristics result principally from poor ion optics at injection into the cyclotron and from the spreading of the external beam caused by the fringing field of the guide field magnet. It is usual, due to the nature of the internal beam, that only about one-fith of the rotating beam at full energy in the machine can be extracted, and of this only a small portion can be usefully employed on a target after energy analysis. There appears to be no fundamental reason why this average performance should not be greatly improved. It is proposed to use the beam from an 8 MeV cyclotron for injection into the 10 GeV proton synchrotron with an air-cored magnet excited from a homopolar generator, which is under construction in Canberra[1]). As the proton synchrotron will only accept a monoenergetic beam of small divergence at injection, investigations were made towards achieving a well defined external beam from the cyclotron. A necessary condition is a well defined internal beam, and to this end measurements have been made on the optics of the ion source and on the effect of beam defining slits and focussing grids near the cyclotron centre. Extensive work with large beams has not been possible owing to inadequate shielding pending transfer of the cyclotron to its final site.

[1]) J. W. Blamey, Published Proceedings of the CERN Symposium (1956) p. 344.

2. Theory

Measurements on the beam during its first revolution have indicated that it conforms closely to the following simplified theory. Assume that ions travel initially in a uniform electric field $E \sin wt$ for a distance d in the x direction perpendicular to the dee face and take $w = eH/m$ so that the ions are in exact resonance, where H is the magnetic field and e/m is the specific charge in e.m.u. The motion near the ion source is not sensibly affected if the accelerating frequency is a few percent off resonance. The voltage between the ion source and the dee will be $V \sin wt = Ed \sin wt$.

To obtain large currents from the ion source d must be small, and the beam will cross the distance d in a time short compared to a period of radio frequency accelerating voltage. If y is the displacement of the ion parallel to the dee face the horizontal motion near the ion source, neglecting space charge effects, is given by

$$\ddot{x} = (eE/m) \sin wt - (eH/m)\ \dot{y} \qquad (1)$$

$$\ddot{y} = (EH/m)\ \dot{x} \qquad (2)$$

with the initial conditions $\dot{x} = \dot{y} = 0$ and $x = y = 0$ at $t = t_0$. Putting $Y = 2mw^2 y/eE$,

$$X = 2mw^2 x/eE,\ D = 2mw^2 d/eE,$$

$wt = \theta$, $wt_0 = \theta_0$ the solutions to these equations are

$$X = \cos^2 \theta_0 \sin \theta + \\ + (\theta_0 - \cos \theta_0 \sin \theta_0) \cos \theta - \theta \cos \theta \,. \quad (3)$$

$$Y = -\cos^2 \theta_0 \cos \theta + (\theta_0 - \cos \theta_0 \sin \theta_0) \sin \theta - \\ - \theta \sin \theta - \cos \theta + 2 \cos \theta_0 \,. \quad (4)$$

In the region free of electric field $x > d$, the ion path will be circular until it again crosses the dees. Eqs. (3) and (4) were solved to give the values of θ, y, $\dot{x}$ and $\dot{y}$ when $x = d$, and thus the orbit centre, energy and phase of the next dee crossing. It is apparent from the calculations

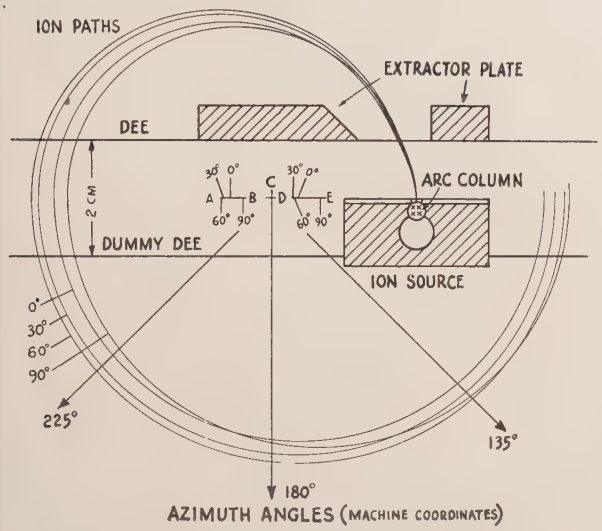

Fig. 1. Calculated initial orbits in the Canberra Cyclotron for ions of starting phases of 0°, 30°, 60° and 90°. AB and DE are the loci of orbit centres for the first and second half turns. C is the centre of the cyclotron.

that with small values of d a group of ions is strongly bunched in energy and orbit centres, but that they possess almost no phase bunching. With large values of d the ions make their first turn in a uniform electric field, and in this case a group of ions is strongly bunched in phase[2]) but lacks energy and orbit centre bunching. If the dee aperture and spacing are sufficiently small the ions may be considered to a first approximation as experiencing an impulsive acceleration on subsequent dee crossings, and their energy gain will be given from the phase of the accelerating voltage at the dee crossing.

[2]) B. L. Cohen, Rev. Sci. Instr. 24 (1953) 589.

Fig. 1 shows the nature of the orbits for the first turn as calculated from the foregoing assumptions and for the ion source to dee spacing of the Canberra cyclotron. This spacing was 1.0 cm but allowing for the electric field

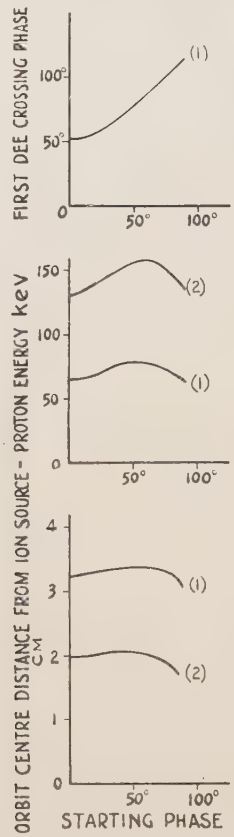

Fig. 2. Calculated phase, energy and orbit centres on the first (1) and second (2) half turns plotted against the initial phase of the ion for the Canberra cyclotron.

penetration into the 1.2 × 1.6 cm slot in the graphite extractor plate on the dee opposite the ion source, the extent of the accelerating field near the ion source was $d = 1.5$ cm. With $H = 12\,300$ gauss, $V = 80\,000$ volts, for protons, $D = 0.8$, and the transit time in the ion source region for the ions of interest is close to 56°. For the subsequent dee crossing the dee aperture was reduced to 3 cm by graphite feeler blocks which with a dee to dummy dee spacing of 2 cm gave a reasonably short transit time for the ions across the dee gap. As shown in fig. 2 the ions leaving the source at initial phases between 30° and 75° are well bunched in orbit centres and in

energy, but essentially no phase bunching occurs. This group of ions can be selected for further acceleration by passing them through a slit in a stop as discussed in section 3.3. These are the ions of highest energy which is given closely from the full ion source to dee voltage, and their small phase range, about 35°, compensates somewhat for the lack of phase bunching. They cross the dees again at phases ranging from 63° to 98°, that is mainly before the dee voltage maximum at phase 90° and thus undergo transit time effect electrical defocussing as discussed in section 4. If this and subsequent dee crossings have small transit times the homogeneity of the group in energy and orbit

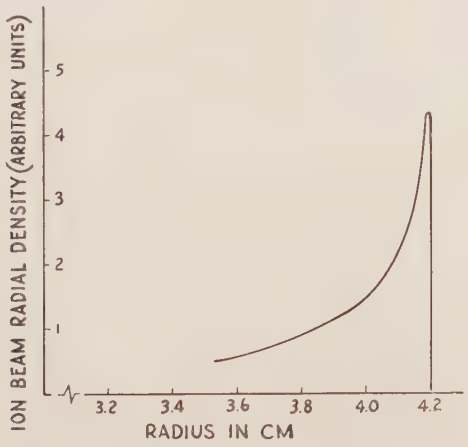

Fig. 3. Calculated radial beam distribution on azimuth 235° for the second half turn.

centres is largely preserved. Fig. 3 shows the beam distribution in radius on the first turn calculated with the assumption that the ion source output varies as the $\frac{3}{2}$ power of the instantaneous dee voltage.

Calculations for other values of D indicate that the shorter the ion source to dee transit time the stronger is the bunching in orbit centres and energy for a group of ions. This group moves closer to those with starting phase 90°, the peak dee voltage, as the ion source to extractor plate distance is reduced. The practical lower limit of this distance is set by flashover and sparking from ion source to dee.

The first integral of eq. (2) shows that all orbit centres are on the axis $x = 0$ if no x component of electric field is present, that is they are on the line through the ion source parallel to the dee edge. Further accelerations cause the orbit centres to oscillate along this line with decreasing amplitude, and neglecting the effects of precession caused by betatron oscillations and other orbit disturbances, the orbit centres of a particular ion will approach a point. The ion source should be offset parallel to the dee edge by an amount which will bring the orbit centres of the high energy ions after many revolutions to the machine centre. Fig. 4 shows the motion of the orbit centres plotted against the number of dee crossings. With a single dee machine the ion source should be offset from the machine centre by 0.76 R, and

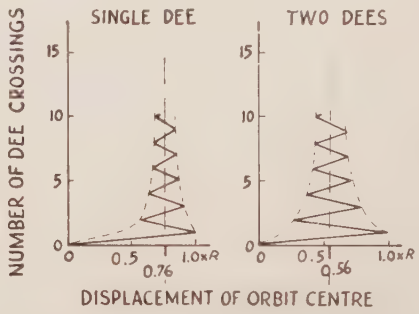

Fig. 4. Displacement from the ion source parallel to the dee edge of the point of bunching of orbit centres plotted against the number of crossings of the dee. The unit of displacement is the radius R of the first turn where $R^2 = 2mV/eH^2$.

in a machine with two dees holding equal voltages the offset should be 0.55 R, where R is the radius of the first turn, $R^2 = 2\,mV/eH^2$. For the Canberra cyclotron the ion source was displaced 2.5 cm from the machine centre to allow for this effect.

3. Measurements

3.1. THE ION SOURCE

The ion source design is similar to that described by Livingston and Jones[3]). The arc body is graphite and the ions are drawn from a slit 1.5 mm wide and 12 mm high. The 12 mm wide and 16 mm high slot in the graphite

[3]) R. S. Livingston and R. J. Jones, Rev. Sci. Instr. 25 (1954) 552.

extractor plate attached to the dee is spaced 10 mm from the ion source and is displaced 5 mm from a position directly opposite the ion source slit towards the machine centre to allow for curvature of the ion beam in the magnetic field. The ion source was observed visually through a lead glass window in the cyclotron tank with an internal target preventing accelerating of the protons beyond 1 MeV. The

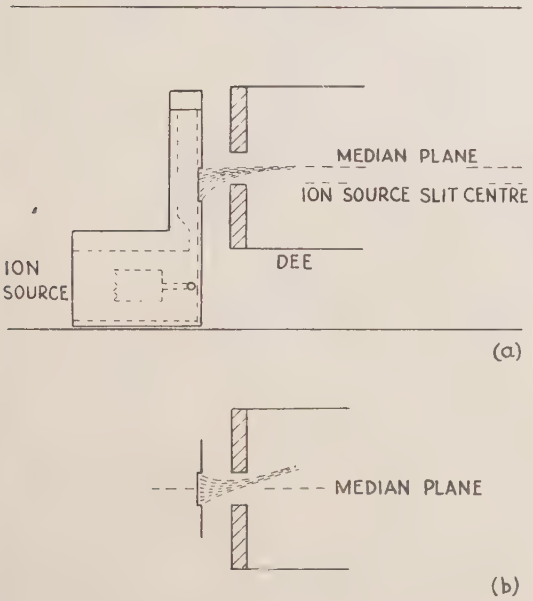

Fig. 5. Vertical focussing near the ion source sketched from visual observation of the glow in the residual gas, (a) with and (b) without the ion source lowered below the median plane.

focussing properties of a given arrangement were estimated from the shape of the glow induced by the ion beam in the residual gas in the tank which could be seen over the first full revolution. With the above arrangement the beam leaving the source is strongly convergent and well focussed vertically, possibly due to curvature of the plasma from which the ions are drawn. The beam however rides up, away from the filament end of the ion source, as might be expected from the presumed shape of the plasma boundary in the arc column. This effect is due to lack of symmetry of the ion source and could possibly be overcome by using a source with a filament at each end of the arc column. The use of an insulated reflecting button on the end of ion source column as discussed by Livingston and Jones[3]) did not overcome this trouble. For the beam from the source to emerge in the median plane it was necessary to lower the ion source slit 8 mm below this plane, whence the diverging action of the ion lens formed by the hole in the extractor plate, pulled the ion beam horizontal, and diverged the converging beam from the source to a nearly parallel beam as is shown in the sketches of fig. 5. The source operated with an arc drop of 70 to 100 volts and 0.75 to 1.0 amperes arc current, and gave beams as high as 25 milliamperes of protons measured on the second half of the first turn.

3.2. EARLY TURNS NEAR THE ION SOURCE

As the Canberra 30 inch cyclotron has a single dee it was possible to insert probes into the dummy dee half of the machine over a wide spread of azimuthal angles and to measure the ion current distribution against radius. A target was introduced to stop the beam immediately before it entered the dee at a suitable radius, and three other targets at different azimuth angles 45° apart were moved separately in small distances (0.050 inches) at a time and the current and power taken by these plotted as a function of target radius. The total beam power was measured in terms of temperature rise of the target cooling water, and this power was differentiated against radius to give the plots of beam intensity against radius at azimuth angles of 225°, 180° and 135° as shown in fig. 6. These measurements confirm that bunching in energy and orbit centres is present and is maintained during at least the first four turns. The peak beam on the first turn was at radial distances from the machine centre of 4.0, 4.25 and 4.65 cm respectively at the 225°, 180° and 135° azimuth angles, as compared with the calculated values of 4.2, 4.5 and 4.9 cm of fig. 1. This discrepancy could be accounted for if the peak dee volts were 73 kilovolts rather than the indicated value of 80 kilovolts on the dee voltmeter, but is also probably partly due to the approximations of the theory. The difference in

radial width of the beam as measured and as calculated is partly accounted for by the 1.5 mm width of the ion source slit.

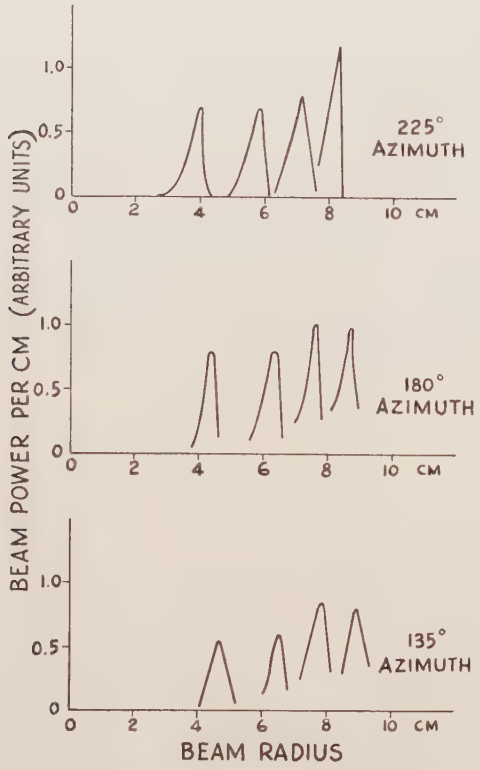

Fig. 6. Beam radial density for the first four turns of the Canberra cyclotron. The ordinate is the measured beam increment for radial increment of 1.25 mm. The integrated beam current for the first four turns respectively is 15, 8, 7 and 6 milliamperes.

0.5 mm. Some of the results as shown in fig. 7 were obtained using two beam defining slits in stops inserted in the first turn, one slit on the 225° azimuth was 3 mm wide, and the other on the 180° azimuth was 1.5 mm wide, both being 1 cm high. These two slits in series reduced the beam at full energy from 3.5 milliamperes to 350 microamperes. The measured orbit centres at small radius form a line of centres 8 mm long lying nearly along the centre line between the dees, in agreement with the theory of section 2 and at large radii this line has rotated in the direction of beam rotation owing to betatron

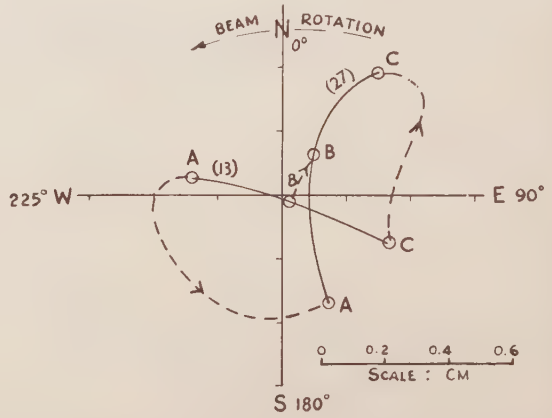

Fig. 7. Measured orbit centres with a 1.5 mm wide defining slit at radii of A 4.3 cm, B 3.7 cm and C 3.1 cm on the first turn. The lines of centres (13) and (27) are for beam radii of 13 cm and 27 cm. The dotted lines show the measured motion of the orbit centres due to precession of the beam.

3.3. BEAM DEFINING SLITS

With the full ion source beam the results of measurements using probe targets at large radii were confused since the beam contained ions which had undergone differing numbers of dee crossings. The behaviour could be resolved by inserting on the first turn water cooled copper stops with slits which would pass for further acceleration only a small selected amount of the ion source beam. These stops and slits could then be moved to allow measurements on the full beam taken in small sections. The measurements at three azimuth angles as previously described enabled the mean orbit centres of the beam or portions of the beam to be determined at different beam radii to within

oscillations or precession of the beam. In measurements made with greater ion source to extractor plate distances and with a lower extraction field at the ion source the line of orbit centres was found to extend for as much as 2 cm. It was found that for good extraction it was necessary that the orbit centre was close to the machine centre on the final orbit, as was assumed in calculations of the extraction system geometry. The final adjustment to bring the orbit centre to the machine centre was made by the use of shimming iron in the shimming gap of the magnet. Extraction of the full ion source beam is not practicable since the orbit centres extend over a line 8 mm long, which at a final radius of 32.5 cm gives a wide variation

of 5% in energy or of 1.5 degrees in angle of approach to the splitter plate. When extraction is attempted under these conditions most of the beam is lost causing a large power dissipation on parts of the extraction system and high background radiation. The 1.5 mm and 3 mm wide slits on the first turn reduce the variation in energy and angle of the final internal beam by a factor of 5, allowing efficient extraction, such that it was possible to have a continuous and steady external beam of 250 microamperes, just over 70% of the internal beam of 350 microamperes. This extraction efficiency was attained in spite of a 2% ripple at 300 cycles on the dee voltage, and it is probable that higher efficiency would result with a more stabilized and ripple free dee voltage. The extraction system consists of a tungsten splitter plate 0.0075 inches thick and 1 inch high and a deflector plate spaced from this about 7 mm and requiring 60 kilovolts DC supplied down the inside of the dee support. In later experiments a final internal beam of 340 microamperes was obtained through a slit on the first turn 0.5 mm wide and 1 cm high, but extraction of this beam was not attempted. The width of the resonance curves, that is internal beam at full energy plotted against magnetic field variations with all other controls fixed, is a measure of the range of phases of the beam injected from the ion source into the machine. With a beam defining slit on the first turn these resonance curves are distinctly narrower than with the undefined beam, confirming that a narrow group of phases is selected by the slit. A slit on the first turn can make the cyclotron unstable when an increase in dee voltage causes a large reduction of the circulating beam, and causes the dee voltage to rise further on account of the reduction in power loading of the oscillator. It is possible to place the defining slit to give the inherently stable condition from the aspect of power load on the oscillator where an increase of dee voltage causes an increase of beam.

Slits defining early cyclotron orbits lead to a beam of precise energy and low angular spread and reduce the general background radiation. This was convincingly demonstrated in an experiment where the external proton beam was used to produce proton capture gamma rays in a number of thin targets[4]). A beam of 1 microampere and cross section 0.5×0.5 cm on a target 12 feet from the machine was required. Three internal beam defining slits, 1 mm, $\frac{1}{2}$ mm and $\frac{1}{2}$ mm wide respectively, each 1 cm high, were used on each of the first three turns. The beam accelerated was controlled by slightly offsetting the slit on the second turn to give a total beam of 10 microamperes on the final orbit. With this low beam and lower power load on the oscillator it was possible to stabilize the dee voltage and reduce dee voltage ripple below $\frac{1}{2}$% by means of a negative feedback circuit involving grid modulation of the oscillator. The expectation that a well defined internal beam would give a well defined external beam was fully realised, and to within the accuracy of measurement the whole of the circulating beam could be extracted, an extraction efficiency of 95% to 100%. With no further energy analysis the energy spread as determined by magnetic deflection of the external beam was of the order of 1%.

An internal target was inserted in the machine 135 degrees in front of the deflector channel and edged in to take 5 microamperes of the internal beam, the other 5 microamperes being extracted. The ratio of the beam to this internal target to the extracted beam was then a very critical function of the magnetic field of the cyclotron, and indicated any slight changes in the precessional history of the beam. When the two beams were held equal, requiring magnet current stabilization to better than 1 in 10 000, the energy of the external beam was constant and homogeneous to better than $\frac{1}{2}$%. The energy of the external beam of 7.7 MeV as measured by its range in aluminium, after allowing for the two further accelerations as the beam entered and left the dee on its final revolution, agreed with the energy determination of 7.6 MeV from

[4]) D. S. Gemmell, A. H. Morton, E. W. Titterton and D. S. Gemmell, A. H. Morton, W. I. B. Smith. Submitted for publication in Nuclear Physics.

measured orbit centre and radius of the final internal beam prior to extraction. The total angular spread of the external beam was 6 milliradians, much of which was probably due to the spreading properties of the cyclotron fringe field. Of the 5 microamperes extracted, 1 microampere was passed through a slit 2 mm wide and 2.5 mm high where the beam emerged from the cyclotron tank, and was focussed by means of a quadrupole magnet on the target 12 feet distant, to an area 5 mm × 5 mm with no further defining slits.

4. Electrical Focussing Bars on the Dees

The use of beam defining slits considerably reduces the beam from the ion source. To obtain large cyclotron beams well defined by such slits it is necessary to either increase the ion source output, or to reduce the large losses of beam usually present during the early stages of acceleration. Most of the loss of beam between the ion source and final turn occurs in the first few turns and is due to the fact that the ions mainly cross the dees on these turns before the dee voltage maximum, and on the latter half of the dee crossing suffer large defocussing forces which exceed the other focussing forces

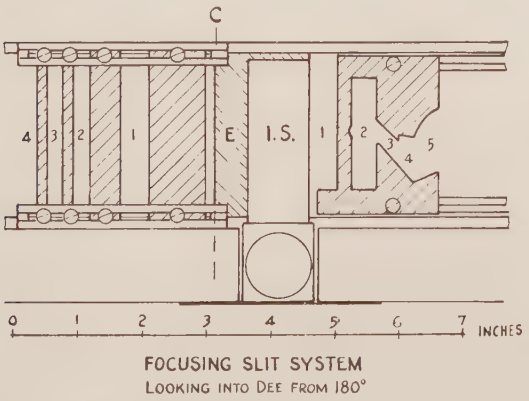

Fig. 8. Focussing slit system attached to the dee and dummy dee. The ion source I.S. is offset 2.5 cm from the cyclotron centre C. E is the ion extraction plate. (1), (2), (3), (4) and (5) refer to the slits for passage of beam on the appropriate turn.

present giving a net defocussing of the beam. This effect is discussed at length by Cohen in ref.[2]). As the early turns in the Canberra cyclotron are well separated as shown in fig. 6, vertical graphite rods were attached to the dee or dummy dee between turns on the down beam side of the dee gap to reduce the vertical defocussing forces and to reduce beam loss on the first four turns. The arrangement of the graphite bars is shown in fig. 8. On the crossings from dee to dummy dee it was possible to place these bars between all turns up to the fourth, but on crossings from dummy dee to dee the third, fourth and fifth turns overlapped to some extent

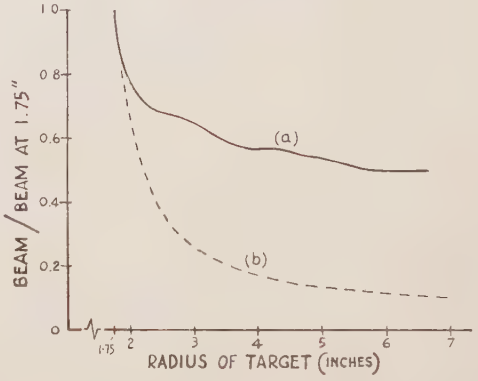

Fig. 9. Beam survival, (a) with and (b) without focussing slits.

and for these turns a carbon plate suitably cut was attached to the dee. The elimination of vertical defocussing forces in this way introduces some horizontal electrical forces which could effect the radial bunching and orbit separation. This effect was noticed but not fully investigated since it seemed advisable first to attempt a more symmetrical beam from the ion source. Fig. 9 shows a plot of beam versus radius with and without the focussing bars on the dees, and indicates a considerable increase in beam survival with the bars. This use of focussing bars is analogous to the use of focussing grids in linear proton accelerators except that in a cyclotron they can be placed between turns and need not intercept useful beam. Similar results have been reported by Blosser and Irwin[5]).

5. Discussion

The use of beam defining slits and electrical focussing bars on the dees have been shown to

[5]) H. G. Blosser and F. Irwin, Bull. Am. Phys. Soc. Series II, Vol. 3 (1958) 180.

improve the beam characteristics and beam survival in a fixed frequency cyclotron. When such slits are used it is necessary to have stabilized and ripple free dee voltage, and highly stabilized magnetic field. Further improvement in reducing the angular spread should be possible by bringing the external beam down the gradient of magnet fringing field rather than across this gradient as is usual. If fixed beam defining slits and a fixed ion source are used on a variable energy cyclotron, it would require that the dee voltage would vary as the final energy of the machine to keep the geometry of the first turn constant. However, as the phase changes through the machine and the precessional history of the beam depend both on the magnetic field fall off with radius and on the relativistic mass increase of the particle during acceleration, a simple variation of dee voltage and frequency cannot keep the beam geometry fixed throughout the whole acceleration as the guide magnetic field is altered. In a variable energy machine it would be necessary as well to change the index of fall off of magnetic field, or otherwise control precession as the energy is altered with change of magnetic field and frequency to fulfil the conditions for efficient extraction at all energies.

The well defined separation of the early turns in a cyclotron should make it possible to pulse the cyclotron beam by the use of deflecting plates near the ion source. Low voltages would be adequate to deflect the low energy beam the order of 1 mm away from a defining slit, and the low capacity of such a system should make it possible to use pulses sufficiently short to select single bunches of ions for further accelerations. In a single dee cyclotron this possibility would appear more attractive than pulsing the beam by deflection after it has achieved its full energy.

Acknowledgments

We wish to thank Professor M. L. Oliphant for initiating the project and for his encouragement. Thanks are due to Mr. R. W. Parkes for his assistance in constructing and operating the cyclotron and for his many useful suggestions. One of us, A. H. Morton, wishes to acknowledge an Australian National University Scholarship which made it possible for him to participate in this work.

NUCLEAR INSTRUMENTS AND METHODS 4 (1959) 44–49; NORTH-HOLLAND PUBLISHING CO.

ACCURATE MAGNETIC FIELD AND FIELD GRADIENT MEASURING INSTRUMENT FOR DYNAMIC LOW FIELDS IN A SYNCHROTRON MAGNET

HANS M. NYSÄTER†

Cambridge Electron Accelerator, Harvard University – Mass. Institute of Technology

Received 25 September 1958

Two biased peaking strips have been combined into a differential magnetic probe. The pulses from the two peaking strips are displayed on an oscilloscope screen with a time separation, for the same bias field, given by the field difference between the locations of the two strips. At the bias current corresponding to the chosen field level, the two peaking strips are given slightly different bias, so as to cancel the time lag between pulses. The field difference is read directly as a D.C. current. The magnetic field itself is measured with one of the peaking strips, as its D.C. bias current. With careful calibration, the accuracy in gradient divided by field (n-value) was estimated to be of the order of 1% in a nearly linear synchrotron field of 25 gauss, varying by 4 percent per cm and 0.15 gauss/μs. The instrument, when applied to the CEA magnets, confirmed the feasibility of an injection field as low as 25 gauss, although at the magnet ends sharp peaks occur in the field and gradient distributions, apparently a remanent field contribution.

1. Introduction

During the course of design for the Cambridge Electron Accelerator, it became imperative to map with precision the magnetic field and field gradient of the magnets at low fields. Since the dynamic behaviour of magnetic fields at the unusually low injection level of 25 gauss is not well known, we had a reason to ask the following questions:

1. How does the remanent field influence the radial gradient distribution across the magnet gap and the absolute n-value at the central orbit location? The n-value, which is a measure of the focusing properties of a magnet, is defined as

$$n = \frac{\mathrm{d}B}{\mathrm{d}r}\,\frac{r_0}{B_0}$$

where r_0 is the particle radius of curvature at the central orbit location in the vertical magnetic field B_0.

2. What are the fluctuations in field and gradient along the length of the magnet?

3. How do remanence and eddy currents affect the fringing fields at the magnet ends, especially with regard to equivalent magnetic lengths?

† On leave from the Royal Institute of Technology, Stockholm, Sweden.

Peaking strips[1,2]) were considered the best approach for measuring these low fields, although the fact that they do not allow directly comparative measurements, such as can be made with search coils at higher fields, constitutes a difficulty when aiming for the desired accuracy of at least 1% in the n-value[3]).

2. Peaking Strips

A review of work on peaking strips is given in ref. [1]). A peaking strip is a thin strip of high-permeability alloy with a μ of the order of 10^5. Because of the high permeability of the strip, it saturates at a very low external field, usually a few tenths of an oersted. A pickup coil wound around the strip will therefore give induced voltage pulses, in an A.C. magnetic field, at the time when the field passes the vertical sides of the almost rectangular hysteresis loop of the strip, as shown in fig. 1. In order to determine the time for passing a certain field

[1]) J. L. Symonds, Methods of Measuring Strong Magnetic Fields, Rep. Progr. Phys., Vol. 18 (1955) 102.

[2]) R. Gabillard, Notes sur la Fabrication des "Peaking Strips", CERN-PS/RGb10 (Apr. 1957).

[3]) G. Diambrini-Palazzi, Measurements, with Peaking Strips in the Gap of a Weakfocusing Electron-synchrotron... of n at the Injection in the Dynamic Field, CERN Symposium 1956, Vol. 1, p. 471.

with a good accuracy, the pulse width has to be made as short as possible by selection of alloy and heat treatment of it to give the maximum

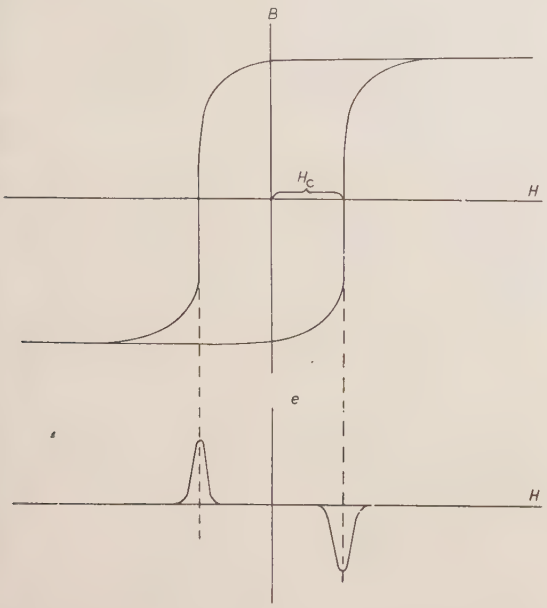

Fig. 1. Hysteresis loop of a peaking strip. B is the magnetic field in the strip, H is the magnetizing force given by the external A.C. magnetic field. A pickup coil around the strip gives voltage pulses e, delayed from zero external field by an amount corresponding to the coercive force H_c.

possible permeability. Another factor governing the effective permeability of the strip, because of the demagnetization effect, is its ratio of length to width, which is usually made at least

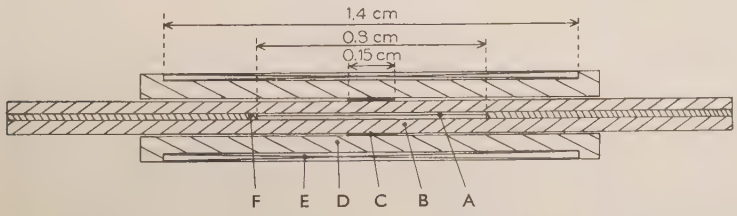

Fig. 2. Biased peaking strip assembly. A is peaking strip, B quarz tube, C pickup coil, D bias coil spool in phlogopite (synthetic mica), E bias coil, and F brushhair for spacing strip.

500. A third consideration is avoiding widening of the pulse because of eddy currents, either in the strip itself or in the surrounding coils. Therefore, it is advisable to make the pickup coil a limited number of turns of fine wire, confined to the center of the strip, since the ends of the strip may have slightly different hysteresis loops. Also, this is another reason for using a very thin strip.

In order to mark in time the passage of a predicted field, the peaking strip is equipped with an additional surrounding coil, the bias coil. Sensitive to the sum of the fields, the peaking strip will fire when the varying external field is equal to and opposing the D.C. bias field plus or minus a correction, corresponding to the coercive force H_c in fig. 1.

Fig. 2 shows the type of peaking strip assembly, used in these measurements. Several different alloys were tried for the peaking strips, the best results being obtained with a 0.025 mm diameter 4–79 Mo-permalloy wire annealed in a "hydrogen flask" at 1100° C for $\frac{1}{2}$ h and subsequently cooled to room temperature in $\frac{1}{2}$ h [4]). With this particular diameter, the strip could be made as short as 0.8 cm before the pulse started to broaden because of decreasing effective permeability. The pulse width from the peaking strips was about 2 μs at half amplitude in the magnet injection field of 25 gauss with a time rate of rise of 0.15 gauss/μs.

A field limit on the dynamic measurements is imposed by the limited heat dissipation in the bias coils. For the type of bias coil shown in fig. 2 the limit set was 50 gauss or 1 A bias current. We could not allow any appreciable heating of the coils because of the strict calibration requirements, described under gradient measurements below.

3. Magnetic Field Measurements

With the magnet excitation waveform shown in fig. 3, the field distribution throughout the magnet at 25 gauss was measured the following way. The biased peaking strip was calibrated in an A.C. magnetic field, known to an accuracy better than 1% and given by a homogeneous

[4]) R. M. Bozorth, Ferromagnetism (Van Nostrand, New York, 1951) p. 137.

field coil, see below. By adjusting a D.C. current in the bias coil to the point, where the peaking pulses just vanished, the bias field was

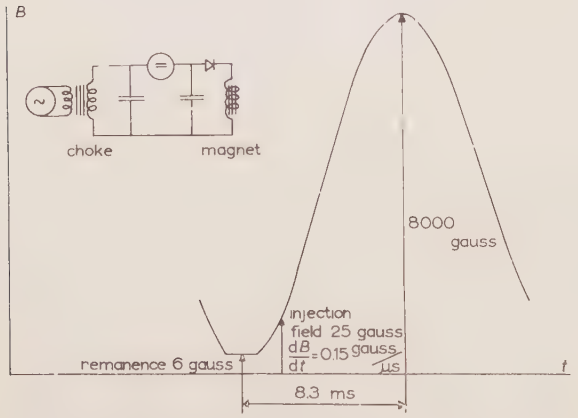

Fig. 3. Magnetic field waveform of the synchrotron magnet models, achieved with rectifiers in series with the magnets. The frequency is 60 cps.

calibrated in terms of bias current. When measuring a magnetic field distribution at 25 gauss, one biased peaking strip at a fixed location in the magnet gap was used to trigger the sweep of an oscilloscope and a second strip was located on the central orbit line inside the magnet, its bias current adjusted to correspond to 25 gauss, and its peaking pulse displayed on the screen. The time for this pulse was the chosen time for the B-distribution to be mapped, and as the peaking strip was moved to scan the magnet, the pulse was always restored to the same time by means of changing the bias current, which was then a measure of the field at the particular location of the strip.

Possible sources of error in this technique were investigated.

1. Since the gap on the orbit was 5 cm compared to the 1.4 cm length of the bias coil, the presence of iron could possibly influence the calibration of the strip. The bias field was recalibrated against a low A.C. field in the magnet, and no difference could be detected as the peaking strip was moved through the fringing field into the magnet gap.

2. Fig. 4 shows an arrangement to measure coercive forces and the results obtained for two peaking strips. The coercive forces are functions of dH/dt and are about 0.5 Oe for the dH/dt valid in our magnets. As mentioned above, these coercive forces represent timing errors, which should cause no noticeable influence on the field distributions inside the magnet gap and a maximum of 1% of the 25 gauss level far out in the fringing fields.

3. To ascertain that the peaking strip did not distort the low fields to be measured, the coercive force was measured with the strip inclined at various angles to a 3.9 gauss peak external A.C. field. To a good approximation, the strip always measured only the field component along the strip, which ruled out field distortion even at this low field.

4. Random errors in the timing of the peaking strips were found to correspond to about 10^{-4} of the 25 gauss field.

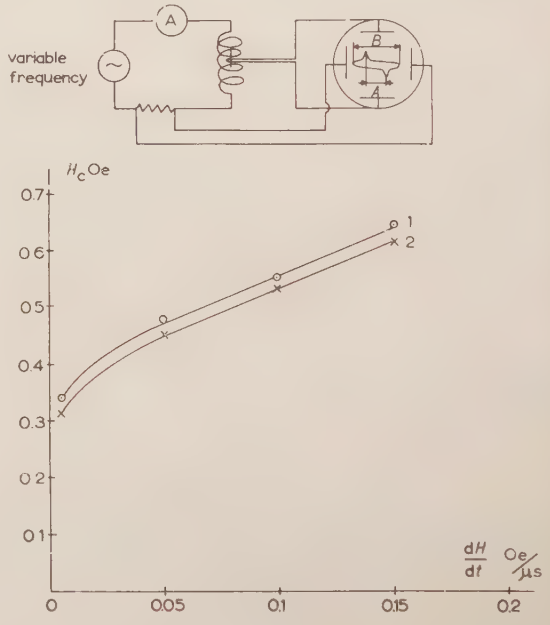

Fig. 4. Measurement of the coercive force H_c of peaking strips, showing the dependence on external dH/dt. The peaking strips were placed in a low external AC field of variable frequency. With the field amplitude 3.9 gauss, the coercive force was obtained from the oscilloscope screen picture shown as $H_c = 3.9\ A/B$ Oe. The plotted curves were taken for the two peaking strips that were combined into a gradient probe.

5. From points 1–4 above it was concluded that the largest source of error in measuring a field distribution at 25 gauss, inside the magnet

gap, was the uncertainty in reading the D.C. bias current, which was done to 0.1%.

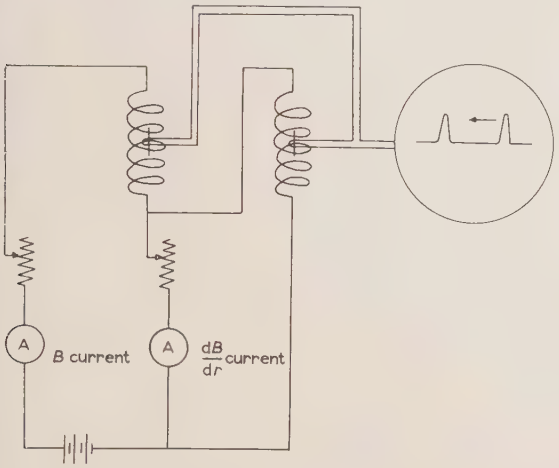

Fig. 5. Principle of field gradient meter. The time lag between the pulses from two peaking strips, a measure of a magnetic field difference, is cancelled by adjusting the dB/dr current, until the series connected pulses add to a sharp maximum. The B current gives the field, at which the gradient is measured as the dB/dr current.

4. Field Gradient Measurements

The principle of the gradient-meter is shown in fig. 5. Two peaking strips were mounted on a probe with a separation of 2.5 cm, estimated to be in error by a maximum of 0.5%. The method of oscilloscope display was the same as for the field measurements. Because of the field difference between the locations of the two strips, for the same bias current there was a time delay between the two pulses. The delay was cancelled by adjusting the bias current of one strip, until the series connected signals added to a sharp maximum. The difference in field was in this way transformed into a difference in bias current, which was read directly on a meter. As the probe scanned the magnet, every reading required another adjustment, namely the setting of the main bias current so that the two superimposed pulses occurred exactly at the time corresponding to the chosen field level (25 gauss). Fig. 6 shows the arrangement of variable resistors used to give a smooth enough variation of the B and dB/dr currents. The circuit also permits switching the meter, a 0.25% "laboratory standard" instrument, between the positions corresponding to measuring B and dB/dr currents.

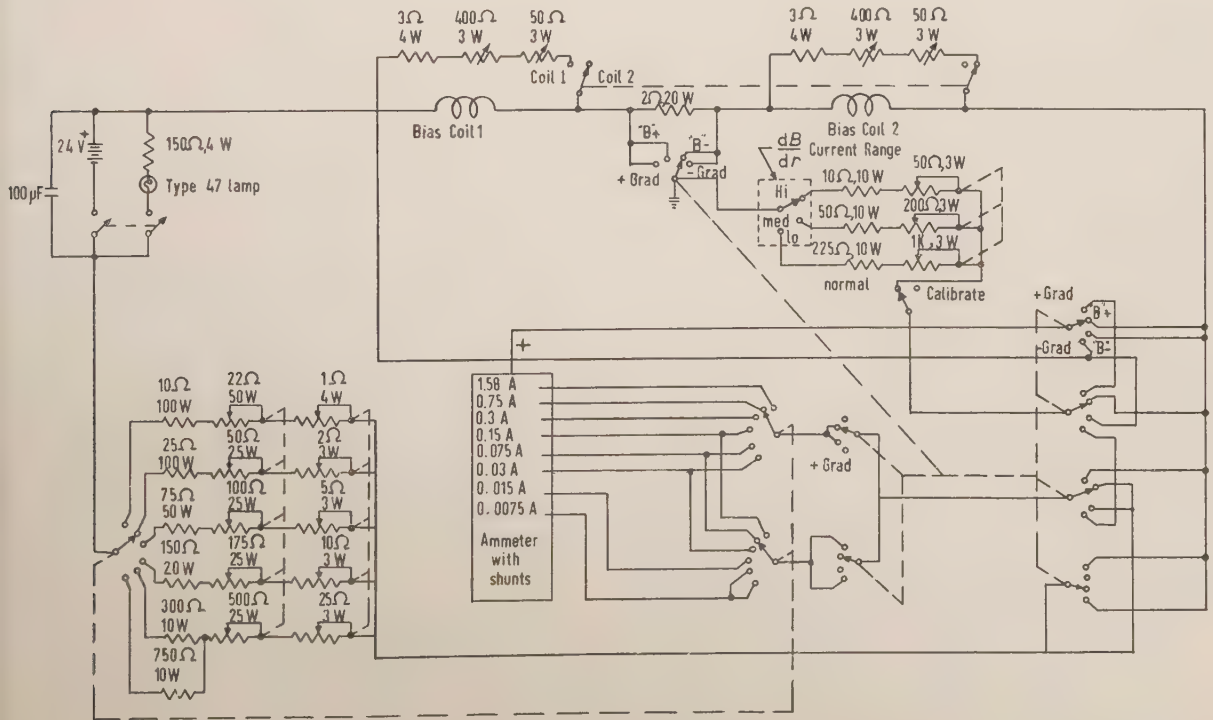

Fig. 6. Detailed circuit for the field and field gradient meter.

Essential for the required accuracy are the calibration circuits, shown connected across the two bias coils in fig. 6. Although extreme care was taken to make the two bias coils identical, they turned out to give 1% different fields for the same current. Since this would give a 10% error in the gradient for a field changing by 10% between strips, it had to be corrected. A variable resistor was connected across the coil giving the higher field and set to the right value by studying the two pulses with the probe in a homogeneous (to better than 0.1%) A.C. field[5]) and with a varying D.C. current through the series connected bias coils.

During the calibration, when the added fields approached a fullbiased state so that the pulses were on the verge of vanishing, the pulses from the two strips (still series connected) started to separate for a constant calibration setting. This error, which could not be taken care of with the calibration, was caused by the slightly different coercive forces of the two strips, 1 and 2 in fig. 4. The relative gradient distributions are not affected but the absolute n-values have to be corrected by 1.0%, as estimated from fig. 4, with a sign depending on the gradient sign.

After correction, the measured absolute n-value was estimated to be correct within $\pm$ 1%. The random error for repeated measurements was $\pm$ 0.5%, and the 2.5 cm separation between peaking strips, which also enters in n, was determined to an estimated accuracy of $\pm$ 0.5%.

5. Some Results of Measurements

With the techniques described above, measurements were made of the vertical fields of the CEA magnet models, which are C-shaped magnets, made of punched laminations of high-silicon (about 4%) hot rolled transformer steel with a lamination thickness of 0.35 mm. The 60 cps, fullbiased excitation waveform is shown in fig. 3.

The questions, put forward as an introduction, are answered as follows:

[5]) M. W. Garrett, Axially Symmetric Systems for Generating and Measuring Magnetic Fields, Part 1, J. Appl. Phys. 22 (1951) 1106.

1. The relative gradient distribution across the magnet gap seems to be almost the same at 25 gauss and 4000 gauss, as shown by fig. 7. The absolute n-value on the central orbit, however, is a few percent higher at 25 gauss than at 4000 gauss.

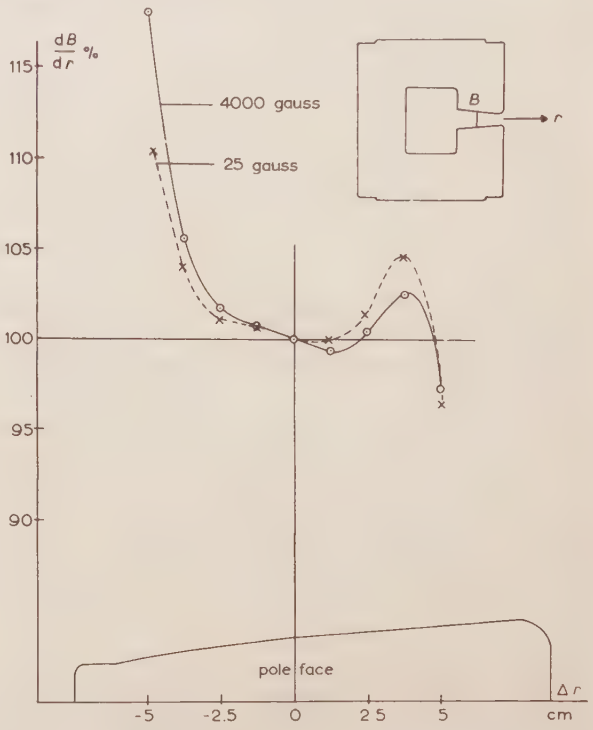

Fig. 7. Field gradient distribution across the gap of a synchrotron magnet model in the dynamic field of 25 gauss, as compared to the 4000 gauss distribution. The gradient measured is the radial gradient of the vertical field.

2. Well inside (at least 10 cm) the magnet ends, no fluctuations could be detected along the central orbit in field and gradient at 25 gauss larger than the random errors, namely 0.1% for the field and 0.5% for the gradient. In spite of the closeness to the remanent field of 6 gauss, the chosen level of 25 gauss for the synchrotron injection field thus seems to give a uniform enough field for alternating gradient operation.

3. In the fringing fields, at the magnet ends, the 25 gauss distributions of field and gradient show a peculiar peak, which is not present at higher fields (above a few hundred gauss). Fig. 8 shows some experimental data. Although the

nature of the peaks is not understood, a few observations will be pointed out.

In trying to account for the peaks as a magnetic after-effect, it was found that 30 cps operation gave much the same effect as 60 cps, and that room temperature of the magnet pole ends gave the same results as 100° C. The effect is not present in fringing fields in the radial end peak, only 8 times weaker. It was observed that the end field peak does not start building up, for varying peak magnet fields, until the latter reaches about 3000 gauss.

The low field peak extends the effective magnetic length for each end by about 5 cm, and special correcting systems, carrying D.C. current, will be needed to cancel the effect.

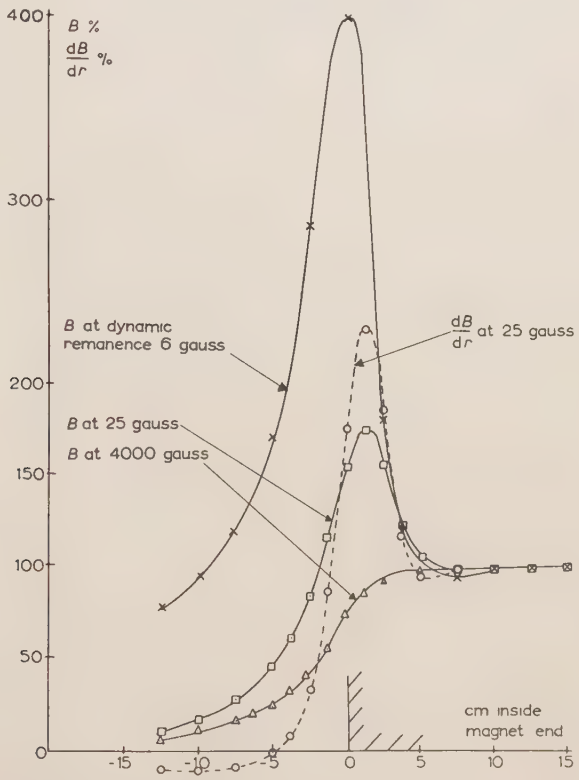

Fig. 8. Measured dynamic distributions of field and field gradient in the fringing field at the end of a synchrotron magnet model. The abscissa is the distance along the magnet, in the direction of the particle orbit. Plotted are distributions at several fields, all normalized to the constant level well inside the magnet end.

(lamination) direction. Yet, it does not seem to be directly associated with eddy currents in the magnet ends. At 25 gauss for falling field, the peak has the same sign, although dB/dt has the opposite sign compared to 25 gauss on the rising side. Fig. 8 shows that the 25 gauss peak is a scaled down influence of a peak in the dynamic remanent field. Also the static remanence, measured with a rotating coil, showed a similar

Acknowledgments

The 4–79 Mo-permalloy wire was kindly supplied by Dr. R. A. Beth, Brookhaven National Laboratory.

The circuit for the peaking strip gradmeter, as shown in fig. 6, was planned and built by Mr. Roland Martick of Boston College.

This work was supported by the U.S. Atomic Energy Commission.

NUCLEAR INSTRUMENTS AND METHODS 4 (1959) 50–51; NORTH-HOLLAND PUBLISHING CO.

AN ABSORBER SYSTEM FOR SCATTERING EXPERIMENTS†

W. J. O'NEILL, E. SUNDAHL and H. OSTRANDER

Argonne National Laboratory, Lemont, Illinois

Received 25 November 1958

In scattering experiments it is often advantageous to degrade the energy of the scattered beam. The following three applications have been used extensively in experiments with the Argonne cyclotron.

1. The resolution of the detector may be improved by taking advantage of the curvature of the range-energy relation. If one uses NaI(Tl) as a detector, it may have a resolution of 2.5% at 22 MeV. If the beam is degraded by a suitable absorber, the effective resolution can be improved readily to better than 2% in spite of the energy straggling.

2. In the case in which two detectors are used in order to identify the scattered particle, it becomes desirable to adjust the available parameters so as to retain a constant value for the $E\,(\mathrm{d}E/\mathrm{d}x)$ pulse for different values of the incident energy E_0.

3. In many cases it is profitable to establish a direct calibration of a pulse-height scale in terms of energy, especially when the response of the detector is not linear with energy.

In order to achieve this it was necessary to have available a great number of absorber thicknesses which could be readily changed. In particular, the change of absorber thickness should not require the presence of the operator near the equipment where the background of radiations is high. In our case the detector unit is operated in a vacuum and therefore remote control is necessary. Furthermore, it was desirable to permit the detector unit to be operated over a wide range of angles, from 4° to 170°. Therefore there were severe space limitations. Finally, the divergence in the scattered beam, because of multiple scattering in the absorber foils, made it desirable to stack the foils closely together. In our particular case a system of three disks with six positions was used. The position had to be accurate to 0.0005 in. The wheels could not be more than 3 in. in diameter and had a maximum thickness of 0.125 in. Furthermore, the spacing between the wheels had to be made as small as possible (actual spacing: 0.0156 in.).

The original system included solenoid actuators used in conjunction with a microswitch bank for indicating the position of the three wheels. These switches, with an actuating range of less than 0.01 in., proved to be difficult to adjust initially and did not remain in adjustment. As an added complication, the solenoids proved to be highly sensitive to temperature changes so they required widely varying voltages.

In order to improve the reliability of the positioning and drive, a search was made for a suitable motor. Our requirements were met by a small ac motor[1]) (1 in. in diameter by 3 in. long) with low speed and high torque. Dc motors could not be used because their magnetic fields might affect the response of the nearby photomultipliers. The only positive method of driving the wheel was to cut a shoulder along its circumference and mount a ring gear on it. The wheel is then directly driven by the motor, thus preventing any backlash which might occur in a gear rack or mechanical linkage. This is illustrated in fig. 1.

The wheel is set accurately at six different positions by using a limit switch riding on a

† Work performed under the auspices of the U. S. Atomic Energy Commission.

[1]) Manufactured by Globe Industries, Dayton, Ohio.

gear-driven cam which makes six revolutions for each revolution of the wheel. The cam is so designed that when the wheel reaches the desired position, the switch actuator suddenly falls into an indentation and opens the motor circuit. The large gear reducer absorbs all overtravel so that the motor stops within 0.005 in. of its mark.

To indicate the position of the wheel, a rotary stepping switch is used in the limit switch circuit of the motor. The limit switch, being of single-pole double-throw construction, simultaneously opens the motor circuit and actuates the rotary stepping switch.

This system has been used in the detection system for the Argonne 60-in. scattering chamber[2]). It provided for the insertion of absorber foils of thicknesses from 0.000 in. to 0.150 in. in steps of 0.001 in. in front of the detecting crystals. It would be equally suitable in other applications in which it is necessary to use remote control to position a wheel accurately in a vacuum, even when the available space is very limited.

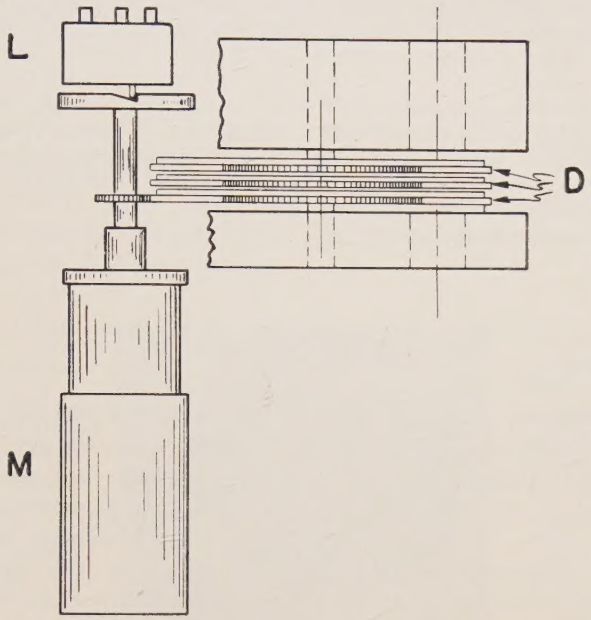

Fig. 1. Diagram showing the location of the motor M, limit switch L and the three disks D. Only one of the three motors and limit switches is shown.

[2]) J. L. Yntema, Argonne National Laboratory Report ANL-5890 (unpublished).

CONFERENCES

SYMPOSIUM ON "CURRENT DEVELOPMENTS IN THE PRODUCTION OF HIGH VACUA"

The Institute of Physics announces that it is arranging a one-day symposium entitled "Current developments in the production of high vacua" to take place in London on 17 April 1959.

There will be three sessions:

(a) Chemical and ionic pumping in kinetic vacuum systems.

(b) Problems in the production of high vacua in large equipment.

(c) Analysis of residual gases in kinetic vacuum systems.

Each of the first two sessions will be opened by invited speakers, and offers of short contributions, especially for the third session, will be considered by the Organizing Committee if outlines are submitted by 15 January next.

The symposium is intended mainly for persons working with high vacua. Abstracts (but not preprints) will be circulated before the symposium, the proceedings of which will not be published in full.

All communications regarding the symposium should be sent to the Secretary, The Institute of Physics, 47 Belgrave Square, London, S.W.1.

CONFERENCE ON "SOME ASPECTS OF MAGNETISM"

The Institute of Physics announces that it is arranging a Conference on "Some aspects of magnetism" to take place in Sheffield from 22–24 September 1959.

The subjects to be covered by the conference are:

(a) Fundamental theories of ferro-, ferri- and antiferromagnetism, including magnetic structure.

(b) Theories of technical magnetization processes, including hysteresis, coercivity, anisotropy and directional effects.

(c) Theoretical and experimental studies of domain phenomena in bulk materials and thin films.

(d) Experimental and theoretical studies of antiferromagnetism in metals and non-metals.

Each session will be opened by an invited speaker and offers of other contributions should be submitted to the Conference Secretary at The Institute of Physics, 47 Belgrave Square, London, S.W.1, before 31 January next. The conference is intended mainly for persons working in the field. Abstracts (but not preprints) will be circulated before the conference, the proceedings of which will not be published in full.

Further particulars will be available in due course from the Secretary of the Institute at the above address.

BOOK REVIEW

J. KISTEMAKER J. BIGELEISEN, A. O. C. NIER (Editors): *Proceedings of the International Symposium on Isotope Separation* (North-Holland Publishing Company, 1958, XX + 704 p., Gld. 55,—)

The first international symposium on isotope separation was held in Amsterdam in April 1957. To judge from the conference proceedings, the somewhat unusual idea of congregating representatives of all the widely differing branches of chemistry, physics, and technology that are involved in the various methods of isotope separation proved very fruitful.

One cannot here enter into a detailed examination of all the 63 chapters in this comprehensive volume. To give a general impression of the contents it may suffice to quote the titles of the 9 parts into which the material has been divided: chemical engineering, molecular interactions, chemical exchange, electromigration, distillation, thermal diffusion, diffusion, electromagnetic separation, ultracentrifuges.

To the student of Nuclear Instruments, the part dealing with electromagnetic separation should be of particular interest. Besides descriptions of some recently constructed apparatus, such as the H(eavy) E(lement and) R(adioactive) M(aterial) E(lectromagnetic) S(eparator) at Harwell (M. L. Smith, K. J. Hill), the calutron type machine in Berlin (F. Bernhard *et al.*), the two-step separator at Saclay (Ch. Cassignol), and the German high frequency mass spectrometer (W. Paul, H. P. Reinhard), there are reports on special techniques, for example the modifications of calutrons at Oak Ridge for high resolution work with heavy elements and radioactive material (R. S. Livingstone, J. A. Martin) and the two-directional mechanical beam scanner developed in Copenhagen (K. O. Nielsen). The possibility of using an isotope separator as an instrument for fundamental research is exemplified by the sputtering experiments performed in Amsterdam (P. K. Rol *et al.*).

As to the editorial work, the inclusion of an element index, which provides a convenient means of reviewing available methods, will certainly be appreciated. It is perhaps too demanding to wish for a subject index in a book like this. The discussions following the various papers make sense surprisingly often, but it is hard to see why most of them have been styled in such a circumstantial way. (Name of lecturer: H. London, Name of questioner: H. C. Urey, Question: ... Answer: (G. H. Reman) ...). In one case a severe critisism must be directed towards the editors. It concerns "A novel magneto-ionic means for separating isotopes in very large quantities", which "separates isotopes of the metals more cheaply than any other method known to the author". This is about all: To leave it at that, without any reference or comment, is not fair to the reader.

In his elegantly written general introduction, H. C. Urey expresses doubt whether any new methods of a decisively advantageous character will be discovered, because differences in the properties of the isotopes other than those of hydrogen are so small. May it be remarked, without any practical considerations, that there is one property that differs considerably between neighbouring isotopes, namely the nuclear spin. G. ANDERSSON

Spotlight on Industry

This section appears each month and features various happenings of interest in the nuclear industrial world and objective information on products of the nuclear manufacturers. It is offered entirely as a service and all nuclear manufacturers are cordially invited to submit clearly objective and descriptive material on their endeavours and product developments for consideration for use in this section.

FILMED STORY OF ACCELERATORS

High Voltage Engineering Corporation, Burlington, Mass.

HIGH ENERGY RADIATIONS FOR MANKIND. 16 mm sound (optical) and color motion picture. Running time: 17 minutes (available with French and German narration).
Versatile radiation source in actual operation.
Industrial accelerators.
Linear accelerator for industrial sterilization.
10 MeV Tandem Van de Graaff.
Van de Graaff X-ray generator.
This film is now available for showing to research, management and educational groups in these fields:
Chemical engineering
Nuclear engineering and physics
Radiology and radiography
Sterilization and radiation processing

ELECTRONIC VOLTMETERS

Metronix, Inc., Chesterland, Ohio

A scale arc of $5\frac{1}{8}$-inches, in a new 6-inch meter case, is announced.

The longer scale, designed for better visibility, compares with the former $4\frac{3}{4}$-inch arc. The new scale is believed

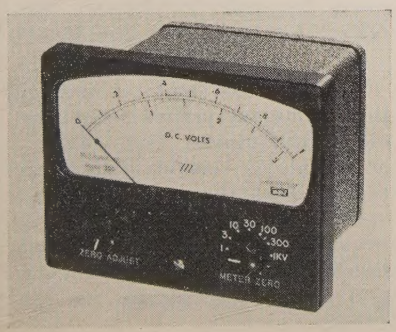

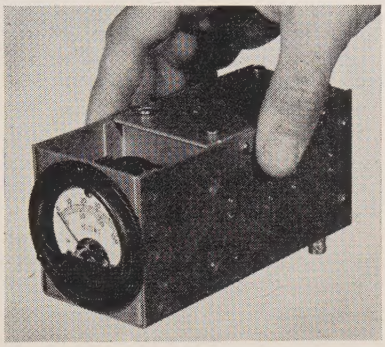

to be the widest available in panel-mounted VTVM's.

Because of improved circuitry and production methods, the new Models 300 (DC) and 310 (AC) are also more accurate over wider temperature ranges than former models.

The high input impedance of these completely self-contained units enables them to measure voltage in a circuit without loading it. They may also be used where voltage reflects other parameters, such as pressure, speed, displacement and temperature.

The DC Voltmeter, with accuracy of plus or minus 3 per cent of full scale deflection, is available in seven discrete ranges, from 1 to 1000 volts. Input resistance is 10 megohms. Model 300-C is a DC centerzero instrument.

The AC model, with frequency response from 20 cps to 100 kc/s, offers 10 ranges from 10 millivolts to 300 volts r.m.s. Input impedance is 1 megohm, 30 $\mu\mu$F.

Model SPD-25 is believed to be the smallest self-contained VTVM ever offered. It operates on power of 400 cycles, 115 volts AC, single phase. The new VTVM occupies panel space of only $2\frac{3}{4}$ by $2\frac{1}{2}$ inches and is less than 6 inches deep. Model SPD-25 is available in any range from 0/30 millivolts to 0/300 volts. Frequency response is 40 cps to 50 kc/s. Input impedance is 1 megohm, 15 $\mu\mu$F. Stability with 10 per cent change in line voltage is better than 2 per cent. Accuracy of the voltmeter is plus or minus 3 per cent.

PANEL METER

Assembly Products Inc., Chesterland, Ohio

A new $3\frac{1}{2}$-inch panel meter, embodying the different design concept introduced last year in the larger Model 561 meter, is announced.

The new Model 361 meter occupies panel space of only $3\frac{1}{2}$ by 2 inches and projects only $\frac{3}{16}$-inch. Like the Model 561, it exposes only its indicating area, with the remainder of the meter fitting snugly behind the panel. The dial and window are slanted for easier reading and may be illuminated through a translucent rear window.

Sensitivity ranges of Model 361 are 0–5 microamperes to 0–50 amperes, and 0–5 millivolts to 0–500 volts.

Model 361 was brought out in response to requests for a smaller meter that could be used with Model 561 to give a "family look" to a panel.

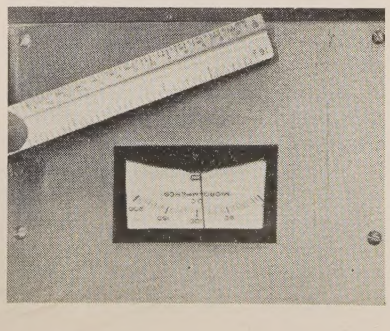

AUTOMATIC SAMPLE CHANGER

Nucleonic Corporation of America, 196 Degraw Street, Brooklyn 31, N. Y., Main

An important development in automatic sample changers for the nuclear laboratory is announced. By using a new type loading and unloading mechanisim, capacities of up to 1 000 planchets with diameters of 5″ or greater are achieved.

Airborne radioactive particulates collected on large filter paper disks can thus be counted. Any type of nuclear counting requirement can be handled by the SC Sample Changer with its associated instrumentation.

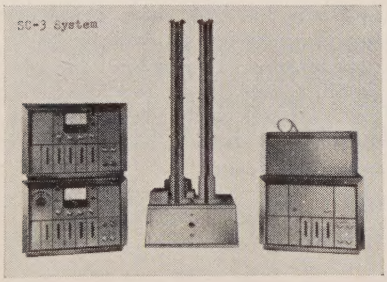

Other features that can be provided are two or more detector heads permitting separate measurements of alpha, beta, and gamma radiation from the sample. Direct print-out of sample number and counts/minute to a preset time, or sample number and time to a preset counts/minute can also be supplied for each type of radiation.

NEW SUNVIC EQUIPMENT

Sunvic Controls Limited, Crown House, Aldwych, London, W.C. 2

A potentiometric recorder, with an integration system suitable for use with gas chromatographs, and a largely transistorised pulse height analyser were shown by Sunvic Controls Limited, at the Physical Society Exhibition, January 19–22, 1959.

The integrating system is fitted into a single trace recorder, potential from the retransmitting slidewire of which is fed to a low-inertia integrating motor. Shaft speed of this is directly proportional to the applied potential. Three sets of cam-operated contacts are included. A pair can be selected according to chart speed, and they

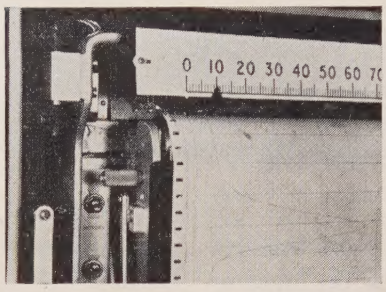

make circuit at a frequency proportional to the deflection of the instrument. The contacts energise two solenoid-operated pens which record the time integral of each trace "peak" immediately beneath the peak. Amplitudes between 10% and 100% f.s.d. can be integrated to better than 1%. Integration commences when the recorder input reaches 1% f.s.d. Output can also be fed to a mechanical counter either internal or external to the instrument.

The new Sunvic PHA will be shown in console form (units can also be rack mounted). Largely transistorised, it uses a ferrite core storage providing 100 channels each with a maximum capacity of 65 535. Counts can be displayed as a CRT analogue trace in which horizontal deflection represents channel number and vertical deflection is proportional to the count. Dekatrons are used to indicate, in decimal form, the total of pulses in any channel selected either manually or automatically in sequence. Totals can also be printed out automatically.

The new Sunvic pulse generator was also shown. Designed primarily for use with the PHA, this has numerous applications in which a shaped pulse of stable and accurately known amplitude is required.

Pulse amplitude is adjustable over the range 0–40 V by the main control and there is also incremental control which provides continuous variation

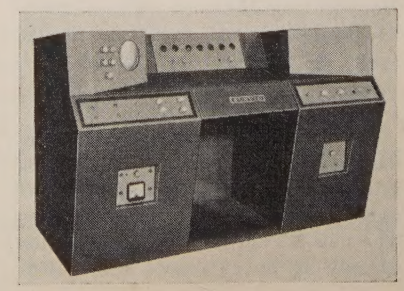

over a range of 0–1.2 V with a linear accuracy of ± 2 mV.

Overall amplitude stability during an 8-hour period is better than ± 0.05% (allowing for mains variation of ± 5%).

NEW 750 MIL MINIATURE SILICON RECTIFIER

Ad. Auriema, Inc., 85 Broad Street, New York 4, N.Y.

Recently developed are Sarkes Tarzian "F" series silicon rectifiers. Rated at 750 milliamperes dc with voltage ratings of 200, 400 and 600 volts, these rectifiers are encapsulated

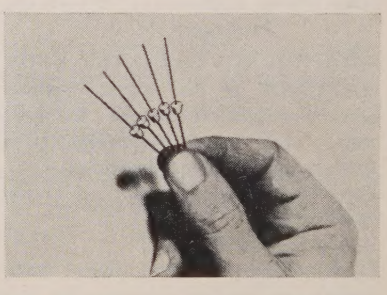

into a volume less than 0.004 cubic inch. Features:

stable form —55° C to 150° C
inrush currents of over 75 A without failure
approximately 0.8 volts drop at 750 mA
reverse currents in the microampere range
extremely shock and vibration resistant

These new "F" series rectifiers are color-coded and finished in a marked sleeving, marking an over-all diameter of about 0.325″ and over-all length of about 0.275″. The "F" series is in production and ready for delivery now.

NEW CATALOG

Anton Electronics Laboratories, Inc., 1226–38 Flushing Avenue, Brooklyn 37, N.Y.

Thirty various types of rack and panel connectors, printed circuit types, special high-current, high-voltage multi-pin-coax combinations, hermetically sealed connectors and other varieties are detailed in the latest edition of the Anton Connector Catalog. Custom design and production accommodations are also described.